

Title page 1 (produced by the Publishing Unit)

Title page 2 (produced by the Publishing Unit)

## ABSTRACT

Tuokko, Sakari

Understanding selective reduction reactions with heterogeneous Pd and Pt: climbing out of the black box

Jyväskylä: University of Jyväskylä, 2016, 85 p.

Department of Chemistry, University of Jyväskylä, Research report Series

ISSN 0357-346X

ISBN 978-951-39-6837-3 (print), 978-951-39-6838-0 (online)

Reduction reactions with heterogeneous metals are one of the most important catalytic methods in synthetic organic chemistry. The reduction products are widely used in academic, pharmaceutical, cosmetics, agro-, and fine-chemical industries. A significant challenge for these reactions is to control chemo-, regio-, and stereoselectivity. Although heterogeneously catalyzed reductions are operationally simple, the origins of selectivity are largely unknown, due the lack of understanding of reaction mechanisms on the metal nanoparticles/colloids.

The first chapter of this thesis presents a short introduction to the heterogeneous metal catalysis and a brief discussion about the past and future research of this field. The chapter includes a preview of the fundamental mechanisms and different selectivities obtained with heterogeneous catalysis. The chapter also reviews different experimental and theoretical methods of studying the mechanism of the heterogeneous catalytic reactions.

The second chapter outlines different methods of controlling chemo-, regio-, and stereoselectivity in reduction reactions with heterogeneous transition metal catalysts. The focus of the review is on how the geometry of substrate can affect the reduction reaction in chemo-, regio-, and stereoselective manners. The discussion is divided into two parts: (1) a basic understanding of the factors that affect the substrates' adsorption geometry, and (2) organic modifiers that interact with the substrate by stabilizing transition states and/or reactive conformations. In each case, selective examples are given; however, the main focus is to understand the underlying reaction mechanisms and origin of the selectivity.

The third chapter consists of research performed by the author towards the understanding of the mechanism of stereo- and chemoselective 1,4-hydrosilylation of enals and enones with heterogeneous palladium catalysts, and further development of the hydrosilylation protocol to a robust and applicable method for industrial use. The chapter also includes studies on selectivity and byproduct formation: (1) first-principle calculations for the mechanism of hydrogenation of acrolein on Pd and Pt, and (2) 3,4-hydroperoxidation of  $\alpha$ -substituted enals with heterogeneous palladium catalyst. The research has been performed by the author by combining experimental and theoretical (i.e. DFT) methods. All results are covered more detail in articles I-IV.

Keywords: hydrosilylation, hydrogenation, hydroperoxidation, reaction mechanism, DFT, heterogeneous, palladium

**Author's address** Sakari Tuokko  
Department of Chemistry and Nanoscience Center  
University of Jyväskylä  
P.O. Box 35  
FI-40014 University of Jyväskylä  
Finland  
sakari.tuokko@jyu.fi

**Supervisors** Professor Petri M. Pihko  
Department of Chemistry and Nanoscience Center  
University of Jyväskylä  
Finland

Associate Professor Karoliina Honkala  
Department of Chemistry and Nanoscience Center  
University of Jyväskylä  
Finland

**Reviewers** Associate Professor Joseph Samec  
Department of Organic Chemistry  
University of Stockholm  
Sweden

Dr. Carine Michel  
Laboratoire de Chimie  
ENS de Lyon  
France

**Opponents** Professor Troels Skydstrup  
Interdisciplinary Nanoscience Center, Department of  
Chemistry  
Aarhus University  
Denmark

Professor Núria López  
Institut Català d'Investigació Química (ICIQ)  
Spain

## ACKNOWLEDGEMENTS

Haluan aloittaa kiittämällä kaikkia jotka ovat auttaneet minua tämän kirjan valmiiksi saattamiseksi. Kiitokset Jyväskylän yliopistolle, Olvi-säätiölle ja innovaatorahoituskeskus Tekesille, jotka ovat rahoittaneet väitöskirjatyötäni 1/2012 - 12/2016 välisenä aikana. Haluan myös kiittää laskentaresursseista CSC - Tieteen tietotekniikan keskusta.

Kiitokset ohjaajilleni Prof. Petri M. Pihkolle ja FT Karoliina Honkalalle. Petriä haluan kiittää synteettisen orgaanisen kemian kiehtovaan maailmaan opastamisesta. Haluan kiittää Petriä myös huolellisuuden, tarkkuuden ja pienten yksityiskohtien huomioimisen opettamisesta. Karoliina haluan kiittää laskennallisen kemian ja heterogeenisen katalyyysin opettamisesta. Erityisesti haluan kiittää Karoliinaa jatkuvasta kannustuksesta ja positiivisten asioiden painottamisesta sekä ylä- että alamäissä väitöskirjatyöni aikana.

Special thanks to Prof. Imre Pápai, Prof. Gokarneswar Sahoo, Dr. Ádám Madarász, Dr. Tanja Lahtinen, Juha Siitonen and Dénes Berta for the fruitful discussions face-to-face or *via* email.

I'm also thankful for Associate Professor Joseph Samec and Dr. Carine Michel for their careful and thorough revision of my manuscript.

Haluan myös kiittää kaikkia joiden kanssa olen läheisesti työskennellyt: Eeva, Sanna, Mikko L., Antti P., Antti N., Jenni, Lauri, Janne, Anna, Mikko M., Jatta, Juha ja Sami. I'm also thankful for post-docs: Meryem, Jun, Hasibur, Sahoo, Rosy, Nicolas, Roshan, Billy and Aurélie, and visiting scientists: Ádám, Ondrej, Martins, Edu and Dénes. Lisäksi kiitos kaikille opiskelijoille jotka ovat työskennelleet samaan aikaan kanssani joko labrassa tai koneella. Kiitos myös kaikille muille kemian laitoksen työntekijöille joiden kanssa olen saanut työskennellä vuosien varrella.

Valtavat kiitokset myös ystäville, perheelle, sukulaisille ja läheisille.

Viimeisenä haluan kiittää rakkaitani Roosaa ja Helviä tuesta, turvasta, elosta ja ilosta.

Helsinki, November 9th, 2016  
Sakari Tuokko

## LIST OF ORIGINAL PUBLICATIONS

This thesis is based on the following original publications, which in the text are referred to by their Roman numerals.

- I Sakari Tuokko and Petri M. Pihko, Palladium on Charcoal as a Catalyst for Stoichiometric Chemo-, and Stereoselective Hydrosilylations and Hydrogenations with Triethylsilane, *Org. Process Res. Dev.* **2014**, *18*, 1740–1751.
- II Sakari Tuokko, Petri M. Pihko and Karoliina Honkala, First Principles Calculations for Hydrogenation of Acrolein on Pd and Pt: Chemoselectivity Depends on Steric Effects on the Surface, *Angew. Chem. Int. Ed.* **2015**, *55*, 1670–1674. (**VIP article**)
- III Sakari Tuokko and Petri M. Pihko, Palladium on Charcoal Catalyzed 3,4-Hydroperoxidation of  $\alpha$ -Substituted Enals with Triethylsilane and Water, *Synlett* **2016**, *27*, 1649–1652. (**Nominee for SYNLETT Best Paper Award**)
- IV Sakari Tuokko, Karoliina Honkala and Petri M. Pihko, Pd/C Catalyzed Hydrosilylation of Enals and Enones with Triethylsilane: Conformer Populations Control the Stereoselectivity, *Submitted*.

### Author's contribution

In paper I, the author conceived the study, performed the experiments and analyses, and wrote the paper together with the co-author.

In paper II, the author initiated and conceived the study, performed the computational modeling and experiments and analyses, and wrote the paper together with the co-authors.

In paper III, the author initiated and conceived the study, performed experiments and analyses, and wrote the paper together with the co-author.

In paper IV, the author conceived the study, performed the experiments and analyses and computational modeling, and wrote the paper together with the co-authors.

## ABBREVIATIONS AND DEFINITIONS

111	surface structure for <i>fcc</i> metals
6-31G(d)	basis set
Ac	acetyl
<i>aq.</i>	aqueous
<i>anti</i>	used in the representation of a stereochemical relationship. <i>Anti</i> means “on the opposite sides” of a reference plane
atm	atmosphere
B3LYP	Becke three-parameter Lee-Yang-Parr (XC functional)
BEEF-vdW	Bayesian error estimation functional with van der Waals (XC functional)
Bu	butyl
CD	cinchonidine
<i>cis</i>	used in the nomenclature of ring systems. Two ligands are said to be located <i>cis</i> to each other if they lie on the same side of a plane
CN	cinchonine
Cy	cyclohexyl
DCM	dichloromethane
DFT	density functional theory
<i>dr</i>	diastereomeric ratio
<i>E</i>	<i>Entgegen</i> (German for “opposite”), used in the nomenclature of stereoisomers. If the groups of the highest precedencies lie on the opposite side of a reference plane passing through the double bond, it is given the description <i>E</i>
<i>ee</i>	enantiomeric excess
e.g.	<i>Exempli gratia</i> (Latin for “for example”)
equiv	equivalent
<i>endo</i>	used in the nomenclature of bridged ring systems. If the group is orientated away from the highest numbered bridge, it is given the description <i>endo</i>
Et	ethyl
etc.	<i>Et cetera</i> (Latin for “and the rest; and the other things”)
<i>exo</i>	used in the nomenclature of bridged ring systems. If the group is orientated towards the highest numbered bridge, it is given the description <i>exo</i>
<i>ex situ</i>	Latin for “outside; off site; or away from the natural location”
<i>et al.</i>	<i>Et alii</i> (Latin for “and others”)
<i>fcc</i>	face-centered cubic
FS	final state
FT	Fourier transform
GDP	gross domestic product
GGA	generalized gradient approximation
GPAW	grid projector augmented wave, the name of a DFT code
h	hour

<i>i-</i>	iso
I	intermediate
i.e.	<i>Id est</i> (Latin for “that is”)
<i>in situ</i>	Latin for “in position; on site; on the premises”
IR	infrared
IS	initial state
IUPAC	International Union of Pure and Applied Chemistry
k	prefix kilo ( $10^3$ )
LCT	liquid chromatography time of flight
LDA	local density approximation
m	prefix milli- ( $10^{-3}$ )
M	metal, mol/L (molarity)
Me	methyl
min	minute
ML	monolayer
NMR	nuclear magnetic resonance spectroscopy
p.a.	puriss analysis
PAW	projector augmented wave
PBE	Perdew-Burke-Ernzerhof (XC functional)
PCET	proton-coupled electron transfer
Ph	phenyl
Pr	propyl
PVP	polyvinylpyrrolidone
QD	quinidine
QN	quinine
R	arbitrary substituent
R	<i>Rectus</i> (Latin for “right”), used in the nomenclature of enantiomers. The designations of absolute configuration of stereogenic centers where the ligands appear in a clockwise order according to Cahn-Ingold-Prelog priority rule
<i>re</i>	a stereoheterotopic face of a trigonal atom on which the ligands appear in a clockwise order according to Cahn-Ingold-Prelog priority
ref	reference
RPBE	a revised Perdew-Burke-Ernzerhof (XC functional)
S	<i>Sinister</i> (Latin for “left”), used in the nomenclature of enantiomers. The designations of absolute configuration of stereogenic centers on which the ligands appear in a counterclockwise order according to Cahn-Ingold-Prelog priority rule
SAM	self-assembled monolayer
<i>s-cis</i>	used in the representation of arrangement of two conjugated double bonds about the intervening single bond, <i>s-cis</i> if the double bonds are synperiplanar

<i>si</i>	a stereoheterotopic face of a trigonal atom on which the ligands appear in a counterclockwise order according to Cahn–Ingold–Prelog priority
SI	Supporting Information
<i>s-trans</i>	used in the representation of arrangement of two conjugated double bonds about the intervening single bond, <i>s-trans</i> if the double bonds are antiperiplanar
<i>syn</i>	used in the representation of a stereochemical relationship. <i>Syn</i> means “on the same sides” of a reference plane
t	time
<i>t-</i>	<i>tert-</i> , tertiary
TDI	TOF-determining intermediate
THF	tetrahydrofuran
TLC	thin layer chromatography
TOF	turnover frequency
<i>trans</i>	Used in the nomenclature of ring systems. Two ligands are said to be located <i>trans</i> to each other if they lie on the opposite sides of a plane
TS	transition state
TSS	transition state scaling
<i>via</i>	Latin for “by; by way of; way; road”
wt %	percentage by weight
XC	exchange correlation
XML	extensible markup language
Z	<i>Zusammen</i> (German for “together”), used in the nomenclature of stereoisomers. If the groups of the highest precedencies lie on the same side of a reference plane passing through the double bond, it is given the description Z
$\alpha$ -	referring to the position adjacent to the functionalized carbon
$\beta$ -	referring to the position one carbon further than $\alpha$
$\Delta$	difference
$\mu$	prefix micro- ( $10^{-6}$ )
$\pi$	a molecular bond type
$\sigma$	a molecular bond type



# CONTENTS

ABSTRACT

ACKNOWLEDGEMENTS

AUTHOR'S CONTRIBUTION

ABBREVIATIONS AND DEFINITIONS

## CONTENTS

1	INTRODUCTION .....	14
1.1	Catalysis .....	14
1.2	Heterogeneous metal catalysis .....	15
1.3	Fundamental mechanisms in heterogeneous metal catalysis .....	17
1.4	Selectivity of the catalytic reaction .....	19
1.5	How to study mechanisms of heterogeneous catalytic reactions .....	21
2	SELECTIVE REDUCTION REACTIONS WITH HETEROGENEOUS TRANSITION METAL CATALYSTS .....	22
2.1	Adsorption geometry as a key to selectivity .....	23
2.1.1	Chemoselective reductions .....	24
2.1.2	Stereoselective reductions .....	26
2.1.2.1	Isomerization mechanisms .....	27
2.1.2.2	Stereoselective reductions of alkynes, dienes, and cumulated allens and polyenes .....	32
2.1.2.3	Diastereoselective reduction of disubstituted cyclohexenes .....	34
2.2	Organic modifiers that interact with the substrate .....	41
2.2.1	Cinchona alkaloids and their derivatives .....	41
2.2.1.1	Requirements for cinchona alkaloid modifiers .....	44
2.2.1.2	Origin of enantioselectivity .....	46
2.2.2	Other organic modifiers .....	48

2.2.3	Self-assembled monolayers (SAMs) .....	51
2.3	Conclusions.....	54
3	RESULTS AND DISCUSSION .....	56
3.1	Aims and background of the work .....	56
3.2	Methods.....	57
3.2.1	Experimental methods .....	57
3.2.2	Computational methods .....	58
3.3	Improving the protocol.....	61
3.3.1	Effect of the catalyst .....	61
3.3.2	Improving the transfer hydrogenation protocol .....	63
3.3.3	Stereo- and chemoselectivity of the improved protocols.....	64
3.4	Mechanistic studies of the hydrosilylation and transfer hydrogenation reactions .....	65
3.4.1	Mechanism of the stereoselective hydrosilylation reaction....	65
3.4.2	Mechanism of the transfer hydrogenation and chemoselectivity of the hydrosilylation reaction.....	70
3.5	First principle calculations for the mechanism of hydrogenation of acrolein on Pd and Pt .....	73
3.6	3,4-Hydroperoxidation of $\alpha$ -substituted enals .....	76
	SUMMARY AND CONCLUSIONS.....	78
	REFERENCES.....	79

(This blank page is for the first chapter to start from odd page.

You may remove this page if the first chapter already starts from an odd page.)

# 1 INTRODUCTION

## 1.1 Catalysis

In the early nineteenth century, a Swedish chemist, Berzelius, defined a term, “catalyst,” to identify a compound that increases the rate of a chemical reaction without itself being consumed.<sup>1</sup> Consequently, the catalyst is both a reactant and product of the reaction. In a thermodynamic sense, the catalyst increases the rate of the reaction by affecting the kinetics of the transformation ( $E_a$ ), not by modifying the overall standard Gibbs energy change ( $\Delta H$ ) in the reaction (Figure 1).<sup>2</sup>

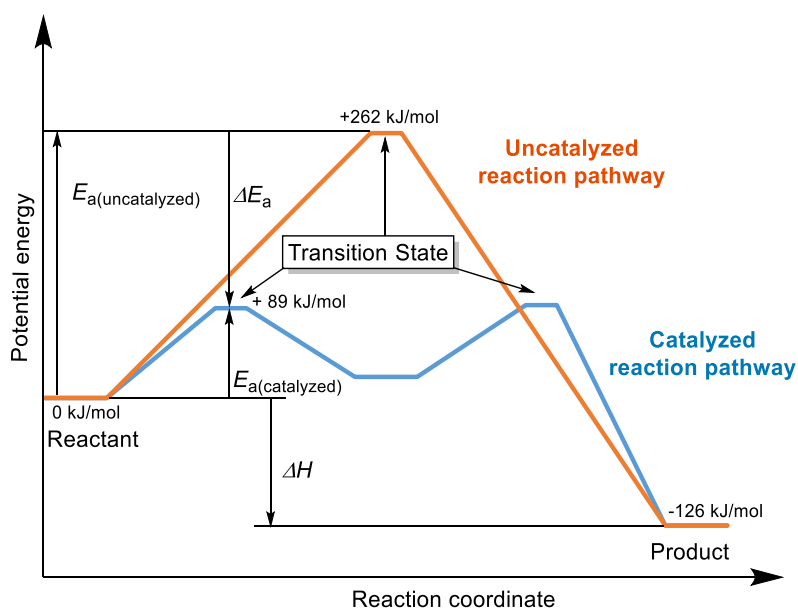


Figure 1. A hypothetical exothermic chemical reaction.

The process in which catalysts are used is called catalysis. Catalysis has been an essential part of most industrial processes since the industrial revolution,<sup>3</sup> including the manufacture of petro-, agro-, and fine chemicals, and the production of pharmaceuticals, cosmetics, foods, and polymers.<sup>4</sup> Catalysis is also in the center of the development of the cleaner energy and bio-based chemicals and plays a key role in the breakdown of environmental pollutants and reducing the amount of waste produced in industrial processes.<sup>4,5,6</sup> At the moment, over 80 % of chemical industrial processes use catalysis. The economic contribution of catalysis is impressive, creating global sales of 1500 billion dollars a year. Estimates are that catalysis contributes directly or indirectly to over 35 % of the world's GDP.<sup>4,7</sup>

From the early stages of catalysis research, the main focus has been on improving the activity of the catalyst.<sup>8</sup> For example, altering the size and stability of metal particles in the heterogeneous catalyst also affects catalytic activity.<sup>8</sup> Increasing environmental concerns require industrial processes to consume less material and produce less waste. These concerns have shifted the focus of catalysis research from improving the activity to improving selectivity as well. Catalytic reactions that are highly selective minimize the use of reactants and prevent the formation of byproducts, i.e., waste. Further, the separation of byproducts from the desired products might need expensive and more waste-producing clean-up procedures. Altogether, more selective processes should ultimately lead to “greener” and in many cases cheaper chemistry than before.<sup>8</sup>

## 1.2 Heterogeneous metal catalysis

Catalysis can be classified into two subdivisions: heterogeneous catalysis and homogeneous catalysis. Homogeneous catalysis includes soluble catalysts such as enzymes (biocatalysts), organocatalysts, and homogeneous metal catalysts. The common factor in homogeneous catalysis is that only one phase is involved during the reaction. In contrast, heterogeneous catalysis occurs at or

near the interface of two phases, most familiarly solid versus liquid or gas, but also for example liquid versus gas or oil versus water.

Most of the catalysts used in industrial processes are heterogeneous. The easy separation and recyclability together with low cost makes the heterogeneous catalysts desirable over homogeneous catalysts.<sup>4,8</sup> The most typical heterogeneous catalyst consists of finely dispersed metal particles adsorbed onto the solid support, such as carbon, alumina, or silica.<sup>9,10,11</sup> Other types of heterogeneous catalysts are, for instance, crystalline solids such as zeolites;<sup>12</sup> the so-called heterogenized catalysts, in which the homogeneous catalysts are immobilized onto the solid support;<sup>13</sup> and the catalysts in which the heterogeneous phase serves as a reservoir for the true homogeneous catalysts, i.e., leached metal atoms.<sup>14,15</sup>

Traditional heterogeneous metal catalysts typically consist of finely dispersed metal particles. However, only a small fraction of the metal atoms, i.e., surface atoms, in the metal particles are active for catalysis. These surface atoms can exist in a variety of different coordination on the metal particle (Figure 2). However, only a small fraction of the coordination sites might be active for the desired transformation, while all the others might be active for the undesired ones. In contrast, homogeneous catalysts usually contain only a single active site, which might explain why they are generally more selective than the heterogeneous catalysts.

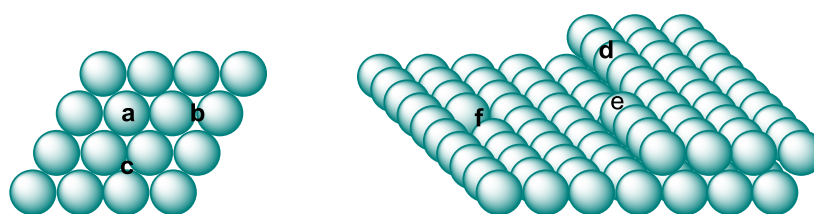


Figure 2. Examples of possible coordination sites on 111-surface. On left, a top view, and on right, a side view of the lattice: a) top-site, b) bridge-site, c) hollow-site, d) step-site, e) edge-site, and f) vacancy-site.

The recent progress in last few decades in spectroscopic and computational methods has advanced the rational design of catalysts to produce single-site

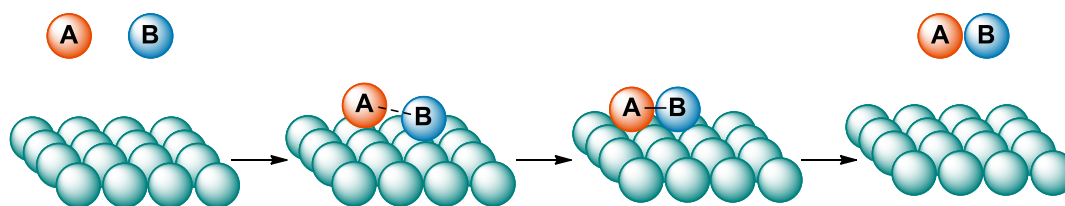
heterogeneous catalysts.<sup>16</sup> To take full advantage of the well-defined surfaces, it is essential to identify the active sites of the catalyst. The identification of the active sites and further development of the catalytic process requires a molecular-level understanding of the reaction mechanism.

### **1.3 Fundamental mechanisms in heterogeneous metal catalysis**

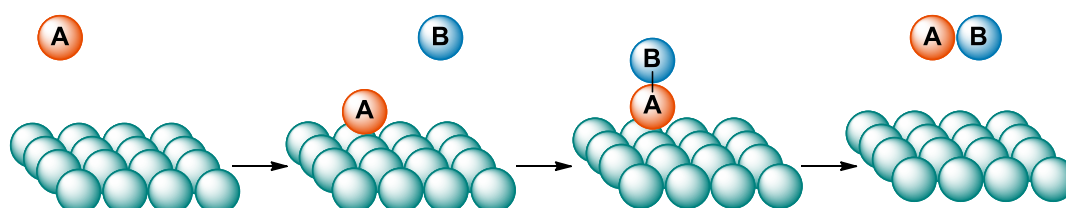
As discussed in the previous section, the design of new catalysts with high selectivity requires a better understanding of the underlying mechanism behind catalytic reactions. Commonly, the first step in every mechanism on the metal surfaces is the activation of the reactant molecule by adsorption. The two types of adsorptions on the surface are called chemisorption and physisorption. In chemisorption, the molecule forms a covalent bond with the surface atom or atoms, and in physisorption the molecules interact with the surface through the van der Waals forces.

In the early years of catalysis, several propositions for the fundamental reaction mechanisms on the metal surface were discussed.<sup>17</sup> Today, the most common and well-established fundamental mechanisms are the Langmuir-Hinshelwood and Eley-Rideal mechanisms (Scheme 1).<sup>18</sup>

a)



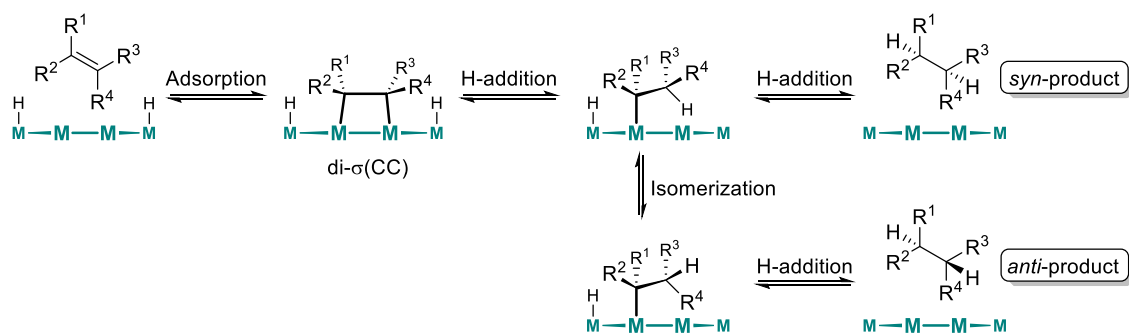
b)



Scheme 1. Fundamental mechanisms on the metal surface: a) Langmuir-Hinshelwood mechanism and b) Eley-Rideal mechanism.

In the Langmuir-Hinshelwood mechanism, each reactant is first adsorbed onto the surface, after which they diffuse towards each other. Contact between the reactants leads to the formation of a new bond or bonds and yields the product, which ultimately desorbs from the surface (Scheme 1a). In contrast, in the Eley-Rideal mechanism, only one of the reactants is initially adsorbed onto the surface. The other reactant, which is still in the solution or gas phase, interacts with the adsorbed reactant, forming the product that desorbs from the surface (Scheme 1b).

In addition to the fundamental mechanisms presented in Scheme 1, more detailed mechanisms have also been proposed for heterogeneous metal catalysis. As an example, the reduction of unsaturated compounds on the metal surfaces proceeds through the well-established Horiuti-Polanyi mechanism (Scheme 2).<sup>19</sup> With most transition metals, the *syn*-addition product is mainly obtained from the reduction of di- $\sigma$ (CC) or  $\pi$ (CC) adsorbed compound (the latter is not shown in Scheme 2).<sup>20</sup> However, with many metals, such as palladium, the *anti*-addition products are often obtained to a large extent. The isomerization leading to *anti*-addition is discussed in more detailed in Section 2.1.2.1.

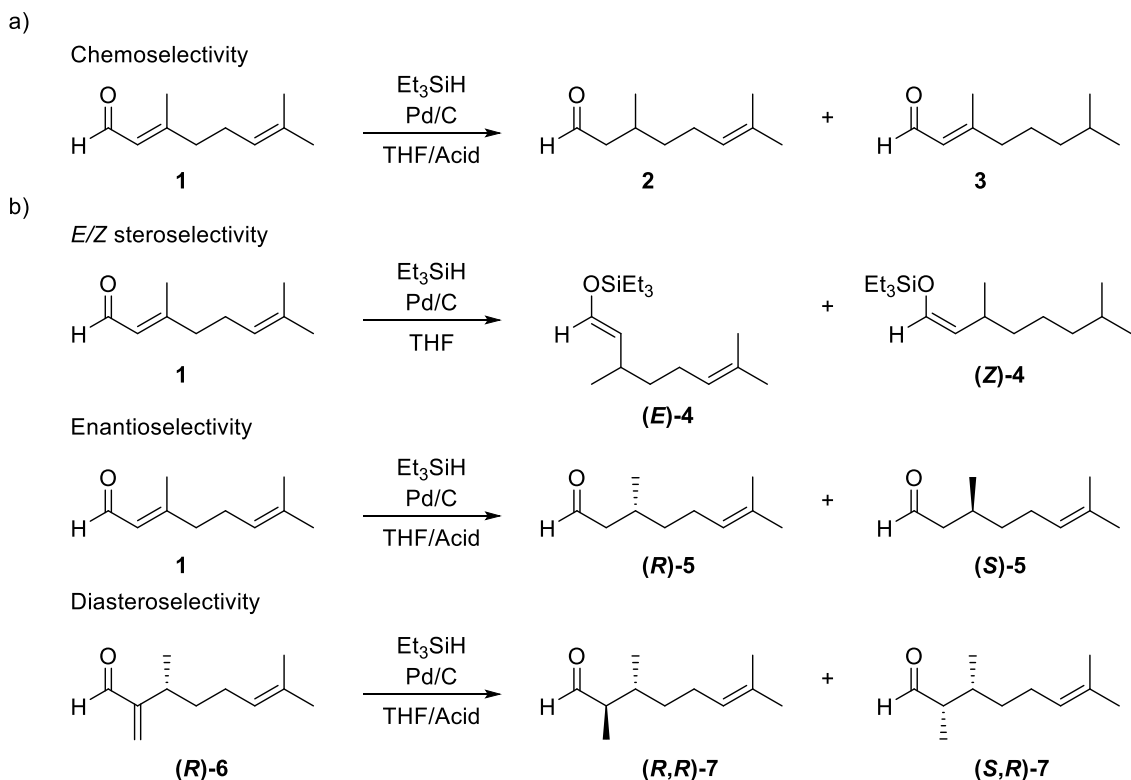


Scheme 2. Horiuti-Polanyi mechanism for the hydrogenation of alkenes on transition metal surfaces: an example of two possible mechanistic pathways leading to *syn*- and *anti*-products.

## 1.4 Selectivity of the catalytic reaction

Catalysts alter only the kinetics of the chemical reaction, not the standard Gibbs energy change.<sup>2</sup> In other words, the catalyst enables the reaction to proceed *via* new kinetic pathway to the desired product (i.e. by lowering the amount of needed external energy,  $E_a$ ; see Figure 1). The possibility to introduce new kinetic pathways to the reaction *via* catalyst also leads to the possibility to modify the selectivity of the reaction.

The term “selectivity” refers to the ratio of products obtained from the reactants.<sup>2</sup> In catalysis, selectivity is a broad concept that includes a wide range of selectivities, such as chemoselectivity and different kinds of stereoselectivities (Scheme 3).



Scheme 3. a) Example of chemoselectivity and b) examples of different stereoselectivities.

The energy differences that distinguish the selectivity of the reaction are generally low compared with the magnitude of  $\Delta E_a$ -value induced by the catalyst in Figure 1. For example, an energy difference of 6 kJ/mol between two pathways leads to a roughly 1:10 difference in product ratio at room temperature.<sup>21</sup> In addition, the methods that have been traditionally used to control the activity, such as pressure, temperature, and the size of the metal particles, usually have similar effects on the different pathways that determine the selectivity of the reaction.<sup>4</sup> As such, alternative (and more specific) methods are required to control the selectivity of the catalytic reaction. This all leads back to understanding the mechanism of the reaction at the molecular level. If we know all the elementary steps leading to the desired and undesired products, we should be able to rationally alter the reaction conditions to completely favor the desired product, i.e., the selectivity of the reaction.

## 1.5 How to study mechanisms of heterogeneous catalytic reactions

The energy difference that determines the selectivity of a reaction is generally very small. To be able to modify the reaction to favor a certain kinetic pathway, it is important to know the exact mechanism of the reaction at the molecular level. However, finding a mechanism to the heterogeneously catalyzed reaction can be challenging. The heterogeneous catalysis occurs at the solid phase on a relatively large metal particle (compared with the size of the reactant). This makes it very difficult to characterize and distinguish the reaction intermediates during the catalytic reaction.

Mechanistic studies of surface reactions are most often made by using *ex situ* investigations, such as labeling experiments.<sup>11</sup> However, as indicated in Section 1.2, the heterogeneous metal catalysts contain a broad distribution of different coordination sites that interact differently with the reactants.<sup>8</sup> This, together with the lack of knowledge of the intermediates of the reaction, makes the determination of the precise reaction mechanism for the surface reaction problematic. The surface reaction is like a black box into which the reactants are put and out of which the products come, but all the steps in between are speculative. Viewed this way, the development of selective heterogeneous metal catalysts is more like trial and error rather than a rational design.

In recent decades, the development of different spectroscopic methods<sup>18,22</sup> has made possible the *in situ* investigation of surface reactions. These advances, combined with the progress of computational chemistry (especially DFT) have enabled researchers to distinguish between the different intermediates and transition states of the surface reaction. This allows for the possibility to determine the reaction mechanism, which ultimately could lead to rational design of the catalytic process towards 100 % selectivity.<sup>8</sup>

## 2 SELECTIVE REDUCTION REACTIONS WITH HETEROGENEOUS TRANSITION METAL CATALYSTS

Reduction reactions are arguably one of the most important catalytic methods in synthetic organic chemistry, both in academia and industry.<sup>9,23,24,25,26,27,28</sup> The scope of functional groups that can be reduced with heterogeneous transition metals is wide, including functionalities, such as alkynes, alkenes, carbonyls, nitro groups.<sup>11</sup> In addition, reduction reactions can be used to synthesize complex molecules in stereo-, enantio-, and diastereoselective manners.<sup>29</sup> Stereochemically complex molecules are highly valuable in academic, fine-chemical, pharmaceutical, and cosmetic industries.<sup>4</sup> However, due the large scope of reducible functionalities, a significant problem is the control of selectivity in reduction processes. This is especially important in industrial settings, where even the traces of byproducts need to be analyzed and characterized.

The selective reduction reactions with heterogeneous transition metals have been covered in numerous books and reviews.<sup>18,22,30,31,32,33,34,35,36,37</sup> The traditional strategies used to control the selectivity are, for instance, modifying the size and shape of the metal particles, using inorganic modifiers or different supporters, or alloying the metal particles with other metals.<sup>30,31,32,33,34,35,36,37</sup> The modification of the size and shape, i.e., the morphology of the metal particle, that commonly affects the number of a different active sites in the catalyst. In turn, inorganic modifiers and supporters induce Lewis acidic or basic sites to the catalyst and alloying affects the redox potential of the catalyst.<sup>30,31,32,33,34,35,36,37</sup>

Selectivity can also be controlled by more sophisticated methods, such as those commonly used in homogeneous catalysis, e.g. ligands, auxiliaries, and cocatalysts.<sup>38</sup> These additives alter either the steric environment around the substrate or/and by activating the reducing functional group. In heterogeneous catalysis, a large number of these methods already exist in a subclass of organic

modifiers.<sup>36</sup> However, because a new trend of single-site catalysts is arising, a more rational approach is possible in a development of selective heterogeneous catalyst systems.<sup>16</sup> This, however, requires a much deeper understanding of the reaction mechanisms on the metal particle, and one of the first steps is to find out how closely the mechanisms of heterogeneous catalysts parallel those established within homogeneous catalysis.<sup>4,39</sup>

## 2.1 Adsorption geometry as a key to selectivity

The adsorption geometry of any substrate on the metal surface depends strongly on several parameters, such as the coordination of the active sites, coverage, hydrogen pressure, solvent, and temperature.<sup>11</sup> Most often, the initial conformation in which the substrate adsorbs onto the metal particle also determines the reaction selectivity.<sup>30,31,32,33,34,35,36,37</sup> However, in some cases, the barriers between alternative adsorption geometries or binding modes can be considerably lower than the activation barriers of the reduction steps.<sup>11</sup> This leads to possibility that the initial adsorption geometry or the most stable adsorption geometry might not always lie on the major reaction pathways.<sup>20</sup> Consequently, all possible conformations, adsorption geometries, and binding modes for the reactant, intermediates, and product need to be considered when trying to determine all the kinetically relevant pathways. This is especially important when one attempts to understand the product distribution of the selective reactions.

In each of the following subsections, some selected examples of selective reductions are given. The aim is to find some generality in how the molecules interact with the surface depending on their structures. For example, although Section 2.1.2 focuses on the reduction of alkenes, it should be noted that identical adsorption structures and intermediates can also be found in the reduction of other functionalities, such as carbonyls, amines, and nitro groups.<sup>11</sup> The factors that affect selectivity, such as steric adsorbate-surface interactions, dissociative

and associative isomerization mechanisms, and influence of the chiral centers are, at least to some extent, universal for reducing any functional group.<sup>11</sup>

### 2.1.1 Chemoselective reductions

The factors that affect the chemoselectivity in reduction reactions with heterogeneous transition metal catalysis mainly depend on the functional groups that are presented in the molecule. For example, if the activation energy to reduce a particular functionality is considerably lower than the energy required to reduce other functionalities (e.g. C=C bond versus phenyl group), most often the optimization of reaction time, hydrogen pressure, temperature, or catalyst loading is sufficient to obtain high selectivities. However, if the activation energies are close to each other, both functional groups might be reduced during the process. In particular, the differentiation of the same (e.g. C=C) or similar (e.g. C=C and C≡C) functionalities is a difficult task.

Some molecules that contain the same or similar functionalities can be reduced with high chemoselectivity if one of the functionalities is sterically crowded.<sup>34</sup> The steric crowding lowers the adsorption energy of the particular functionality and in most cases this leads to a lower reduction rate by the Sabatier principle, which connects the binding energy to the reaction rate.<sup>8</sup> The explanation for the lower adsorption energy is that, in order to form the geometry for an optimal metal-substrate bond, the repulsive adsorbate-surface interaction leads to the deformation of the molecule and surface. These deformations are energetically costly. The energetic cost directly lowers the adsorption energy of the particular functionality, as illustrated in Figure 3 for DFT calculated adsorption energies for crotonaldehyde (**8**) and prenal (**9**) on Pt(111) surface.<sup>40</sup>

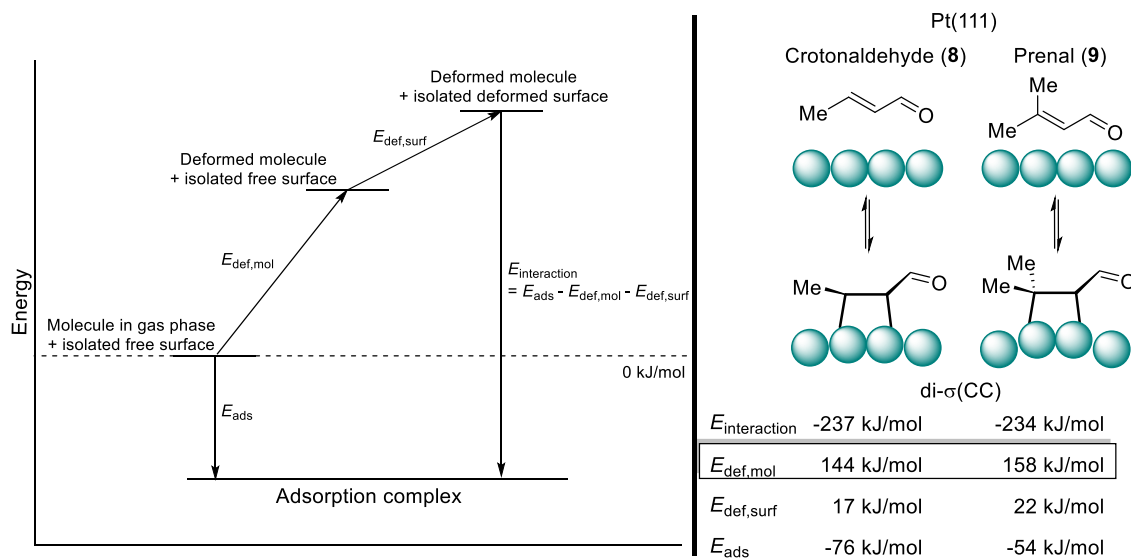
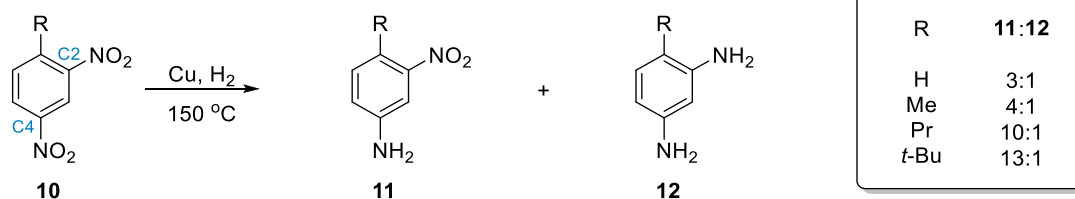


Figure 3. The lower adsorption energy of prenal (9) compared with crotonaldehyde (8) is mainly due to the repulsive adsorbate-surface interaction of methyl substituents. This leads to the higher deformation of the molecule in order to form the geometry for optimal bonding.<sup>40</sup>

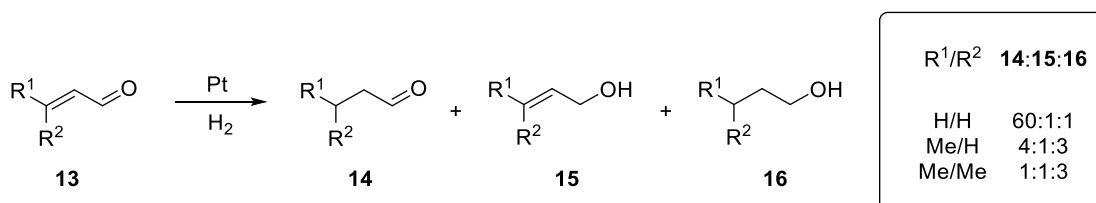
The effect of the steric crowding on the chemoselectivity is illustrated in selected examples in Scheme 4. The selectivity toward reducing only the 4-nitro group of the 1-substituted-2,4-dinitrobenzene **10** increases hand in hand with the bulkiness of the substituent near the 2-nitro group (Scheme 4a).<sup>41</sup> The reason for the increased selectivity is that the molecule can easily adapt an adsorption geometry in which the interaction between the 4-nitro group and the catalyst surface is not disturbed by the substituent.<sup>42</sup> However, the interaction between the 2-nitro group and the catalyst surface is inevitably affected by the size of the substituent at the 1-position. This leads to a lower reduction rate of the 2-nitro group simultaneously as the size of the substituent increases.

The steric crowding also affects the chemoselectivity in hydrogenation of  $\alpha,\beta$ -unsaturated aldehydes (Scheme 4b).<sup>43</sup> Although the origins of the chemoselectivity are still under debate,<sup>44,45,46</sup> it has been found that the reduction rate of the C=C double bond is lowered by the steric crowding around it. With increased steric crowding of the C=C bond, the chemoselectivity changes towards C=O double bond reduction (Scheme 4b).<sup>43</sup>

a)



b)



Scheme 4. a) The bulkiness of the R-group affects the chemoselectivity of the reduction reaction.  
 b) The steric crowding reduces the rate of C=C bond reduction, which induces the chemoselectivity of the reaction.

## 2.1.2 Stereoselective reductions

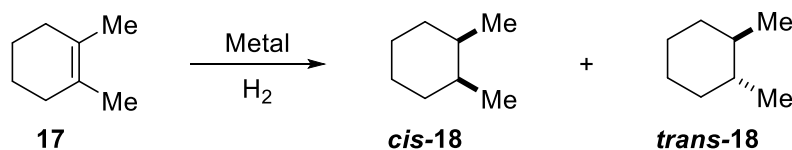
The stereoselectivities of reduction reactions are highly dependent on the reaction mechanisms. As discussed in Section 1.3, the hydrogenation on the metal particles usually occurs by *syn*-addition. However, in some cases *anti*-addition is observed, which results from the isomerization during or after the reaction.

Typically, a mixture of *E/Z* isomers are observed in reductions, in which a C=C double bond is left in the product. Such reactions include the reductions of alkynes and semireductions of conjugated double bonds, allenes, and cumulated trienes and polyenes. Diastereoselectivity, in turn, becomes possible with substrates containing chiral centers. The chiral center present in the substrate influences the direction of the hydrogen addition. The influence is much more apparent in the case of rigid cyclic compounds than acyclic ones. Most of the examples of diastereoselective reductions are hydrogenations of C=C, C≡C, C=O, or C=N bonds. In these reductions, the structural/conformational factors affecting the selectivity are very similar, such as *E/Z* isomerization and double bond migration.<sup>11</sup>

### 2.1.2.1 Isomerization mechanisms

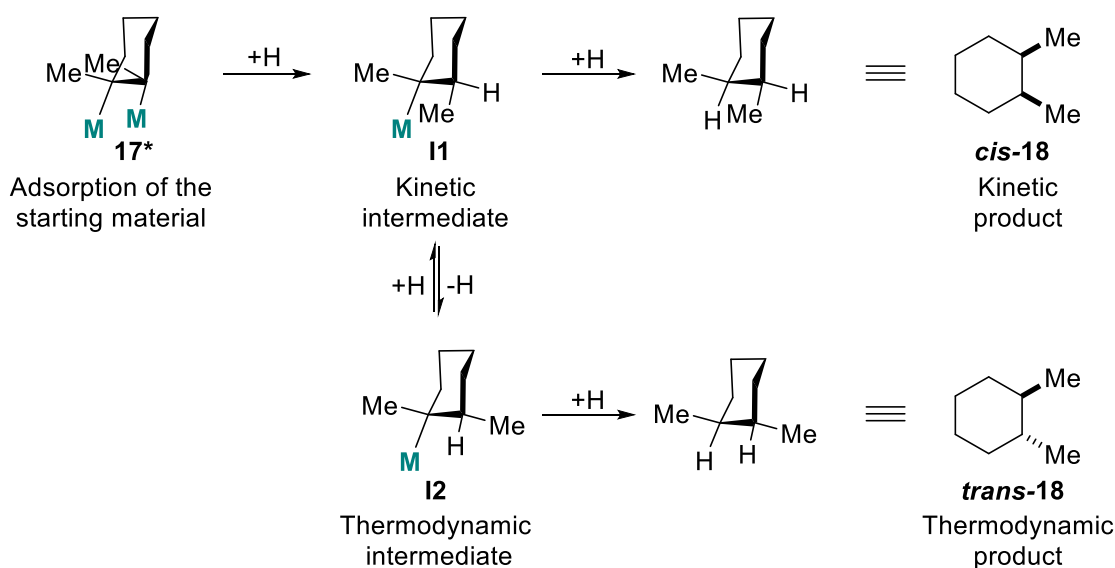
To understand the stereoselectivities of reduction reactions with heterogeneous transition metal catalysts presented in the literature, it is important to distinguish among different mechanistic pathways leading to the different product isomers. In general, the reduction reactions on metal surfaces proceed *via syn*-addition (see Scheme 2 in Section 1.3). However, depending on the reaction conditions, in most cases an *anti*-addition product is obtained as a result of isomerization. Isomerization mechanisms include dehydrogenations, rehydrogenations, and  $\sigma$ -bond rotations, which enable the substrate to adapt thermodynamically the most stable geometry at the TOF-determining intermediate (TDI).<sup>47</sup> In other words, if any dehydrogenation or  $\sigma$ -bond rotation has a reaction barrier smaller than or equal to either of the H-additions of the hydrogenation sequence, by the Curtin-Hammett principle,<sup>2</sup> some extent of isomerization will occur. Generally, the isomerization ratio varies with different metals in the sequence Pd>>Pt,Ru,Rh>Os>Ir (Scheme 5a).<sup>11,48</sup>

a)

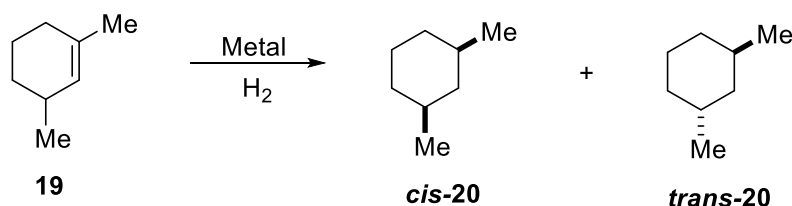
Metal ***cis-18:trans-18***

Pd	25:75
Pt	80:20
Ru	94:6
Rh	88:12
Os	99:1
Ir	99:1

b)



c)

Metal ***cis-20:trans-20***

Pd	80:20
Pt	76:24

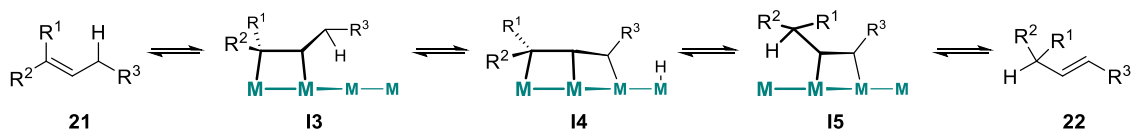
Scheme 5. a) Reduction of 1,2-dimethylcyclohexene (**17**) with different heterogeneous transition metal catalysts. b) The semihydrogenated intermediate **I2** resembles the gas phase product. Consequently, the thermodynamic intermediate leads to thermodynamic product *trans*-1,2-dimethylcyclohexane (**trans-18**). c) Reduction of 1,3-dimethylcyclohexene (**19**) with heterogeneous palladium and platinum catalysts: *Cis*-20 is both a thermodynamic and kinetic product.

With platinum, ruthenium, rhodium, osmium, and iridium catalysts, the adsorption of the starting material is the TDI and the reduction produces a kinetic product *cis*-1,2-dimethylcyclohexane (**cis-18**) by *syn*-addition (Schemes 5a and 5b). However, in the case of palladium, the semihydrogenated intermediate is the TDI, and the thermodynamically more stable intermediate **I2** builds up on the surface by

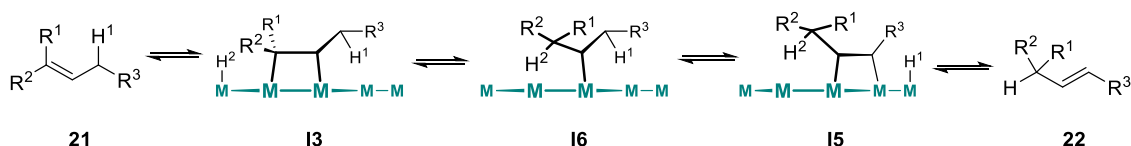
isomerization. The intermediate **I2** binds to surface only from the one carbon atom, and consequently, this geometry resembles the thermodynamically most stable product *trans*-**18** in solution or gas phase. As a result, in the case of reduction of 1,2-dimethylcyclohexene (**17**) with palladium, a *trans* isomer is obtained as the major product by *anti*-addition (Scheme 5b).<sup>37</sup> However, in the reduction of 1,3-dimethylcyclohexene (**19**), with both palladium and platinum catalysts, the *cis* product (*cis*-**20**) is obtained as the major isomer, because it is both a kinetic and thermodynamic product (Scheme 5c, see also Section 2.1.2.3.).<sup>49</sup>

The isomerization discussed above can take place *via* many different mechanisms, or it might be a combination of several of them. One type of isomerization is migratory isomerization, i.e., double bond migration.<sup>11</sup> For example, if the functionality that binds to the metal catalyst, such as C=C double bond, is sterically very hindered, it is possible that one of the allylic C-H bonds contacting the metal surface is cleaved, leading to dissociative adsorption (intermediate **I4**, Scheme 6a).<sup>50</sup> This leads to double bond migration, which enables the molecule to adopt an energetically more stable and structurally different adsorption geometry **I5** with less steric adsorbate-surface interaction than in **I3** (see Figure 3 in Section 2.1.1.).<sup>11</sup> Hydrogenation of the structurally different molecule, even by *syn*-addition, might lead to a different isomer product than the hydrogenation of the starting molecule, as presented in Scheme 7. This eventually appears as “*anti*-addition” product and results in lower stereoselectivity of the reaction. In addition, the migratory isomerization can also occur associatively *via* semihydrogenated intermediate **I6** (Scheme 6b).<sup>11</sup>

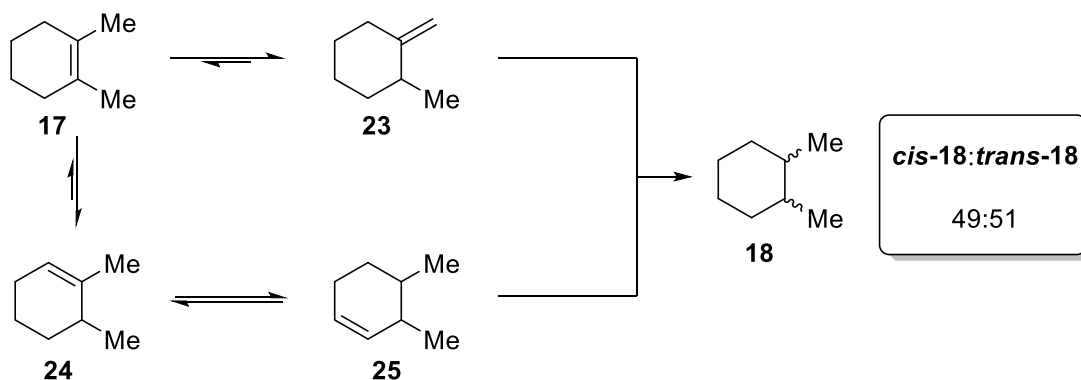
## a) Dissociative migratory isomerization of alkenes



## b) Associative migratory isomerization of alkenes



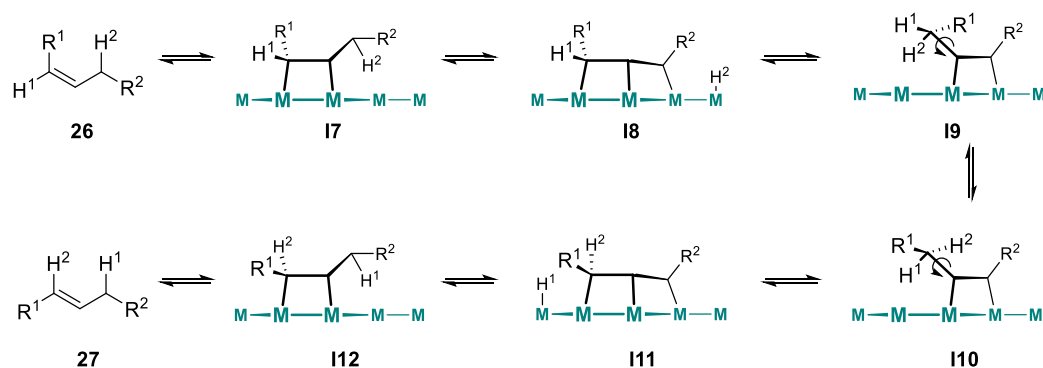
Scheme 6. a) The dissociative migratory isomerization of alkenes and b) the associative migratory isomerization of alkenes.



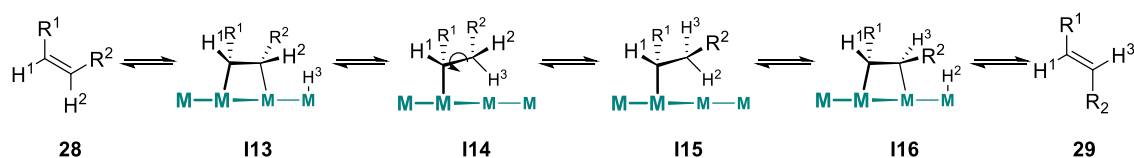
Scheme 7. Dissociative migratory isomerization during the reduction of 1,2-dimethylcyclohexene (17) with a nickel catalyst. The *cis:trans* ratio of the product 18 reflects isomer distribution obtained in the reduction of mixture of molecules 23, 24, and 25.

Alkenes can also undergo dissociative and associative *E/Z* isomerization (Scheme 8). For example, at the reductive conditions the acyclic alkenes can undergo an associative isomerization with  $\sigma$ -bond rotation at the half hydrogenated intermediate **I14** (Scheme 8b).<sup>11</sup> This leads to change in the *E:Z* ratio of the starting material and eventually to erosion in stereoselectivity of the reduction reaction. As an example, this mechanism is believed to be the main reason for the appearance of (*E*)-isomer in the semireduction of alkynes to alkenes with the heterogeneous metal catalyst (see Section 2.1.2.2).<sup>11</sup>

## a) Dissociative isomerization of alkenes



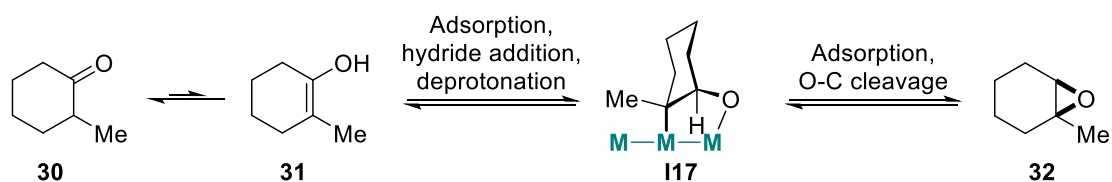
## b) Associative isomerization of alkenes



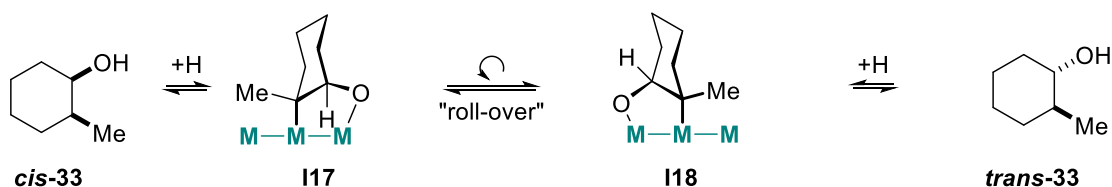
Scheme 8. a) The dissociative *E/Z* isomerization of alkenes and b) the associative *E/Z* isomerization of alkenes.

In addition to the mechanism illustrated in Schemes 6 and 8, it is possible that the isomerization occurs *via* “roll-over” mechanism.<sup>51,52,53</sup> This mechanism is especially relevant if the molecule contains oxygen. The “roll-over” mechanism is illustrated in Scheme 9 with the reduction of two different oxygen-containing compounds **30** and **32**. The hydrogenation of 2-methylcyclohexanone (**30**) and the hydrogenolysis of 1,2-epoxy-1-methylcyclohexan (**32**)<sup>54</sup> share a similar intermediate **I17** along one of the possible mechanistic pathways (Scheme 9a). In both reactions, this intermediate **I17** (Scheme 9b) can “roll over,” presumably *via* formation of alkoxide ion or alcohol (by protonation). This leads to different adsorption geometry **I18** and, eventually after the H-addition, to a different product isomer.

a)



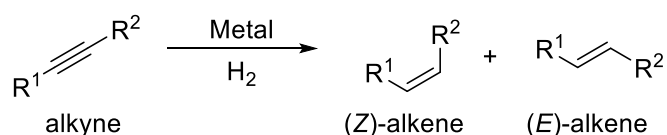
b)



Scheme 9. a) The hydrogenation of 2-methylcyclohexanone (**30**) and the hydrogenolysis of 1,2-epoxy-1-methylcyclohexane (**32**) share a similar intermediate **I17** along the possible reaction pathway. b) The intermediate **I17** can "roll over," leading to intermediate **I18**, and eventually to the opposite isomer. See the main text for more detailed discussion.

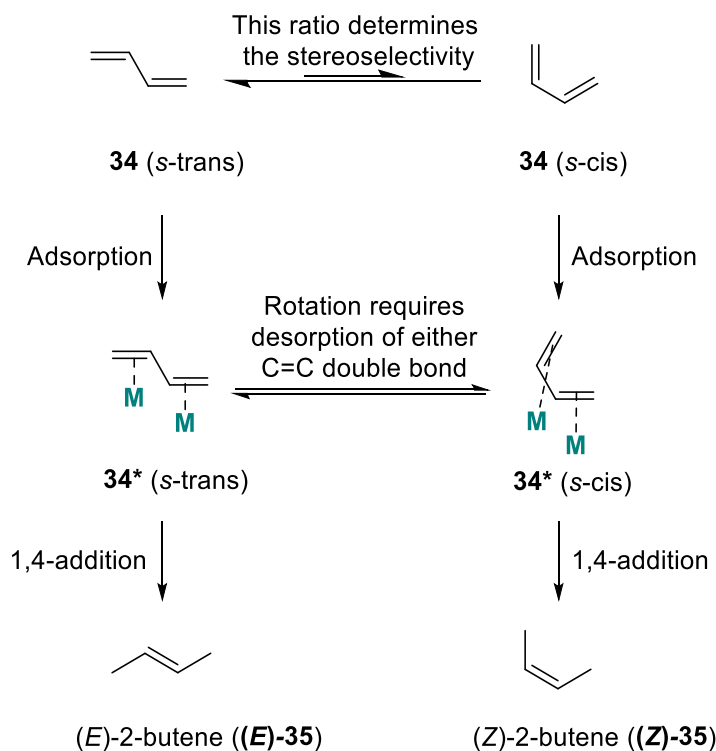
### 2.1.2.2 Stereoselective reductions of alkynes, dienes, and cumulated allens and polyenes

*E/Z*-isomeric products are obtained in selective reductions in which the product contains a C=C double bond. The most well-known example is the reduction of the C≡C triple bond to C=C double bond (Scheme 10). The (*Z*)-isomer is the main product, because the *syn*-addition occurs predominately on the metal surfaces. However, the formation of the *anti*-addition product, i.e., (*E*)-isomer, is usually observed as a minor product, as a result of *E/Z*-isomerization (Scheme 10).<sup>11</sup>



Scheme 10. The stereoselective hydrogenation of alkynes results mainly in (*Z*)-alkenes and secondarily (*E*)-alkenes.

In the semihydrogenation of conjugated double bonds, such as 1,3-butadiene (**34**), the main product is 1-butene by a 1,2-addition.<sup>55</sup> However, the formation of the side-product 2-butene (**35**) by 1,4-addition is theoretically interesting, because the newly formed monoene exists mainly as a (*E*)-isomer and only traces of (*Z*)-isomer are detected (Scheme 11).<sup>55</sup>

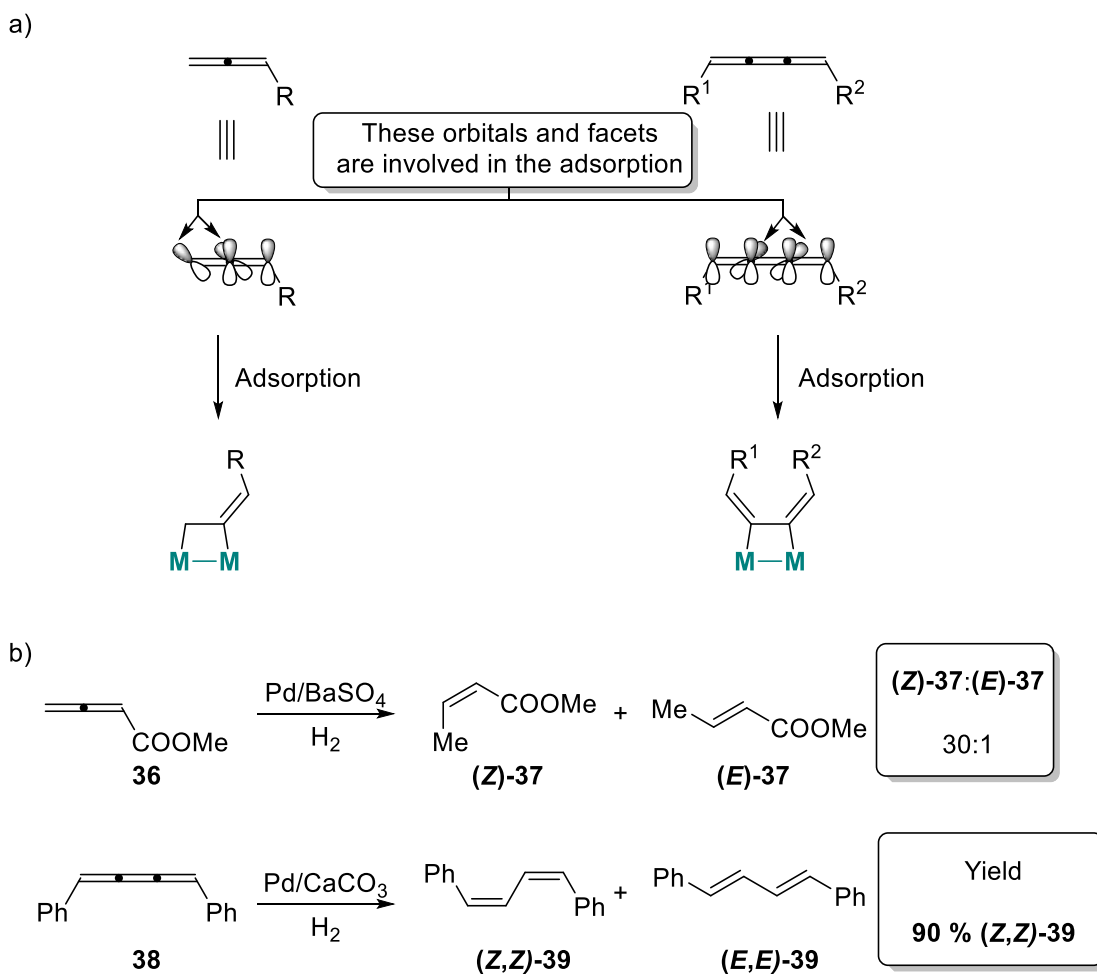


Scheme 11. Stereoselective formation of the side-product in the semihydrogenation of 1,3-butadiene (**34**).

1,3-butadiene (**34**) can exist in two rotamers *s-trans* and *s-cis*, and the *syn*-addition to these rotamers yields (*E*)- and (*Z*)-isomers, respectively. The adsorption energy difference between two rotamers is too small to explain the observed isomer distribution of the product.<sup>55</sup> In addition, the *s-trans* to *s-cis* rotation on the catalyst surface would require the desorption of either C=C double bond. However, in the experiments, the *E*:*Z* ratio of the 2-butene (**35**) was found to mimic the gas-phase ratio of two rotamers of the 1,3-butadiene (**34**).<sup>55</sup> This leads to the conclusion that the stereoselectivity of the reaction is determined by the stability of the gas-phase conformations of the starting material **34**. Similar reasoning can also explain the stereoselective 1,4-hydrosilylation of enals and enones on a palladium surface (see Article IV).

Allenes and cumulated trienes are adsorbed on the metal surface only *via* one of the C=C double bonds as a result of the  $\pi$ -orbital geometry (Scheme 12a).<sup>55</sup> The steric hindrance around the double bonds affects the binding energy, as discussed in Figure 3 in Section 2.1.1. Primarily, the allenes and cumulated trienes are adsorbed through the least hindered double bond and from the least hindered

facet of it. This selection explains why 1,2-hydrogenation of 3-substituted allenes, such as **36**, mainly produces (*Z*)-**37** (Scheme 12b).<sup>56</sup> Moreover, the cumulated trienes, such as **38**, are mainly hydrogenated to produce (*Z,Z*)-**39** (Scheme 12b).<sup>57</sup> Semihydrogenation of other cumulated polyenes proceeds analogously to the cumulated triene hydrogenation.<sup>58</sup>



### 2.1.2.3 Diastereoselective reduction of disubstituted cyclohexenes

Most of the diastereoselective reactions on metal surfaces are C=C, C=O, or C=N double bond reductions.<sup>11</sup> High diastereoselectivities can be obtained if both of the prochiral centers are presented in the reducing functionality (see Scheme 5a in Section 2.1.2.1). Moreover, if the substrates already have chiral centers in the structures, it can influence the direction from which the hydrogen addition occurs to the reducing double bond. The closer the chiral center is to the

reaction center, the more influence it will have on the selectivity. The influence is much more apparent in the case of rigid cyclic compounds than with acyclic ones. Consequently, most of the high diastereoselective reductions with heterogeneous transition metal catalysts are obtained with cyclic compounds, such as cyclohexenes.<sup>11</sup> Herein, we present a selected example of how the position of the chiral center and the size of the substituent affects the diastereoselectivity.

Cyclohexene (**40**) can adsorb on the metal surface in various conformations (Figure 4).<sup>59,60,61</sup> Although the half-chair conformation is the most stable in the solution and gas phases, experimental investigations<sup>59</sup> and DFT calculations<sup>61</sup> suggest that, for example, on the Pt(111) surface, the di- $\sigma$  bonded boat-up (Figure 4c) conformation is 12 kJ/mol more stable than the second most stable geometry chair di- $\sigma$  (Figure 4a). This has been rationalized by the steric adsorbate-surface interactions (see Figure 3 in Section 2.1.1). In the boat conformation, the bulkiest groups next to the C=C double bond (i.e. methylenes) are farthest away from the surface, and the molecule and surface are least deformed. In other words, the stabilizing energy gained from the less deformed molecule and surface overcomes the energy difference of chair and boat conformations.

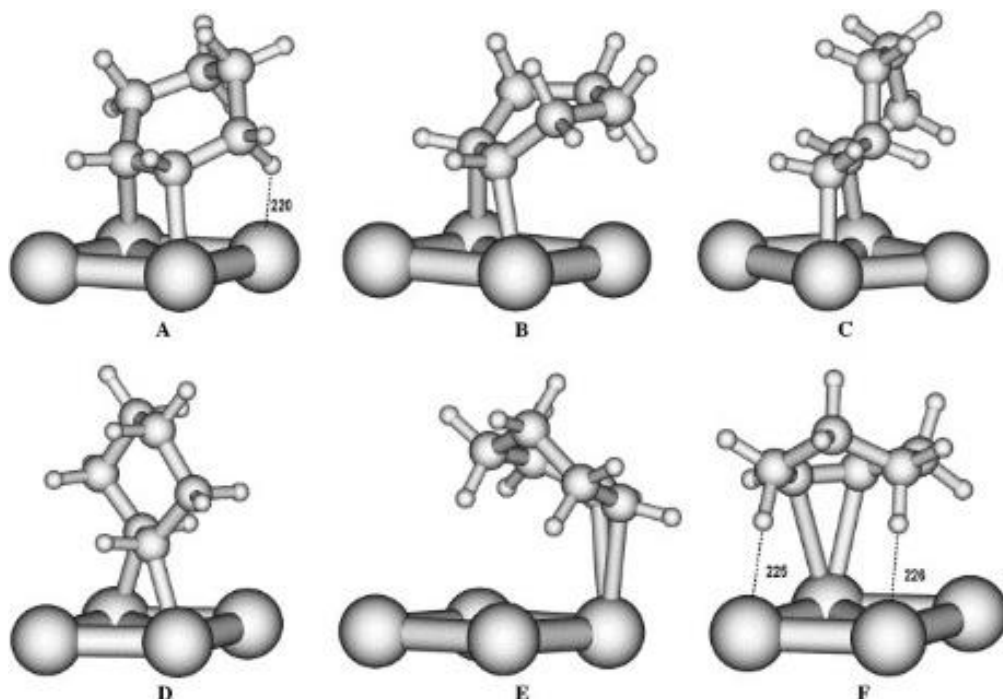
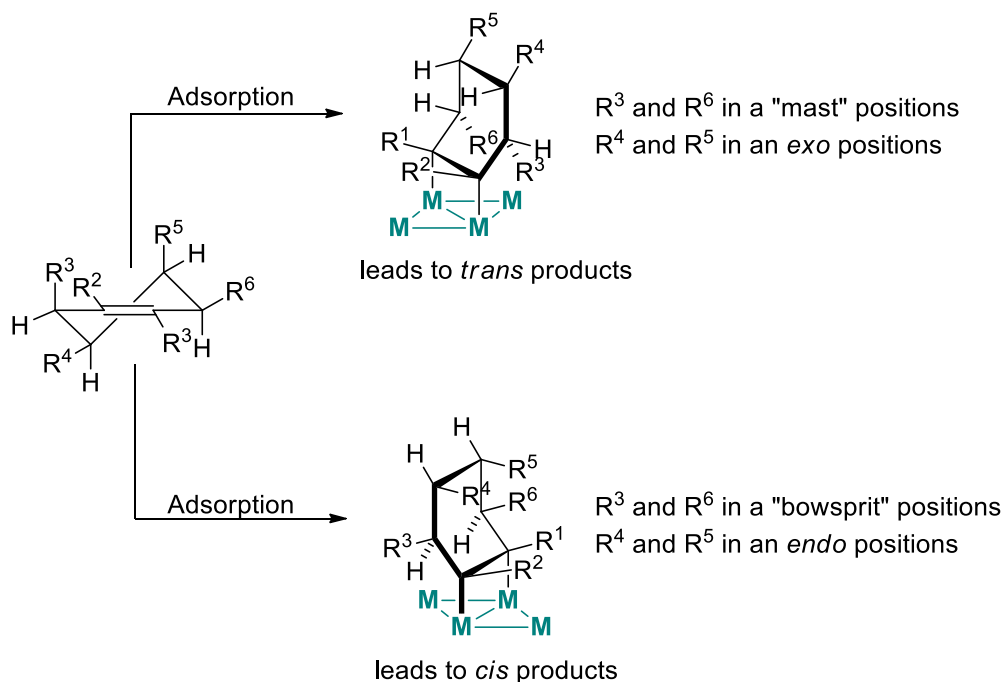


Figure 4. Different adsorption modes and calculated adsorption energies for cyclohexene (**40**) on a Pt(1 1 1) surface: a) chair di- $\sigma$ ,  $E_{\text{ads}} = -69.2$  kJ/mol, b) boat di- $\sigma$  down,  $E_{\text{ads}} = -63.8$  kJ/mol, c) boat di- $\sigma$  up,  $E_{\text{ads}} = -81.1$  kJ/mol, d) trans-di- $\sigma$ ,  $E_{\text{ads}} = -68.0$  kJ/mol, e)  $\pi$  A,  $E_{\text{ads}} = -31.9$  kJ/mol, f)  $\pi$  B,  $E_{\text{ads}} = -43.4$  kJ/mol. Adapted with permission from Saeys, M.; Reyniers, M.-F.; Neurock, M.; Marin, G. B. *Surf. Sci.* **2006**, *600*, 3121–3134. DOI: 10.1016/j.susc.2006.05.059, Copyright © 2006 Elsevier B.V. All rights reserved.

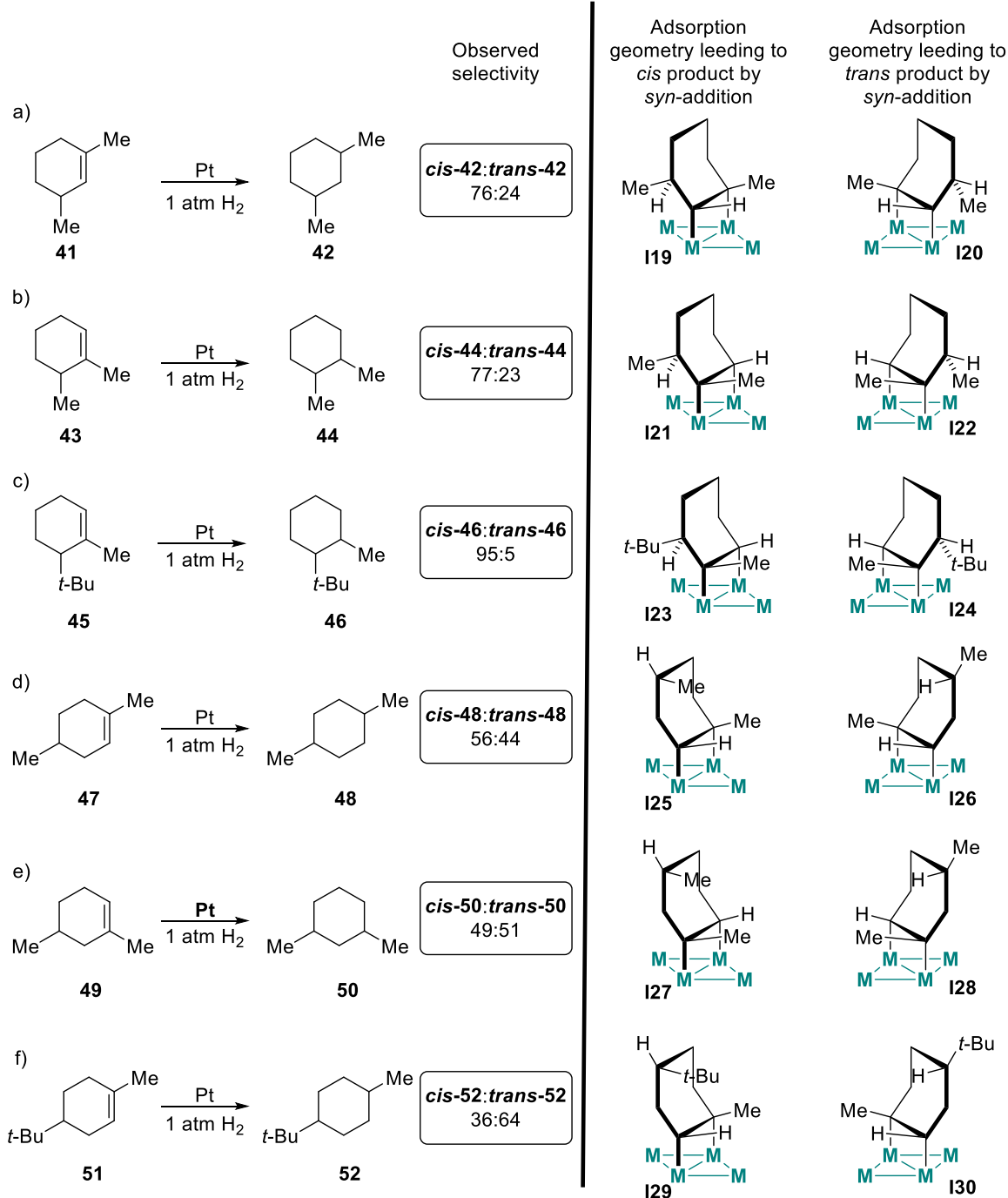
With transition metals, such as platinum, that have a low isomerization rate (see Section 2.1.2.1), the observed diastereoselectivities of the reduction of substituted cyclohexenes can be rationalized with the most stable adsorption geometry. Generally, the substituted cyclohexenes can adsorb onto the metal surface, as boat-up conformation, from two different faces of the C=C double bond (Scheme 13).<sup>62</sup> The substituents R<sup>3</sup> and R<sup>6</sup> can adapt either a “bowsprit” or a “mast” position, and the substituents R<sup>4</sup> and R<sup>5</sup> can adapt either an *endo* or an *exo* position in the boat-up conformation.



Scheme 13. Two possible adsorption geometries of substituted cyclohexenes as a boat-up conformation.

The substituents  $R^3$  and  $R^6$  in Scheme 13 prefer to adapt the “bowsprit” position, in which it faces outward from the molecule itself and is tilted away from the surface. In the “mast” position, the substituent would experience steric hindrance from the other “mast” position and from the metal surface (the interaction with the surface can be envisioned better from Figure 4c). In general, larger substituents in the  $R^3$  or  $R^6$  positionw lead to better diastereoselectivities (Schemes 14a–c).<sup>62,63</sup>

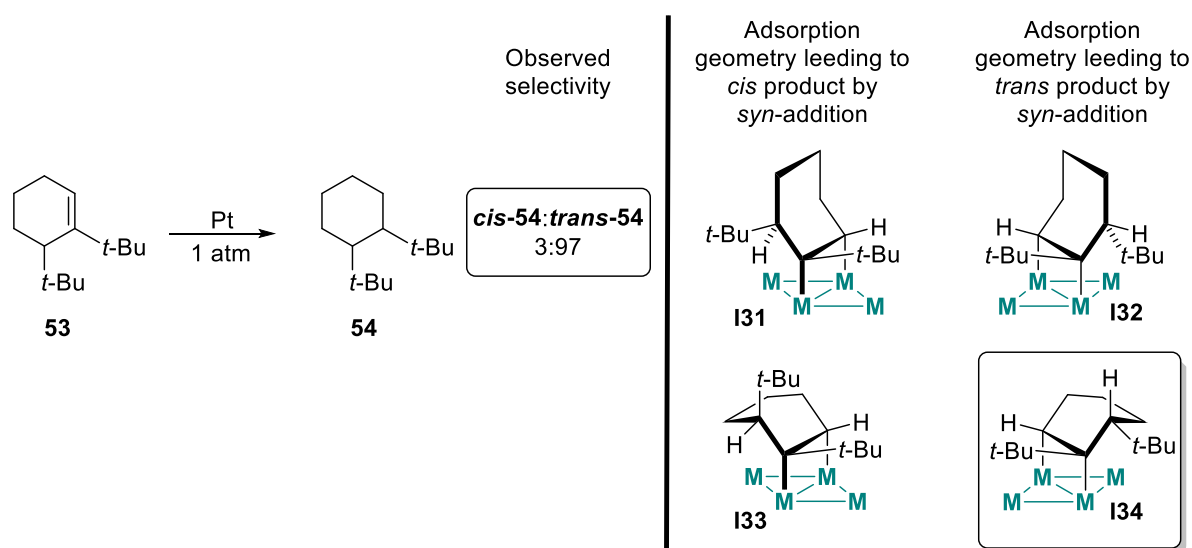
The  $R^4$  and  $R^6$  have only minor influence on the stereoselectivity, because the substituent can rather easily (i.e., without a large difference in steric hindrance) adopt either an *exo* or *endo* position (Schemes 14d and 14e).<sup>62</sup> More of *trans* isomer is observed with the 2,4-disubstituted **49** than with 1,4-disubstituted cyclohexene **47**. The steric interaction of the 4-methyl substituent in the *endo* position with the 2-methyl (Scheme 14e) substituent is higher than with the 1-methyl substituent (Scheme 14d). Changing the methyl substituent to *t*-butyl in the  $R^4$  position drives the selectivity further to the *trans* product, but with only moderate diastereoselectivity (Scheme 14f).<sup>62</sup>



Scheme 14. Hydrogenation of several disubstituted cyclohexenes on Pt-catalyst, and adsorption geometry-based rationalization for the observed diastereoselectivity.

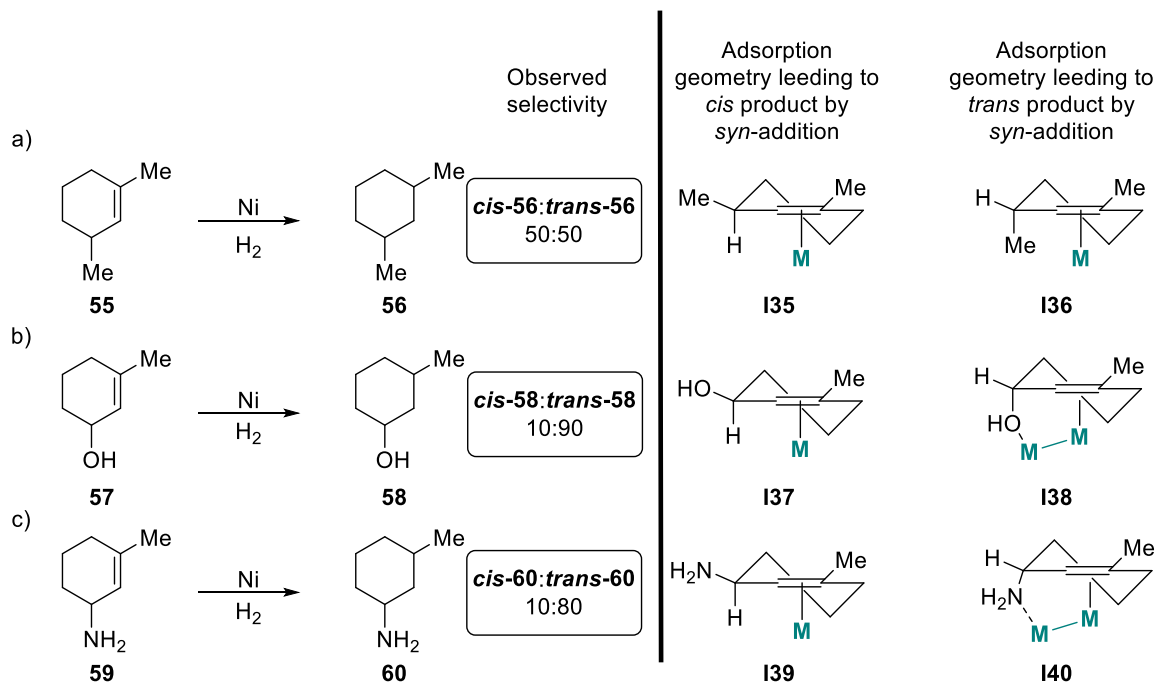
The above analysis is not universal for each substituted cyclohexene, and with every molecule all of the conformation should be considered when one tries to understand the observed selectivities. For example, in the case of 2,3-di-*t*-butylcyclohexene (**53**), a boat-down adsorption geometry (Figure 4b) explains the observed diastereoselectivity of the reduction reaction (Scheme 15).<sup>64</sup> In the boat-

up adsorption geometry (Figure 4c), the *t*-butyl group at the “bowsprit” position would experience a high torsional angle strain with the R<sup>2</sup>-*t*-butyl. Moreover, at the “mast” position, the bulky *t*-butyl would experience high steric interactions with the surface. Consequently, the most stable adsorption geometry is boat down, in which the methylene-group of the cyclohexene skeleton is at the “mast” position, and the *t*-butyl group is tilting away from the molecule at “bowsprit” position (**I34** in Scheme 15).<sup>64</sup>



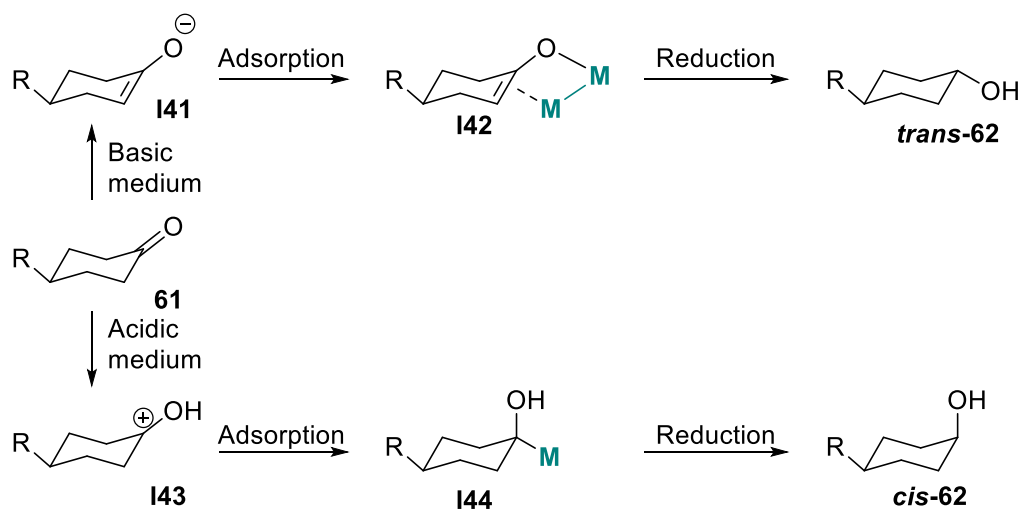
Scheme 15. Hydrogenation of the 2,3-di-*t*-butylcyclohexene (**53**), and the adsorption geometry-based rationalization for the observed diastereoselectivity. The adsorption geometry **I34** that explains the obtained diastereoselectivity is highlighted.

In addition to the above exception, some functional groups, such as hydroxyl, ether, amine groups, and carboxylic acids, can interact with the surface and assist the substrate to a certain conformation.<sup>11</sup> This is especially significant with Ni catalyst, which has a strong affinity for oxygen and nitrogen.<sup>65</sup> The anchoring effect of the hydroxyl and amine group on the diastereoselectivity is illustrated in Scheme 16.<sup>49,65,66</sup> It should be noted that nickel catalysts also readily promote the isomerization of the substrate, which affects the isomer distribution presented in Scheme 16a.<sup>11</sup>



Scheme 16. Hydrogenation of the 1,3-disubstituted cyclohexenes with the nickel catalyst, and the adsorption geometry-based rationalization for the observed diastereoselectivity.

As mentioned at the beginning of the section, the structural/conformational factors affecting the selectivity are very similar to the reduction of C=C and C=O double bonds. A similar adsorption structures, as in the reduction of the C=C double bond, can also be found along the reaction pathway of reduction of substituted cyclohexanones (Scheme 17).<sup>67</sup>



Scheme 17. The simplified reaction mechanism of the hydrogenation of the 4-cyclohexanone (**61**) in basic and acidic mediums. The medium affects the adsorption geometry of the molecule and the diastereoselectivity of the reaction.

## 2.2 Organic modifiers that interact with the substrate

In this chapter, we discuss only the organic modifiers that interact with the substrates and assist them to certain conformations/orientations on the surface to enable selective reduction. Most of the published data, mainly patents, contain organic modifiers that act as promoters, poisons, or traps for the desired product.<sup>36</sup> Promoters are modifiers that increase the activity of the catalyst, and poisons are modifiers that decrease the activity, both by changing the catalyst redox potential.<sup>68</sup> In addition, poisons may be used to block the undesired sites of the catalyst. A classic example of such a poison is the addition of quinoline during the hydrogenation of alkynes to alkenes with Lindlar catalyst.<sup>69</sup> Quinoline acts as an electron donor to the metal particle, which inhibits the alkene interaction. Additionally, it also inhibits the oligomerization reaction by competing with alkyne for the adsorption sites. The large size of the quinolone leaves isolated small ensembles on the metal surface, in which only a single alkyne can adsorb and further react.<sup>69</sup> An example of using organic modifiers as a trap is adding acetic anhydride to the reaction mixture in the reduction of nitriles. The acetic anhydride trap the primary amines as an amide and prevent the further reactions to secondary amine.<sup>70</sup>

The organic modifiers discussed herein are the ones that interact with the substrate by weak interactions, by inducing steric hindrance, or by covalently bonding to the substrate. These interactions assist the substrates to certain conformations/orientations and enable either chemo- or stereoselective reductions on the transition metal particle. The most studied class of this type of organic modifiers are cinchona alkaloids and their derivatives,<sup>71,72,73,74,75,76,77,78,79,80,81</sup> and the latest are self-assembled monolayers (SAMs).<sup>82</sup>

### 2.2.1 Cinchona alkaloids and their derivatives

An intensively studied class of organic modifiers that interact with the reactants in heterogeneous catalysis are cinchona alkaloids (Figure 5).<sup>73,74,76,77</sup>

These modifiers adsorb onto the metal (usually Pt or Pd) surface and form chiral sites, enabling the reactant to be hydrogenated in an enantioselective manner. In the chiral sites, the other enantioface of the prochiral substrate is usually favored only by the energy difference of a few kJ/mol.<sup>77</sup> However, a precise mechanism of the system is difficult to determine, because the heterogeneous metal catalyst has atoms with different coordinations. In other words, the enantiodifferentiating sites may not be uniform and there could be several different types of active sites. The energy difference between the pathways leading to two enantiomers may vary or even reverse in different sites. Additionally, some of the sites may remain unmodified, which leads to racemic reaction pathways.<sup>75,77</sup>



	R <sup>1</sup>	R <sup>2</sup>	R <sup>3</sup>		R <sup>1</sup>	R <sup>2</sup>	R <sup>3</sup>
Cinchonidine ( <b>63</b> )	H	vinyl	H	Cinchonine ( <b>68</b> )	H	vinyl	H
Quinine ( <b>64</b> )	H	vinyl	OMe	Quinidine ( <b>69</b> )	H	vinyl	OMe
MeOCD <b>65</b>	Me	vinyl	H				
HCD <b>66</b>	H	vinyl	H				
MeOHCD <b>67</b>	Me	vinyl	H				

Figure 5. The list of natural cinchona alkaloids used as organic modifiers in heterogeneous catalysis.

Despite the difficulties in determining the active site structures, numerous systematic studies have been carried out for the requirements of cinchona alkaloid-modified catalyst systems.<sup>71,72,75,83</sup> These studies have generated the collection of natural alkaloids derivatives and structurally simpler synthetic modifiers that mimic the properties of cinchona alkaloids (Figure 6).<sup>78,79,80,81</sup> However, the natural cinchona alkaloids are still the most versatile, and in most cases the most selective, modifiers that exist.<sup>75,77</sup>

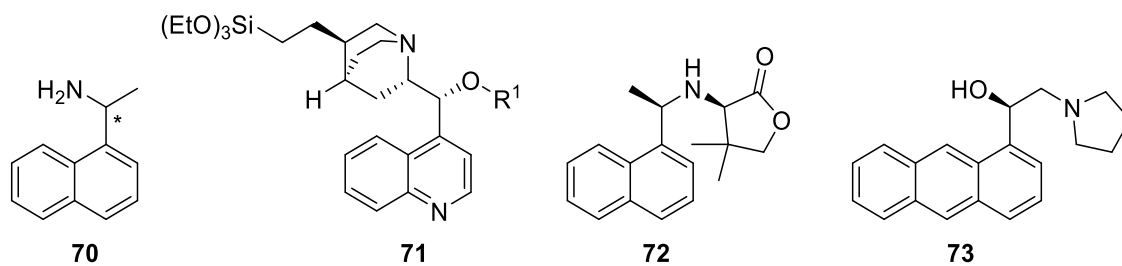
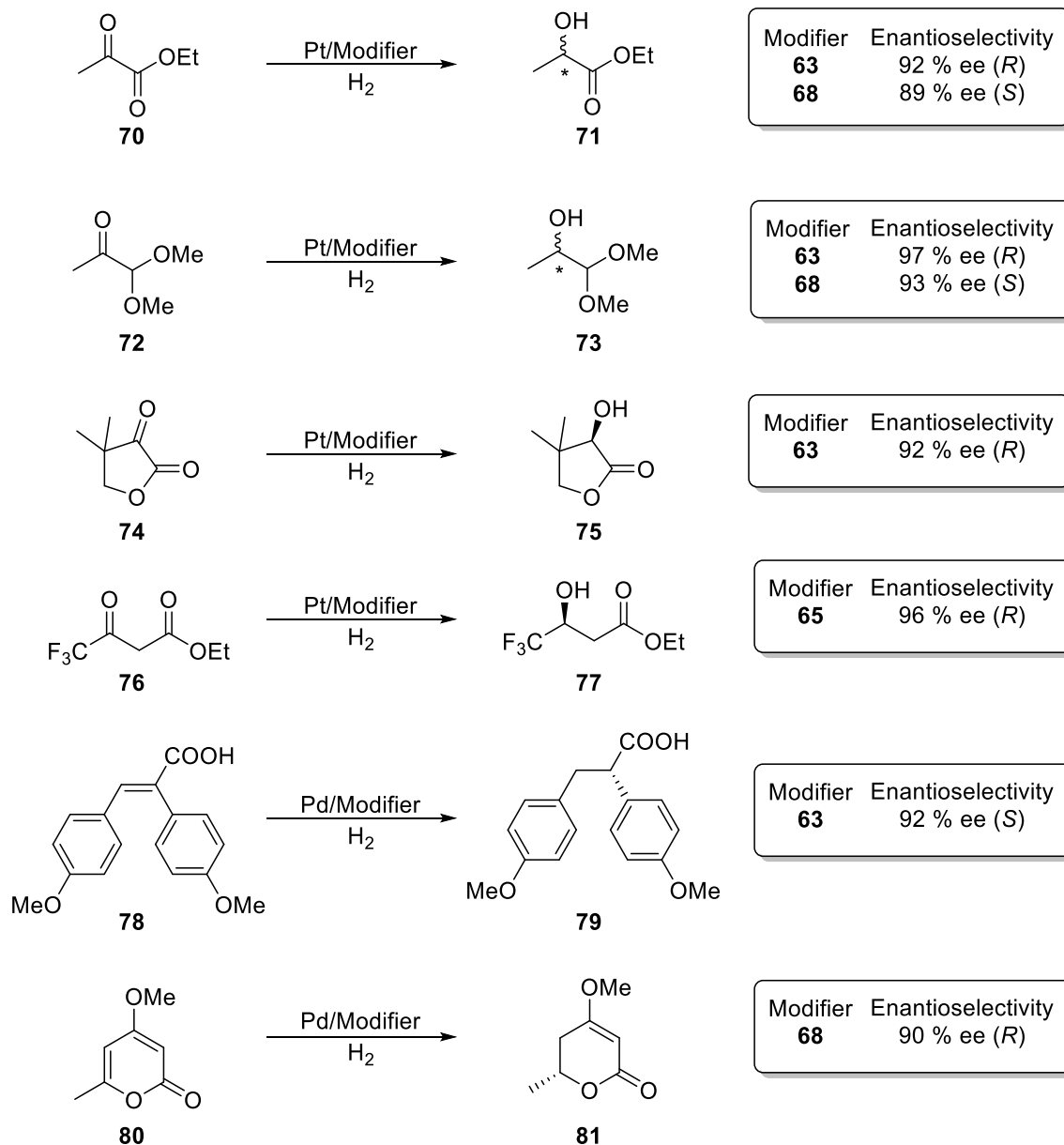


Figure 6. Selected synthetic cinchona-mimics used as organic modifiers.

In general, cinchona-platinum systems are commonly used to reduce  $\text{C}=\text{O}$  double bonds and the cinchona-palladium systems are used to reduce  $\alpha$ -functionalized  $\text{C}=\text{C}$  double bonds. Scheme 18 presents selected examples of the substrates that give high  $ee$ 's with cinchona-platinum<sup>84,85,86,87,88</sup> and -palladium systems.<sup>89,90</sup>



Scheme 18. Selected examples of enantioselective hydrogenations with cinchona modifiers.

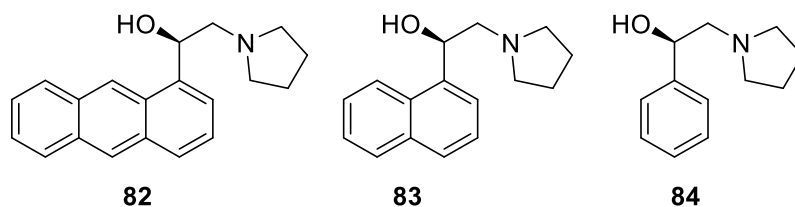
### 2.2.1.1 Requirements for cinchona alkaloid modifiers

The basic requirements for the cinchona alkaloid modifier are (i) an anchor that adsorbs to the metal surface, (ii) an amine functionality that interacts with the carbonyl group, and (iii) a stereogenic center or centers that induces the enantioselectivity to the reduction reaction.<sup>75,77</sup>

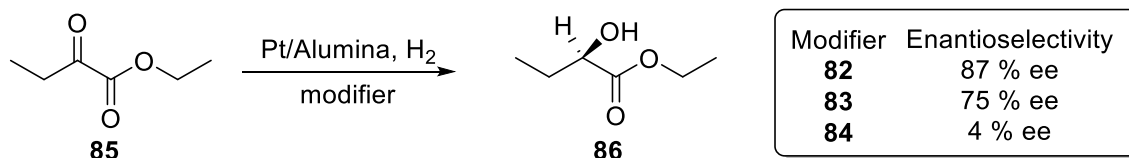
(i) The purpose of the anchor group is to adsorb on the metal particle and form a chiral site where the enantioselective reaction can occur. The anchor needs to cover the surface to ensure that only chiral sites are present during the reaction.

If the anchor is only weakly adsorbed to the metal particle, racemic sites, i.e., not modified sites, are also present during the reaction. This may lead to poor enantioselectivity. However, too-strong adsorption leads to the complete coverage of the metal particle with the modifier, and consequently to inhibition of the reaction. The anchor is usually an aromatic ring, and the most suitable groups found in the experiments are quinoline, naphthalene, and anthracene.<sup>77</sup> Smaller anchors, such as benzene, pyridine, or aromatic systems that are not flat, show no or very low chiral induction.<sup>77</sup> An example of the size effect of the anchor group on the enantioselectivity is presented in Scheme 19.<sup>80,91,92</sup>

a)



b)



Scheme 19. a) Three similar modifiers with different anchor groups. b) Size of the anchor group affects the enantioselectivity in the hydrogenation of ethyl pyruvate with Pt/alumina.

(ii) The interaction with the amine and the carbonyl group of the reactant is crucial for the enantiodifferentiation. The surface complex (1:1 substrate:modifier) formed *via* hydrogen bonding (N-H $\cdots$ O) between the protonated *N*-atom of the modifier amine group and *O*-atom of the reactant carbonyl group is one of the proposed interaction modes. In addition, other hydrogen bonds can also be involved with the interaction between substrate and modifier. However, these interactions depend on the substrate, modifier, and reaction conditions. The possible interaction modes are discussed in more detail in the next section.

(iii) The strongest influencing factor on the enantioselectivity with cinchona alkaloids is the steric environment on the O-C9-C8-N part (Figure 5). In recent theoretical studies of the reduction of carbonyl compounds on the platinum surface, the absolute configuration of the product was found to depend on the configuration of the C8. The C9 position was less influential and only affected the rate and enantiomeric excess, even if the absolute configuration of the C9 was changed.<sup>93</sup> In palladium-catalyzed hydrogenation of olefins, the enantiodifferentiation is more sensitive, and only a right combination of the C8 and C9 configurations has found to lead good enantioselectivities.<sup>93</sup>

### 2.2.1.2 Origin of enantioselectivity

While the requirements for the modifier are rather simple to understand, to be able to design an efficient and robust modifier with a large substrate scope is a demanding task. A rational design of new modifiers needs a full understanding of the mechanism on the metal particle. However, the chosen metal, different sites in the catalyst, support, hydrogen pressure, and solvent all have effects on the mechanism and outcome of the reaction.<sup>75,77</sup> Consequently, most of the cinchona systems are very specific and resemble the lock-and-key interaction of enzymatic catalysis.<sup>77</sup> For example, cinchonidine (**63**) is generally the best modifier with platinum; however, with nickel and ruthenium, it is more or less ineffective.<sup>71,94</sup>

Most of the mechanistic studies have been done on the reduction of activated ketones with cinchonidine (**63**) modified platinum surface.<sup>77</sup> Through the years, a variety of different mechanisms have been proposed for the enantiodifferentiating interaction at the chiral site (Figure 7).<sup>95,96,97,98</sup> Some of the models assume a N-C (Figure 7a and 7b) and others a N-H...O (Figure 7c and 7d) type interaction. Lately, it has been shown that the proton in the N-H...O type interaction originates either from protonation (protic solvents) or from dissociatively adsorbed H<sub>2</sub> (aprotic solvents).<sup>99,100</sup> Nevertheless, *N*-alkylation of the amine group leads to a complete loss of the enantioselectivity.<sup>71,72</sup>

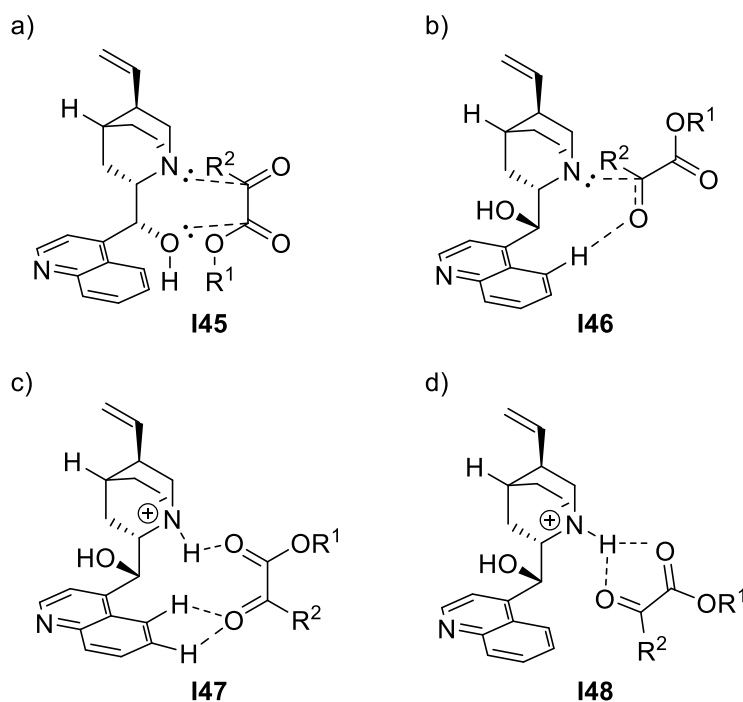
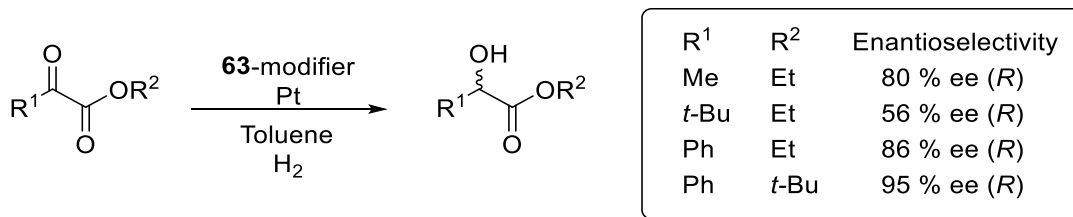


Figure 7. Different mechanisms proposed for the modifier-substrate interaction on cinchonidine (**63**) modified Pt surface: a) by Bartók **I45**, b) by Augustine **I46**, c) by McBreen **I47**, and d) by Baiker **I48**.

Only a few studies have attempted to explain the preferred adsorption of the *re* or *si* face of the reacting ketone.<sup>75,77</sup> The most recent studies show that the directing effect is a combination of steric and electronics.<sup>101,102</sup> However, the steric effects have a lesser role, because the outcome of the reaction seems to be independent of the relative hindrance of the substituents (Scheme 20).<sup>101,102</sup> The dominant effect that determines the energy difference of the *re* and *si* face is believed to be an asymmetric electron distribution in the reducing carbonyl group (Figure 8). This asymmetry directs the substrate to adsorb from the other face and ultimately leads to enantioselective reduction on the surface.<sup>102</sup> With very rough DFT calculations without the metal slab, the Pro(*R*) complex was found to be 0.5 kcal/mol lower in energy than the Pro(*S*) complex (Figure 9).<sup>102</sup> The calculated energy difference is believed to originate from the charge-dipole interaction.



Scheme 20. The relative size of the substituents does not affect the absolute configuration in the hydrogenation of  $\alpha$ -ketoesters with Pt and cinchona alkaloid **63**.

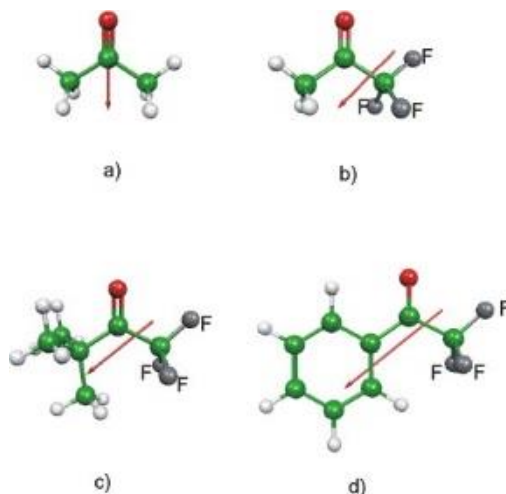


Figure 8. Calculated dipole moments (vectors) of several of ketones and trifluoroacetophenone. In prochiral fluorinated ketones the vector of the dipole moment strongly deviates from the axis of the keto-carbonyl group. Adapted with permission from Vargas, A.; Hoxha, F.; Bonalumi, N.; Mallat, T.; Baiker, A. *J. Catal.* **2006**, *240*, 203–212. DOI: 10.1016/j.jcat.2006.03.022, Copyright © 2006 Elsevier Inc. All rights reserved.

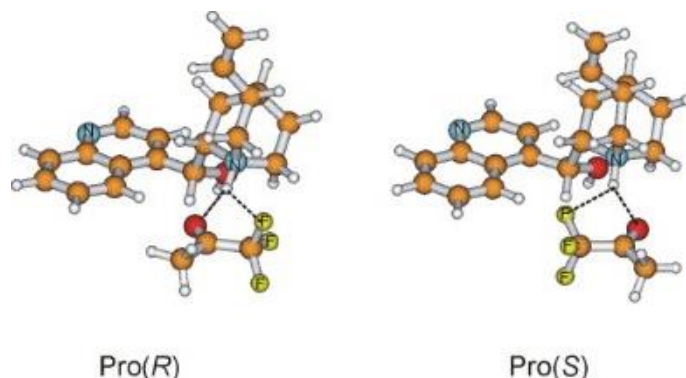
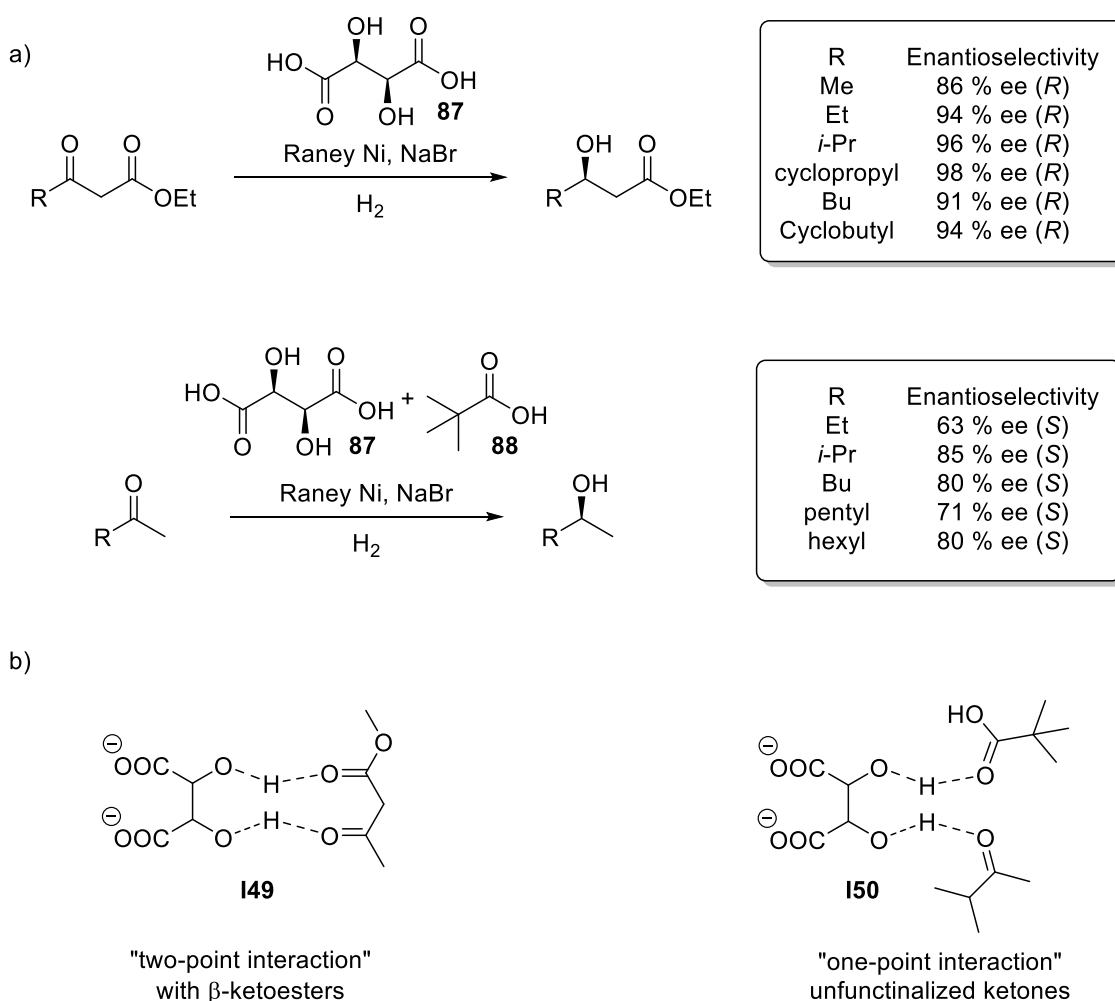


Figure 9. The interaction model between cinchonidine (**63**) and trifluoroacetone using surface constraints to force the quinoline ring and the ketone to be coplanar. Adapted with permission from Vargas, A.; Hoxha, F.; Bonalumi, N.; Mallat, T.; Baiker, A. *J. Catal.* **2006**, *240*, 203–212. DOI: 10.1016/j.jcat.2006.03.022, Copyright © 2006 Elsevier Inc. All rights reserved.

## 2.2.2 Other organic modifiers

In addition to cinchona alkaloids and their derivatives, other modifiers have also been successfully used in enantioselective reductions with heterogeneous transition metal catalysis.<sup>75</sup> For example, Raney nickel–tartaric acid–NaBr system

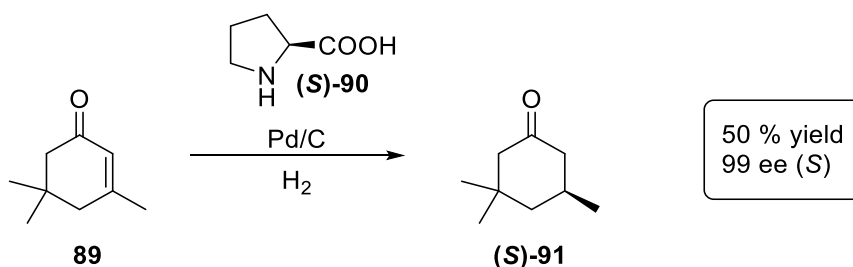
gives high enantioselectivities in reduction of  $\beta$ -ketoesters and unfunctionalized ketones to alcohols (Scheme 21a).<sup>103</sup> The origin of the enantiodifferentiation is much more complicated and less understood than with cinchona alkaloids. However, with  $\beta$ -ketoesters, the enantioselection is believed to originate from the "two-point interaction" (**I49**), and with unfunctionalized ketones, from "one-point interaction" (**I50**) with the assistance pivalic acid (**88**) (Scheme 21b).<sup>104</sup>



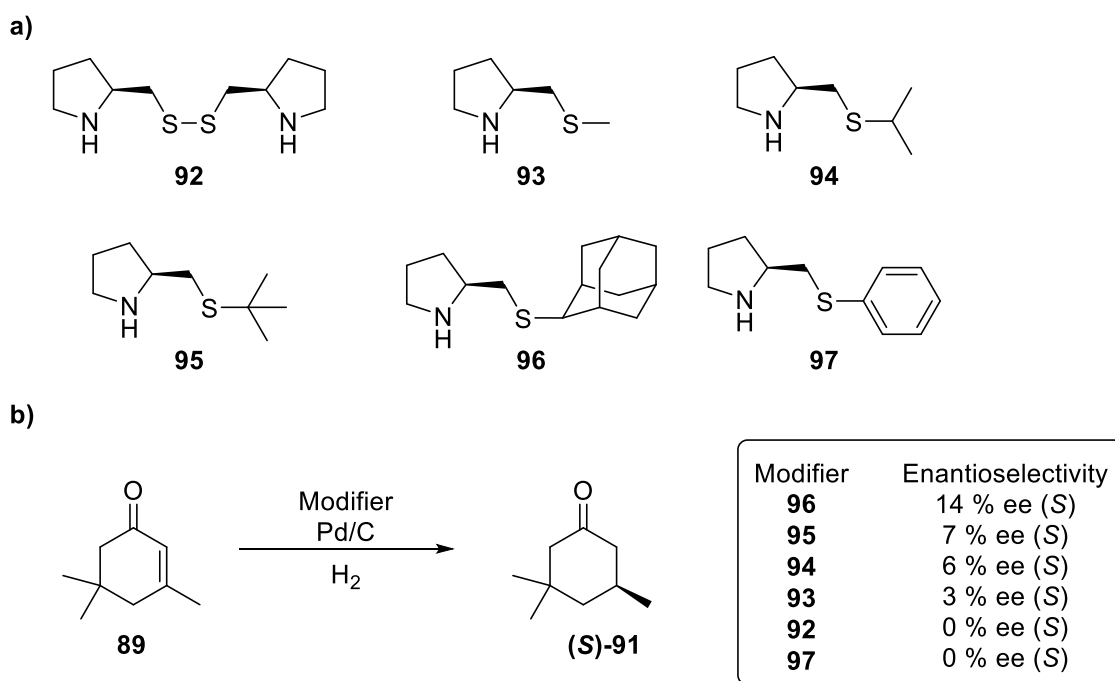
Scheme 21. The selected examples of enantioselective reductions with Raney nickel–tartaric acid–NaBr system: a) reduction of  $\beta$ -ketoesters and unfunctionalized ketones and b) proposed interaction for the enantiodifferentiation.

The other example is the use of proline derivatives in the reduction of isophorone (**89**) with heterogeneous palladium (Scheme 22).<sup>105,106</sup> In this reaction, the proline (**90**) acts as a chiral auxiliary that forms a precomplex with the reactant. This precomplex is further hydrogenated in an enantioselective manner on the metal particle. Recent studies have shown that under certain reaction

conditions, the enantiomeric excess originates from the chiral resolution after the hydrogenation.<sup>107,108</sup> In other words, the enantiodifferentiation is not completely surface mediated. Nevertheless, later studies have led to the development of proline derivatives possessing a thio-group anchor that forms a covalent bond with the metal catalyst (Scheme 23).<sup>109</sup>



Scheme 22. Enantioselective reduction of isophorone (**89**) with Pd catalyst and (*S*)-proline modifier (**90**).



Scheme 23. The enantioselective reduction of isophorone (**89**) with thio-group anchored proline derivatives as modifiers for Pd/C: a) List of thio-group anchored proline derivatives and b) their use in the enantioselective reduction of isophorone.

Although currently the enantioselectivities of these reductions are only moderate, the concept of covalently anchoring a modifier onto the metal surface is new and interesting, and it has also been extended to cinchona alkaloid derivatives.<sup>110</sup> The benefit of the system is that now the catalytic system is completely heterogeneous and no further separation is needed, as in the case of

traditional solution-phase modification. The disadvantage is that both of the C-S bonds can dissociate rather easily on the metal catalyst. Consequently, the modifier binds more strongly to the catalyst, which in this case leads to the inhibition of the catalyst (see Sabatier principle in Section 2.1.1) and the formation of a self-assembled monolayer.<sup>109,110</sup>

### 2.2.3 Self-assembled monolayers (SAMs)

In contrast to the previous examples, in which the organic modifiers were added to the reaction mixture, an alternative method of enhancing the selectivity of the heterogeneously catalyzed reduction reactions is to pretreat the metal catalyst with covalently bonding organic modifiers to form a self-assembled monolayer (SAM).<sup>82</sup> Traditionally, SAMs have been used as sensors or etch resists, or to stabilize nanoparticles.<sup>82</sup> However, the use of SAMs as catalyst modifiers is a rather new research area.<sup>111,112</sup>

At the moment, SAMs have been successfully used to induce steric hindrance onto the metal particles in catalytic reductions. The steric hindrance affects the geometry/orientation in which the reactant can approach the metal surface. For example, with the unmodified heterogeneous Pd-catalyst, the chemoselective reduction of 1-epoxy-3-butene (**98**) to 1-epoxybutane (**99**) produces only 11 % of the desired product.<sup>113</sup> However, with the SAM-modified catalyst (Figure 10), the reaction selectivity towards the 1-epoxybutane (**99**) jumps up to 94 % (Scheme 24). The reason for the increased chemoselectivity is that SAMs induce steric hindrance on the surface and decrease the ensemble-adjusted surface atoms. Consequently, the 1-epoxy-3-butene (**98**) interacts and adsorbs only *via* the C=C double bond (**I53**) to the surface. Eventually, only the C=C double bond is reduced and the epoxy group remains unreduced (Scheme 24).<sup>114</sup>

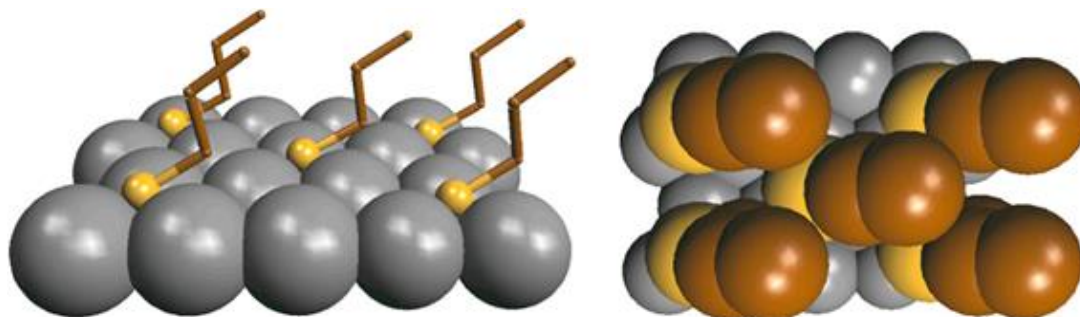
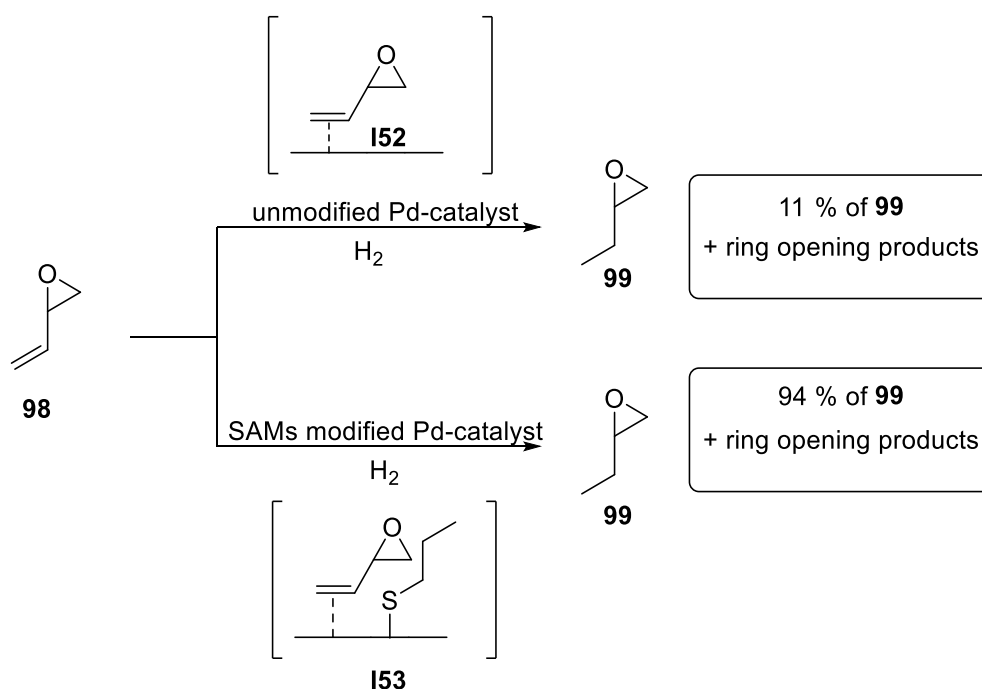
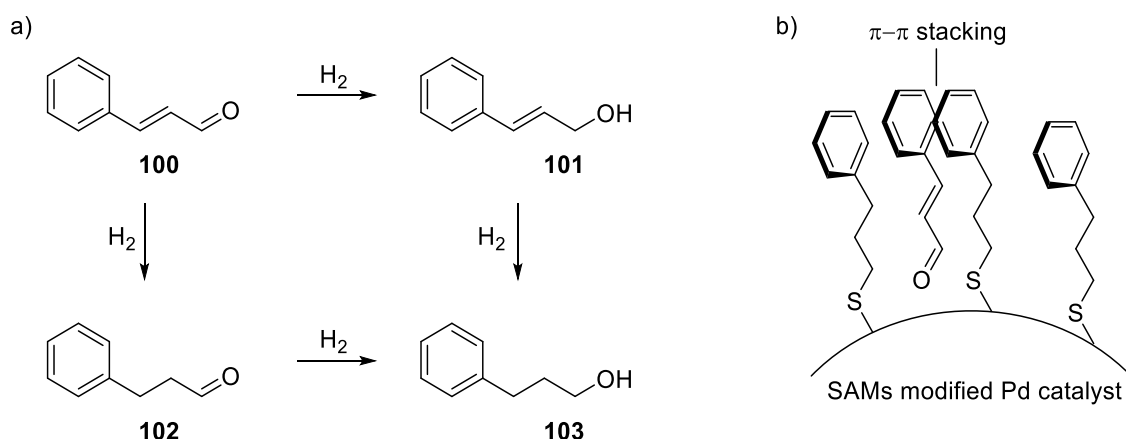


Figure 10. An example of a SAMs-modified surface. Adapted with permission from Marshall, S. T.; O'Brien, M.; Oetter, B.; Corpuz, A.; Richards, R. M.; Schwartz, D. K.; Medlin, J. W. *Nat. Mater.* **2010**, *9*, 853–858. DOI: 10.1038/nmat2849, Copyright © 2010, Rights Managed by Nature Publishing Group.



Scheme 24. Chemoselective reduction of 1-epoxy-3-butene (**98**) to 1-epoxybutane (**99**) with unmodified and SAMs-modified Pd-catalyst. Steric hindrance induced by SAMs prevents the epoxy-group from interacting with the Pd surface.

Another example of using SAMs to enhance the chemoselectivity is the reduction of cinnamaldehyde (**100**) to cinnamyl alcohol (**101**) with heterogeneous Pt-catalyst (Scheme 25a). On the unmodified platinum surface, the cinnamaldehyde (**100**) favors adsorption *via* the C=C double bond.<sup>115</sup> This leads predominately to C=C double bond reduction as discussed in Section 2.1.1, and cinnamyl alcohol (**101**) is obtained with only 25 % selectivity. However, when the Pt catalyst is modified with SAM of 3-phenyl-1-propanethiol **I59**, the cinnamyl alcohol (**101**) obtained is over 90 % selectivity.<sup>116</sup>



Scheme 25. a) Three products of the hydrogenation of cinnamaldehyde (**100**) and b) effect of SAMs on the geometry/orientation of the cinnamaldehyde molecule on the surface of palladium metal.

The reason for such a drastic change in the chemoselectivity can be rationalized similarly as in the previous example: the SAMs lower the number of an ensemble and the adjusted surface atoms. In this case, the adsorption *via* the C=C double bond becomes less favorable. Additionally, the chemoselectivity is further increased with non-covalent interaction ( $\pi$ - $\pi$  stacking) between the reactant and a SAM (Scheme 25b).<sup>116</sup> The  $\pi$ - $\pi$  stacking holds the C=C double bond away from the surface, which prevents it from the reduction. The effectiveness of the non-covalent interaction is illustrated by varying the length of the SAMs alkyl chain. The best selectivity was obtained with SAM of 3-phenyl-1-propanethiol **I59**, which is roughly the same size as the cinnamaldehyde (**100**) (Figure 11).<sup>116</sup>

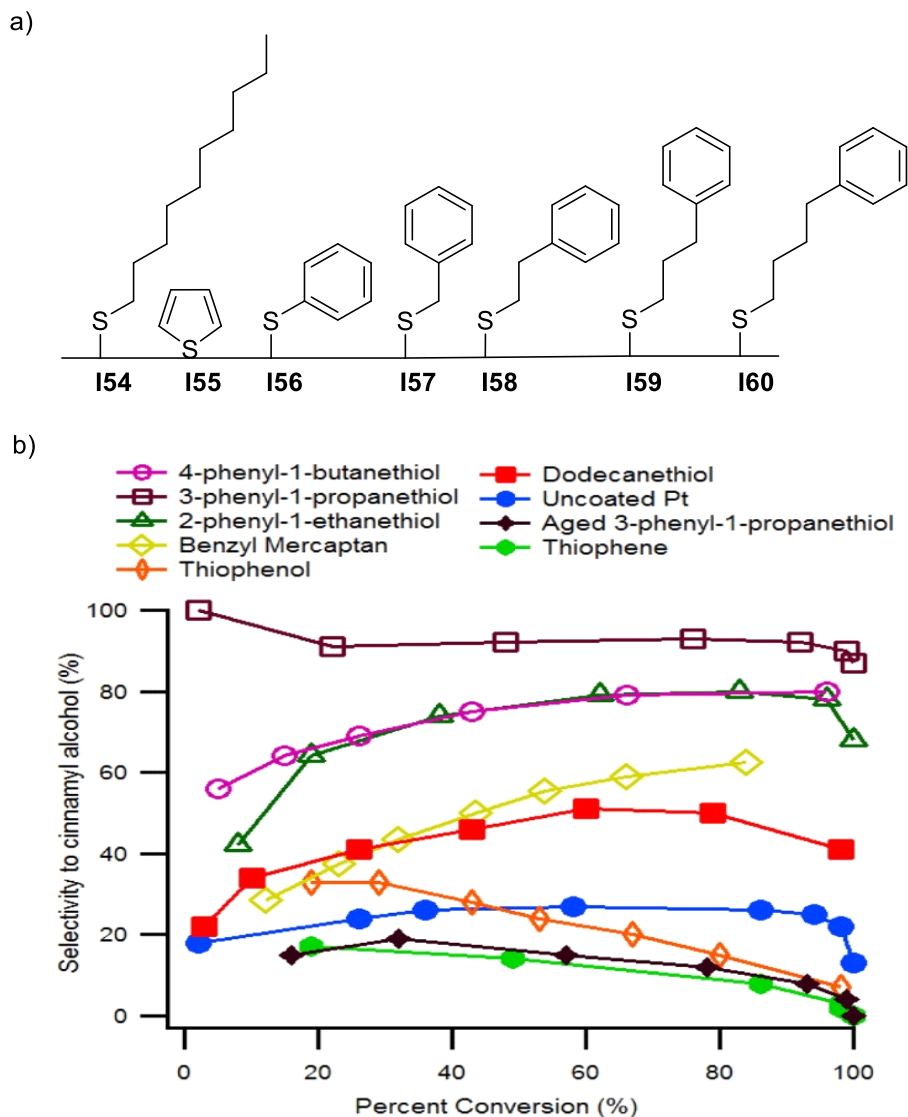


Figure 11. a) A list of different SAMs explored in the chemoselective reduction of cinnamaldehyde (**100**) and b) selectivity to cinnamyl alcohol (**101**) for the hydrogenation of cinnamaldehyde over Pt/Al<sub>2</sub>O<sub>3</sub> catalysts with different SAMs. Figure 11b adapted with permission from Kahsar, K. R.; Schwartz, D. K.; Medlin, J. W. *J. Am. Chem. Soc.* **2014**, *136*, 520–526. DOI: 10.1021/ja411973p, Copyright © 2014, American Chemical Society

## 2.3 Conclusions

As has been presented in the above pages, the reduction reactions with heterogeneous transition metals catalysts can be used to synthesize complex molecules in chemo-, regio-, and stereoselective manners. The tools available for selective reductions are extensive, such as catalyst morphology, inorganic modifiers, supporters, alloying, and organic modifiers. However, due to the

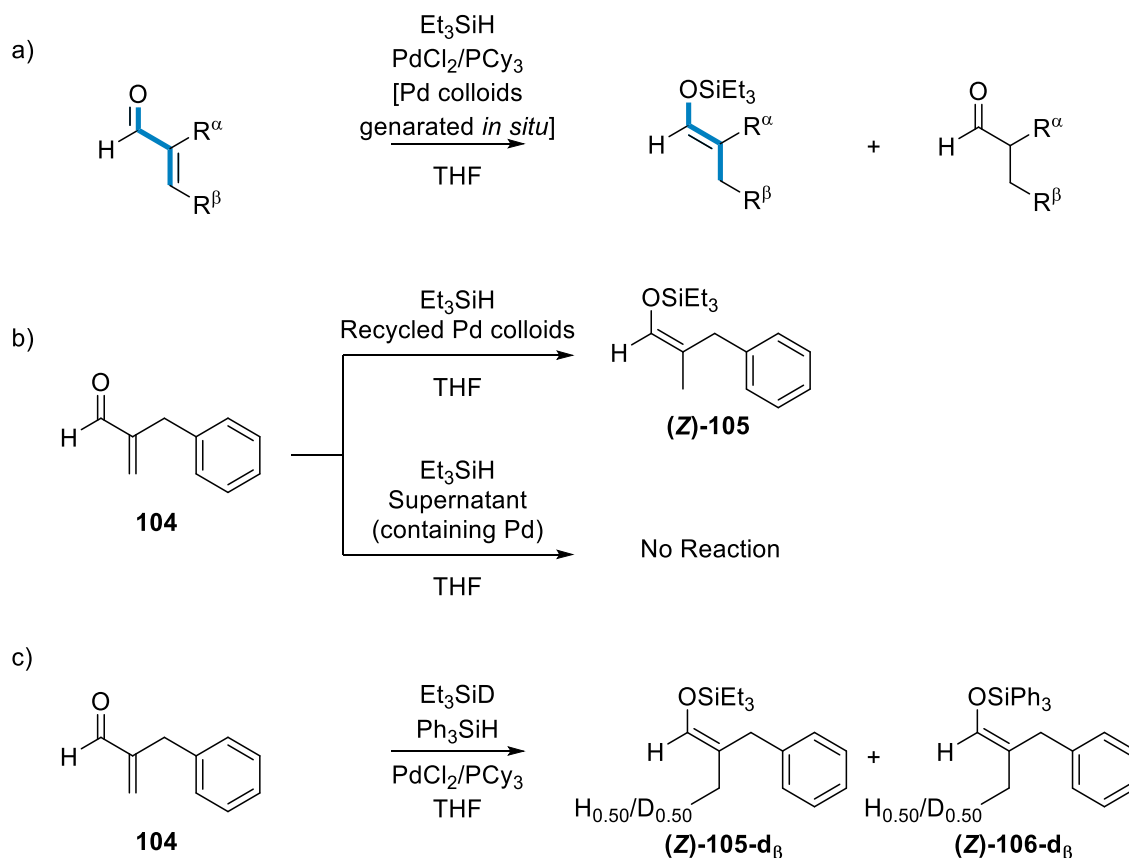
broad distribution of different coordination sites in the catalysts and with challenges in reaction monitoring, the determination of precise reaction mechanisms is difficult. Consequently, development of new and selective heterogeneous catalyst-systems is more like "trial and error" rather than a rational design. Nonetheless, as a new trend of single-site heterogeneous catalysts is arising, a deeper understanding of the reaction mechanisms is needed. As a result, one of the first steps is to find out how closely the mechanisms of heterogeneous catalysts parallel those established within homogeneous catalysis.

## 3 RESULTS AND DISCUSSION

### 3.1 Aims and background of the work

The aim of the work was to study the mechanism of our previously published reaction of stereo- and chemoselective 1,4-hydrosilylation of enals and enones with *in situ* generated colloidal palladium and triethylsilane (Scheme 26a).<sup>117</sup> With the knowledge that would be gained from the mechanistic studies, the plan was to further develop the protocol into a robust, industrially applicable method, and possibly to expand the concept for other similar reactions.

Single enol silane stereoisomers are very valuable compounds in many stereospecific transformations, such as Mukaiyama aldol and Mannich reactions or transmetalation.<sup>118,119,120,121,122</sup> The hydrosilylation protocols usually display a preference for (*E*)-enol silanes, and methods to uniformly produce (*Z*)-enol silanes are rare.<sup>123,124</sup> Our protocol enabled access to (*Z*)-enol silanes from  $\alpha$ -substituted enals and (*E*)-enol silanes from  $\beta$ -substituted enals (Scheme 26a).<sup>117</sup> However, the most interesting aspect of the reaction was that the active catalyst was heterogeneous, and leached palladium atoms were not likely to be active in catalysis (Scheme 26b).<sup>14,15</sup> The stereo- and chemoselective hydrosilylation reaction occurred on the surface of the *in situ* generated palladium colloids. As discussed in the previous sections, among the selective reduction reactions, the truly heterogeneous surface reactions are usually simple hydrogenations, in which the H<sub>2</sub> is the e source.<sup>9,10,11</sup> In this reaction, both the silyl-species and the H-species seemed to react with the substrate on the metal surface, as indirectly demonstrated by crossover experiments with two different silanes in Scheme 26c.<sup>117</sup>



Scheme 26. a) Previously published protocol for the stereo- and chemoselective 1,4-hydrosilylation of enals and enones. b) Proof of the heterogeneity of the active catalyst. c) Crossover experiments provide evidence for the dissociation of a silane on the palladium surface.

## 3.2 Methods

### 3.2.1 Experimental methods

All reactions were carried out in screw cap glass vials or septum cap glass flasks under air or argon atmosphere. For more details, please see the supporting information of each publication. THF, Et<sub>2</sub>O, DCM, MeCN, and toluene were obtained by passing deoxygenated solvents through activated alumina columns (MBraun SPS-800 Series solvent purification system). Other solvents and reagents were used as obtained from the supplier; see articles' supporting information for more details. Analytical TLC was performed using Merck silica gel F254 (230–400 mesh) plates and analyzed by UV light or by staining upon heating with vanillin solution (6 g of vanillin, 5 mL of conc. H<sub>2</sub>SO<sub>4</sub>, 3 mL of glacial

acetic acid, 250 mL of EtOH) or  $\text{KMnO}_4$  solution (1 g of  $\text{KMnO}_4$ , 6.7 g of  $\text{K}_2\text{CO}_3$ , 1.7 mL of 1 M NaOH, 100 mL of  $\text{H}_2\text{O}$ ). For silica gel chromatography, the flash chromatography technique was used, with Merck silica gel 60 (230–400 mesh) and p.a. grade solvents. A small pad of alumina (neutral) columns was prepared by filling plastic syringes (5–20 mL) with Sigma-Aldrich purum p.a. grade alumina. The  $^1\text{H}$  NMR and  $^{13}\text{C}$  NMR spectra were recorded in  $\text{CDCl}_3$  on Bruker Advance 500, 400, 300, and 250 spectrometers. The chemical shifts are reported in ppm relative to residual  $\text{CHCl}_3$  ( $\delta$  7.26) for  $^1\text{H}$  NMR. For the  $^{13}\text{C}$  NMR spectra, the residual  $\text{CDCl}_3$  ( $\delta$  77.16) was used as the internal standards. IR spectra were recorded on a Tensor27 FT-IR spectrometer. High-resolution mass spectrometric data were prepared using MicroMass LCT Premier Spectrometer.

### 3.2.2 Computational methods

The calculations in this thesis were performed using the density functional theory (DFT). In recent decades, as discussed in Section 1.5, DFT has become an important tool for investigating the mechanism of surface reactions. In this chapter, a very short introduction to the theory is given. A more detailed mathematical and theoretical discussion can be found in several books<sup>125,126,127</sup> and review articles.<sup>128,129</sup>

The theoretical background of DFT is based on two Hohenberg-Kohn theorems.<sup>130</sup> The first Hohenberg-Kohn theorem states that the external potential  $V_{ext}$  and also the energy of the system are a unique functional of the electron density  $\rho(\vec{r})$ :

$$E[\rho] = \int d\vec{r} \rho(\vec{r}) V_{ext}(\vec{r}) + F[\rho] \quad (1)$$

$F[\rho]$  is a universal functional that does not depend on external potential,  $V_{ext}$ . In other words, there cannot be two different external potentials yielding the same ground state density. The second theorem states that the ground state density can be achieved by minimizing the functional (1), and by the ground state density  $\rho_0(\vec{r})$  it is possible to obtain ground state energy  $E_0$ .

The unknown universal functional,  $F[\rho]$  contains kinetic energy and electron-electron interactions. One way to address the unknown universal functional is by the Kohn-Sham approach,<sup>131</sup> in which the universal functional is divided into fictive non-interacting particles. The non-interacting part generates the same density as any of the interacting particles.<sup>129,131</sup> The non-interacting part can be calculated with the Kohn-Sham equation:

$$\left(-\frac{1}{2}\nabla^2 + v_{eff}\right)\varphi_i(\vec{r}) = \epsilon_i\varphi_i(\vec{r}) \quad (2)$$

$v_{eff}$  is effective potential where the electrons move. This creates a set of a non-interacting one-electron states ( $\varphi_i$ ), i.e., Kohn-Sham orbitals. With the Kohn-Sham equation, the large part of the kinetic energy can be calculated with good accuracy. The remaining part is mixed with the non-classical electron interaction. Now the universal functional  $F[\rho(\vec{r})]$  can be divided into:

$$F[\rho(\vec{r})] = T_s[\rho(\vec{r})] + J[\rho(\vec{r})] + E_{xc}[\rho(\vec{r})] \quad (3)$$

The kinetic energy,  $T_s[\rho]$ , describes the non-interacting particles,  $J[\rho]$  is the Hartree energy and describes the classical Coulomb interaction, and the non-classical part,  $E_{xc}[\rho]$ , includes the exchange and correlation energies and the residual part of the kinetic energy. The exchange and correlation functional ( $E_{xc}$ ) contains all the parts that need to be approximated.

The exchange and correlation functional is the most important part of the DFT calculations. Even though the  $E_{xc}$  contribution to the total energy is very small (~6 %), the quality of the DFT calculation depends on the accuracy of the  $E_{xc}$  approximation.<sup>132</sup> Several different types of functionals have been developed over time to cover the XC effects.<sup>133</sup> The simplest description of XC effects is local density approximation (LDA), which treats the XC energy as uniform electron gas with the same electron density.<sup>130</sup> Most of the functionals used in surface calculations, such as PBE<sup>134</sup> and RPBE,<sup>135</sup> are based on a generalized gradient approximation (GGA), in which the XC energy is expressed as a function of

electron density and density gradient. To further improve the XC functionals from GGA, several approaches have been used.<sup>136,137</sup> One approach has been to add a part of Hartree-Fock exchange to the XC functional. For example, B3LYP, which is routinely used in gas-phase calculations, is this kind of hybrid functional.<sup>138,139</sup>

Density functional theory (DFT) calculations in this study were performed mainly with the GPAW code,<sup>140,141</sup> which implements the projector augmented wave method (PAW),<sup>142</sup> which is a generalization of the pseudopotential method. The PAW method implements a real-space grid, in which the Kohn-Sham equations are solved at each point of the real-space grid and no basis set is involved. The most important advantage of the real-space grid is that the parallelization of the calculation is easier, which makes it possible to use massively parallel supercomputers. The Kohn-Sham equations were solved self-consistently using the RPBE<sup>135</sup> or BEEF-vdW<sup>143</sup> to describe exchange and correlation effects. The metal particles were modeled with four-atom-layer-thick 111-surface slabs using periodic boundaries in the x- and y-directions, while in the z-direction (perpendicular to the surface), a vacuum was used to separate the cells below and above the slab. The Brillouin zone was sampled with Monkhorst-Pack k-points for the supercells. The transition states were determined using a Nudge Elastic Band (NEB) method<sup>144</sup> or a constraint method, under which the interatomic distance of a forming bond is fixed to several values and the remaining degrees of freedom are relaxed. For the found transition states, harmonic frequencies were calculated and only a single imaginary frequency was obtained in each case. The visualization of the vibration mode showed bond stretching along a reaction coordinate. A small set of the calculations were performed at the B3LYP/6-31G(d) level with Jaguar from Schrödinger LLC.<sup>145</sup> Maestro was used as a graphical user interface to import or modify the input structures and generate the input files for Jaguar.<sup>145</sup> A more detailed description of the computational methods used in this study can be found in articles' supporting information.

### 3.3 Improving the protocol

The previous PdNP protocol (see Section 3.1) was not fully chemoselective for the hydrosilylation reaction, as a significant amount of saturated aldehyde was formed as a side product.<sup>117</sup> The other problem with the protocol was that the reaction failed to proceed if the nucleation of the catalyst did not initiate properly. Additionally, scaling up the protocol was difficult due to the fast aggregation of the active catalyst.

#### 3.3.1 Effect of the catalyst

In the previous protocol, the best selectivity towards the hydrosilylation was obtained with the PdCl<sub>2</sub>/PCy<sub>3</sub> catalyst combination (Table 1, entries 1–4). We screened several different colloidal palladium catalysts and the best results were obtained with Pd-PVP colloids and Pd-thioether colloids (entries 5 and 6). However, the chemoselectivity was only slightly improved with Pd-thioether colloids compared with the PdCl<sub>2</sub>/PCy<sub>3</sub> catalyst system (entry 1). Above all, the practicality of the reaction was still questionable.

Table 1. The chemoselectivity of the hydrosilylation reaction with different palladium catalysts.

Entry	Catalyst	Catalyst loading <sup>a</sup>	Product <sup>b</sup>	
			105	107
1	PdCl <sub>2</sub> /PCy <sub>3</sub>	1.3 mg/4.2 mg	84 %	16 %
2	Pd(OAc) <sub>2</sub> /PCy <sub>3</sub>	1.1 mg/2.8 mg	50 %	5–10 %
3	PdCl <sub>2</sub> /PPh <sub>3</sub>	0.9 mg/2.6 mg	20 %	5–10 %
4	Pd/C (5 wt %) [Not Activated] <sup>c</sup>	2 mg	19 %	39 %
5	Pd-PVP colloids <sup>d</sup>	12 mg	29 %	42 %
6	Pd-thioether colloids <sup>e</sup>	2 mg	90 %	10 %
7	Pd/C (5 wt %) [Not Activated] <sup>f</sup>	2 mg	83 %	17 %
8	Pd/C (5 wt %) [Vacuum] <sup>g</sup>	2 mg	91 %	8 %
9	Pd/C (5 wt %) [Washed] <sup>h,i</sup>	2 mg	100 %	0 %
10	Pd/C (5 wt %) + Acid <sup>j</sup>	2 mg	0 %	100 %

Reaction conditions: **104** (44 mg, 0.30 mmol, 1.0 equiv), catalyst, triethylsilane (53  $\mu$ L, 0.33 mmol, 1.1 equiv), THF (1 mL), room temperature. [a] Catalyst loading presented as a mass because the active catalytic surface differ with catalyst's particle size. [b] Determined by <sup>1</sup>H NMR analysis. **104** was also detected in the entries 2–5. [c] Reaction done during the preparation of the ref 117 paper [d]. All of the details are provided in ref 117. [e] Catalyst was prepared using the procedure described by Obare *et al.* in ref 146. [f] Pd/C was taken from a different batch than in entry 4. [g] Pd/C was kept in a vacuum for 10 min. [h] Pd/C was washed three times with acetone and dried in a vacuum; see protocol in Article I: the Supporting Information. [i] The same selectivity was observed with five different batches of Pd/C (5–10 wt %) from different sources (Sigma-Aldrich, Fluka and other suppliers). [j] *Aq.* H<sub>2</sub>SO<sub>4</sub> or *aq.* HCl (20  $\mu$ L, both 1 M).

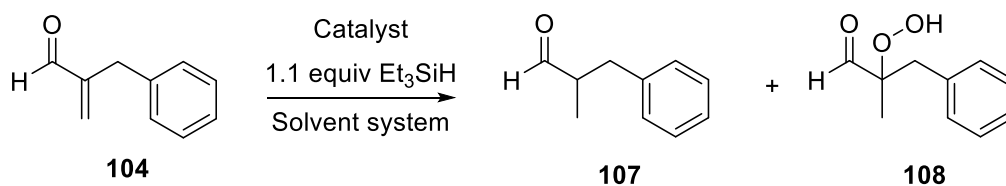
Another experiment with Pd/C unexpectedly gave completely different results compared with the previous screenings (compare entries 4 and 7). Even a small amount of water is enough to promote the formation of the saturated aldehyde **107** (Table 2). The charcoal can adsorb up to 55–60 wt % of water,<sup>147</sup> and presumably the amount of residual water varies with different Pd/Cs. We then tried to dry the charcoal as effectively as we could (Table 1, entries 8 and 9). Eventually, washing the Pd/C with acetone and drying it in vacuum (Table 1, entry 9) led to complete selectivity towards the hydrosilylation with  $\alpha$ -

substituted enal **104**. In addition to solving the chemoselectivity problem, the use of activated commercially available Pd/C also solved the scale-up and practicality problems, as the reaction worked well in gram-scale with enal **104** (3.3 g, 92 % (Z:E > 50:1)).

### 3.3.2 Improving the transfer hydrogenation protocol

The transfer hydrogenation conditions to produce the saturated aldehyde product **107** were also optimized. In the previous protocol, the reaction was completely selective toward the formation of **107** when 1:1 mixture of THF and water was used as the solvent system (Table 2, entry 1). With the same solvent mixture and Pd/C, surprisingly, the main product was the  $\alpha$ -hydroperoxy aldehyde **108** (entry 2, see Section 3.6). The attempt to reduce the amount of the water in the solvent system failed (entry 3). However, in the previous protocol, the pH of the reaction mixture was 2.6 due to HCl generated from the PdCl<sub>2</sub> precatalyst.<sup>117</sup> We then tried to add just a small amount of acid [*aq.* H<sub>2</sub>SO<sub>4</sub> or *aq.* HCl (20  $\mu$ L, both 1 M)] into the reaction mixture (entries 4 and 5). This changed the outcome of the reaction, and full conversion to the corresponding saturated aldehyde **107** was obtained in less than 5 minutes.

Table 2. The chemoselectivity of the transfer hydrogenation reaction with catalysts and solvent systems.



Entry	Catalyst	Solvent system	Product <sup>a,b</sup>	
			107	108
1	PdCl <sub>2</sub> /PCy <sub>3</sub>	1 mL THF/H <sub>2</sub> O (1:1)	100 %	0 %
2	Pd/C	1 mL THF/H <sub>2</sub> O (1:1)	40 % <sup>c</sup>	60 %
3	Pd/C	1 mL THF/H <sub>2</sub> O (20 μL, 1 M)]	31 % <sup>c</sup>	69 %
4	Pd/C	1 mL THF/HCl (20 μL, 1 M)]	100 %	0 %
5	Pd/C	1 mL THF/H <sub>2</sub> SO <sub>4</sub> (20 μL, 1 M)]	100 %	0 %

Reaction conditions: **104** (44 mg, 0.30 mmol, 1.0 equiv), catalyst, triethylsilane (53 μL, 0.33 mmol, 1.1 equiv), solvent system (1 mL), room temperature, reaction time: entries: 1-3 1 h and 4-5 5 min. [a] Determined by <sup>1</sup>H NMR analysis. [b] Enol silane **105** were not detected in any entry. [c] For more details, see Section 3.6.

### 3.3.3 Stereo- and chemoselectivity of the improved protocols

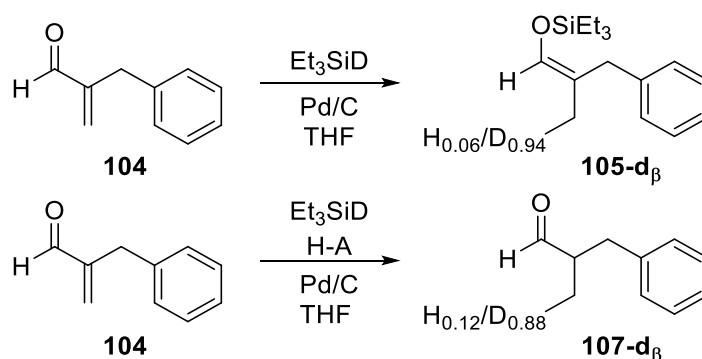
With  $\alpha$ -substituted enals, the stereoselectivities of the reaction were generally high, favoring the (*Z*)-enol silanes (typical *Z*:*E* > 50:1). With  $\beta$ -substituted enals, the reaction favored the (*E*)-enol silanes; however, the stereoselectivity was considerably lower (typical *Z*:*E* was ca. 10:90). The substrate scope for the hydrosilylation and for the transfer hydrogenation was quite wide (see Article I). Both reactions worked well with enals and cyclic enones. However, in case of acyclic enones, only the transfer hydrogenation gave the desired product.

Maybe the most interesting aspect of the study was that Et<sub>3</sub>SiH can be used as stoichiometric source of H atoms. Consequently, both reactions tolerated several reducible functional groups, such as non-conjugated C=C double bonds, benzyl protection, carbonyls, and nitro group (see substrate scope in Article I). In addition, other C=C double bonds, remote from the enal or enone functionalities,

were also successfully hydrogenated with 2.2 equivalents of Et<sub>3</sub>SiH (see substrate scope in Article I).

### 3.4 Mechanistic studies of the hydrosilylation and transfer hydrogenation reactions

The mechanism and the origin of the stereo- and chemoselectivity in the hydrosilylation reaction, together with the mechanism of the transfer hydrogenation reaction, were not completely understood. From the previous experiments, we knew that the hydrosilylation reaction was catalyzed by the heterogeneous palladium (Scheme 26c). We also knew that, in both the hydrosilylation and transfer hydrogenation reactions, the hydrogen atom (“hydride”) adding to the β-position of the α,β-unsaturated carbonyl was originated from the Et<sub>3</sub>SiH (Scheme 27, also see Article I).



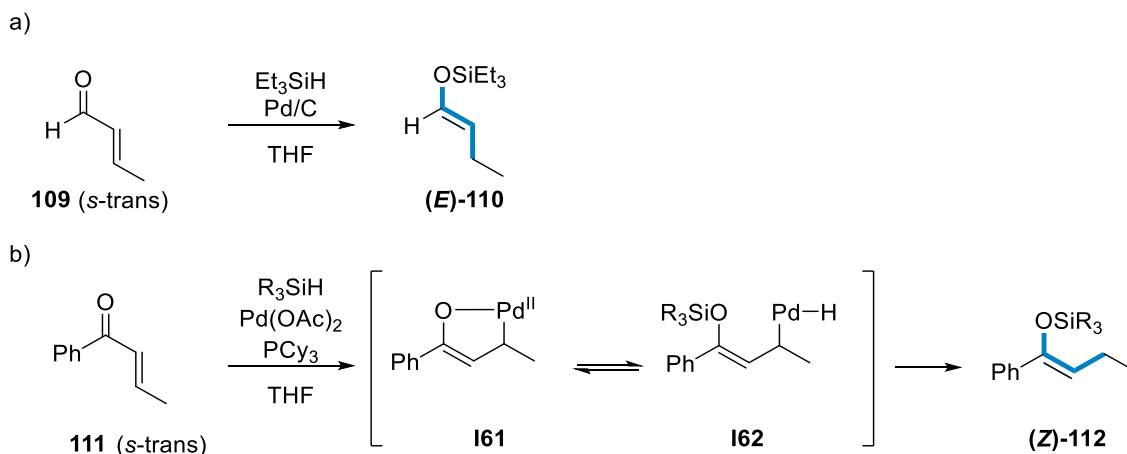
Scheme 27. Labeling experiments for the hydrosilylation and transfer hydrogenation reactions with Et<sub>3</sub>SiD.

The mechanistic studies of the hydrosilylation and transfer hydrogenation reactions were carried out by combining experimental investigations and theoretical, i.e. DFT, calculations.

#### 3.4.1 Mechanism of the stereoselective hydrosilylation reaction

In the previous experiments, we observed a clear trend in the stereoselectivity of the hydrosilylation reaction. The major isomer of the product, enol silane **105**, corresponded to the *s*-trans conformation of the starting material

enal **104** (Scheme 28a). The observed isomer was the opposite of what Oshima *et al.* had previously obtained in similar reaction conditions.<sup>124</sup> However, in their reaction, the active catalyst was homogeneous palladium and the stereoselectivity originated from the five-membered intermediate **I61** (Scheme 28b).



Scheme 28. a) Our protocol: the enol silane isomer **(E)-110** corresponds to the *s*-trans conformer of the starting enal **109**. b) Oshima protocol: the enol silane isomer **(Z)-112** originates from the five-membered intermediate **I61**.

The stereoselectivity of the hydrosilylation reaction was addressed by DFT calculations, and the simplest  $\alpha,\beta$ -unsaturated aldehyde, acrolein (**4a** in Figure 12), was chosen as a model substrate. In summary, the DFT calculations suggested that the hydrosilylation reaction is not under a Curtin-Hammett control (Figure 12). The individual adsorbed enal conformers cannot equilibrate from a *s*-trans to *s*-cis conformer on the Pd-surface and the *O*-silylation elementary step is irreversible. This indicates that the stereoselectivity of the reaction is determined by the ratio of the *s*-trans and *s*-cis conformers of the enal in the solution phase.

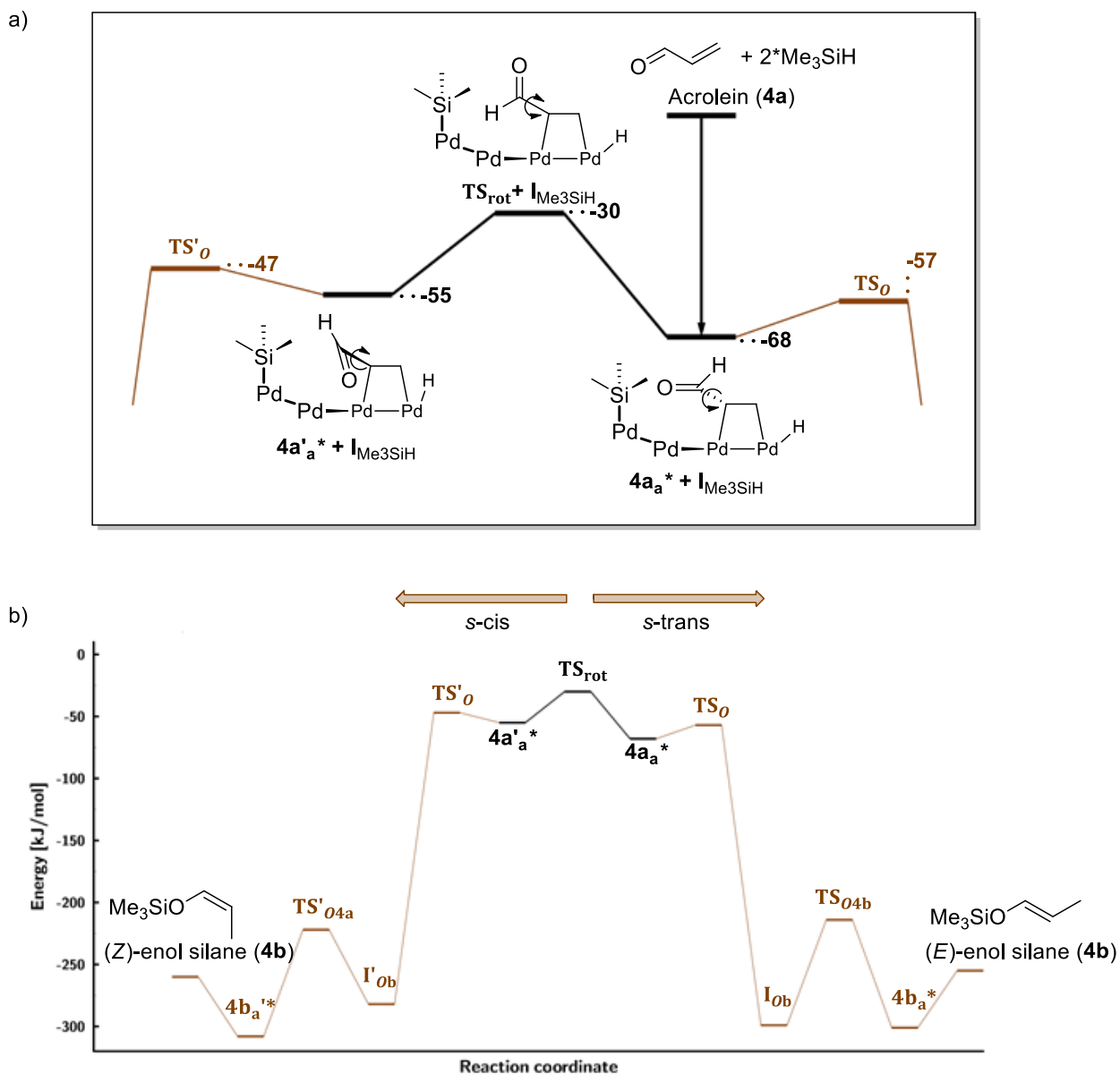


Figure 12. Stereoselectivity of the hydroxylation reaction of acrolein **4a** is not under Curtin-Hammett control: a) a close-up of the *O*-silylation step and b) full picture. (See the naming convention from the Article IV.)

We then calculated the gas-phase energies of the *s*-trans and *s*-cis conformations of several  $\alpha$ - and  $\beta$ -substituted enals, and found out that the Boltzmann populations of two conformers corresponded especially well with the isomer ratio of the enol silane products (see Article IV). In addition, in the control experiments with citral (**113**), a small solvent effect on the stereoselectivity was observed. The isomer ratio of the enol silane product could be affected with the choice of the solvent.

Interestingly, only the enol silanes formed from the  $\beta$ -substituted enals underwent isomerization after the completed reaction (see  $^1\text{H}$  NMR experiments in Figure 13). The isomerization of the enol silanes in the reaction conditions occurs associatively (Scheme 8c) from the  $\beta$ -position enol silane (see the Supporting Information in Article IV). With 2-substituted enol silanes (from  $\beta$ -substituted enals), this mechanism leads to *E/Z*-isomerization. However, with the 2,2-disubstituted enol silanes (from the  $\alpha$ -substituted enals), this mechanism always leads to the same isomer that initially adsorbs to the surface, and no isomerization can occur (see Article IV).

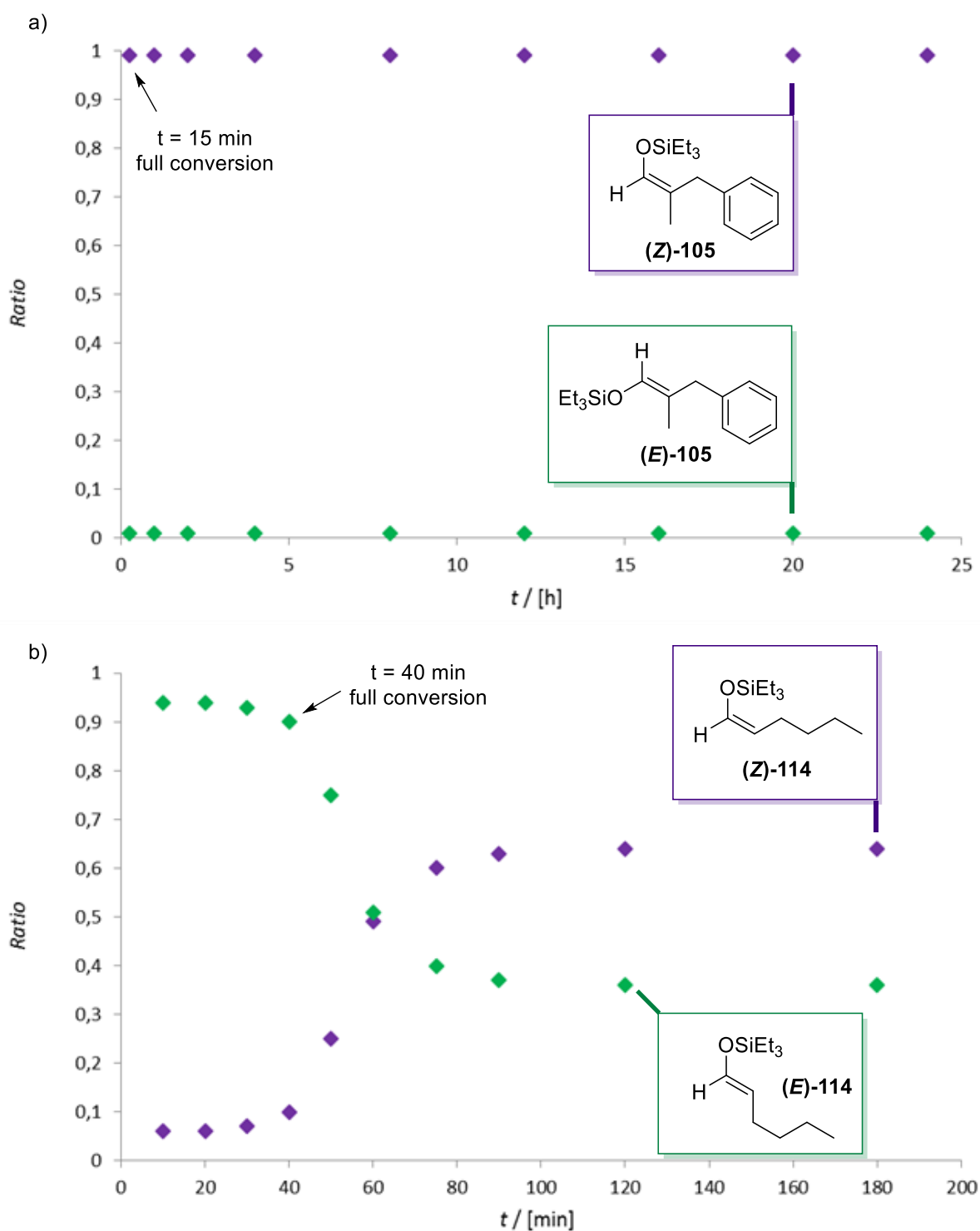
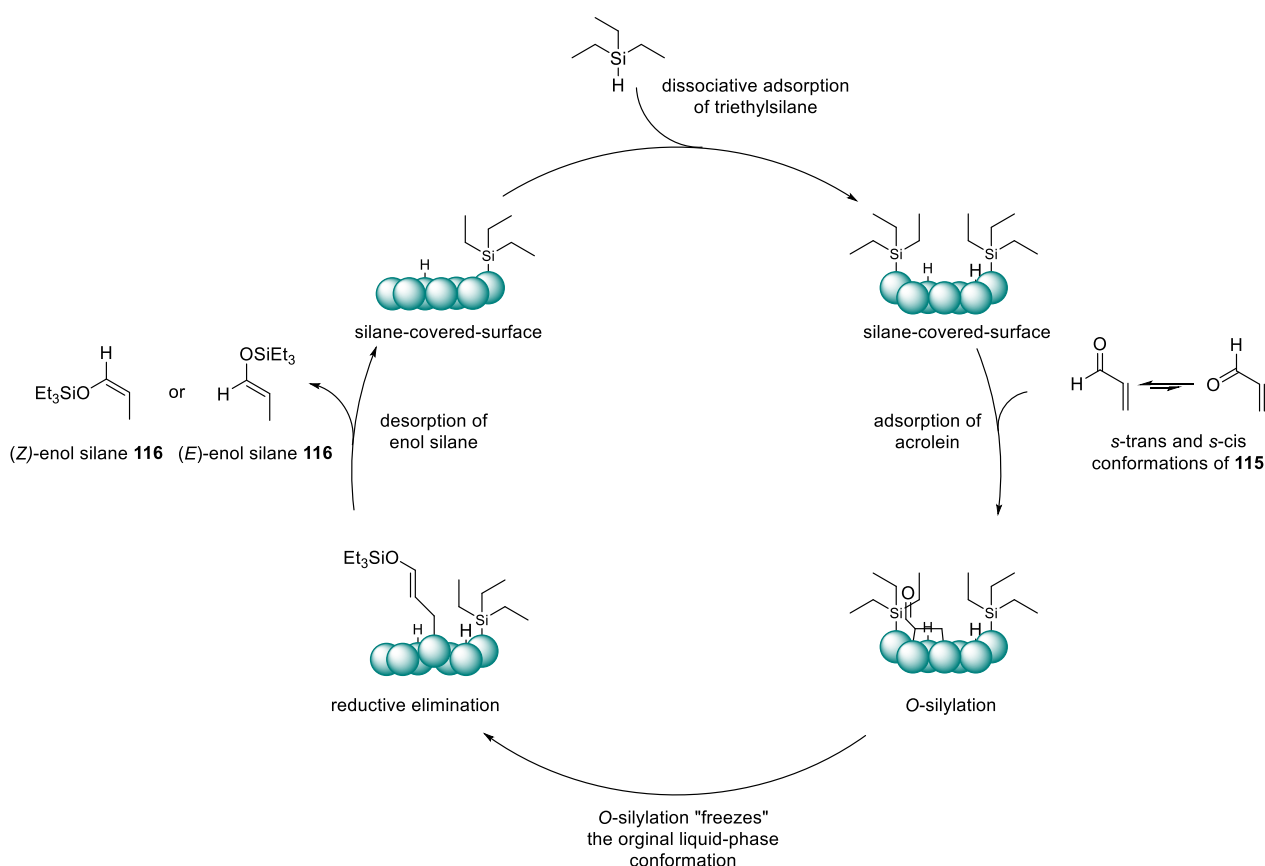


Figure 13. Isomerization during and after the hydrosilylation reaction. a) With  $\alpha$ -substituted enol silane **105** and b) with  $\beta$ -substituted enol silane **114**.

The proposed mechanism for the hydrosilylation reaction is presented in Scheme 29. The catalytic cycle begins with the dissociation of the triethylsilane onto the Pd-surface. Onto this triethylsilyl- and hydride-covered surface an enal **115** adsorbs from the C=C double bond. Before the individual enal can rotate

from *s*-trans to *s*-cis conformation or vice versa, it undergoes a rapid and irreversible *O*-silylation that “freezes” the original solution-phase conformation. The enol silane **116** then desorbs from the surface. The *Z*/*E* ratio of the product is then determined by the solution phase ratio of the enal *s*-trans and *s*-cis conformations, like in the case of 1,3-butadiene (**34**) hydrogenation (discussed in Section 2.1.2.2).

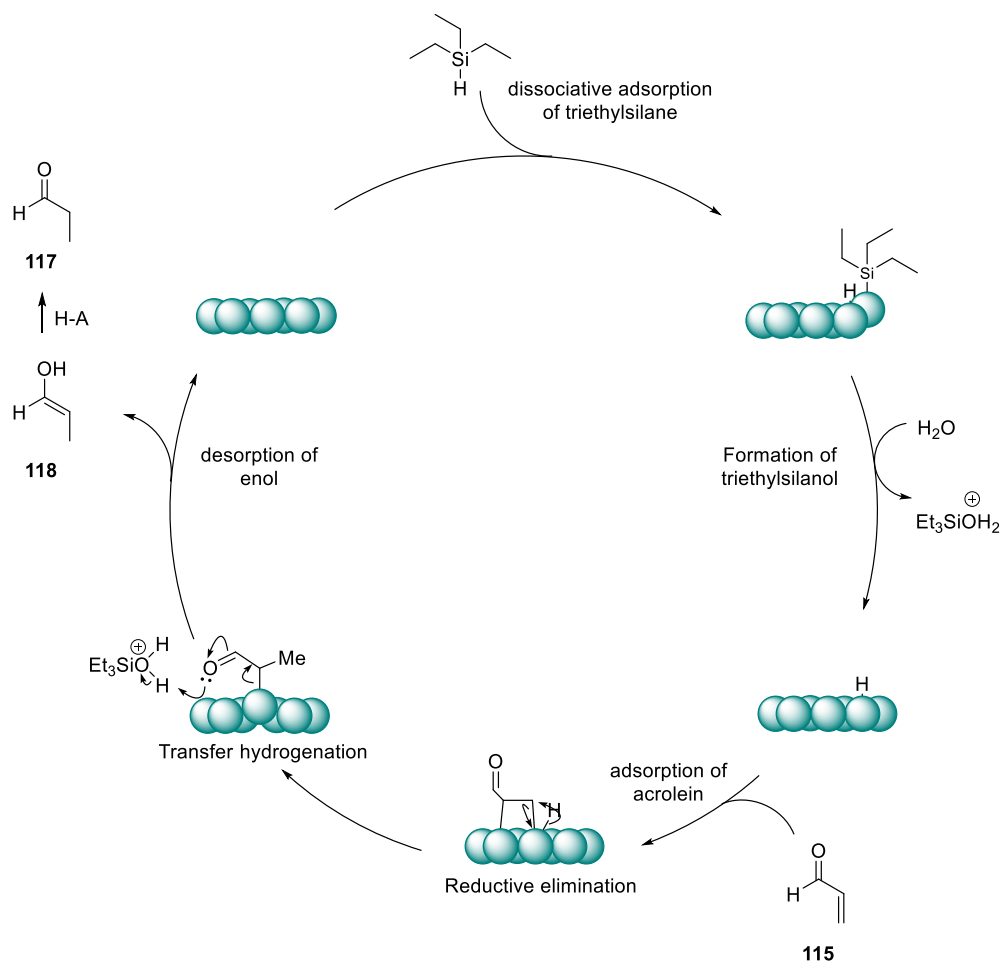


Scheme 29. Proposed catalytic cycle for the 1,4-hydrosilylation of enals with triethylsilane and Pd/C.

### 3.4.2 Mechanism of the transfer hydrogenation and chemoselectivity of the hydrosilylation reaction

Under aqueous and acidic conditions (Table 2, entries 4 and 5), the studied reaction gives saturated aldehyde **117** as a major product. The proposed mechanism for the transformation is presented in Scheme 30. The catalytic cycle begins, like the hydrosilylation reaction, by the dissociation of the triethylsilane onto the Pd-surface. However, in aqueous conditions, the triethylsilyl on the palladium surface reacts with water to produce triethylsilanol (see Article III: the

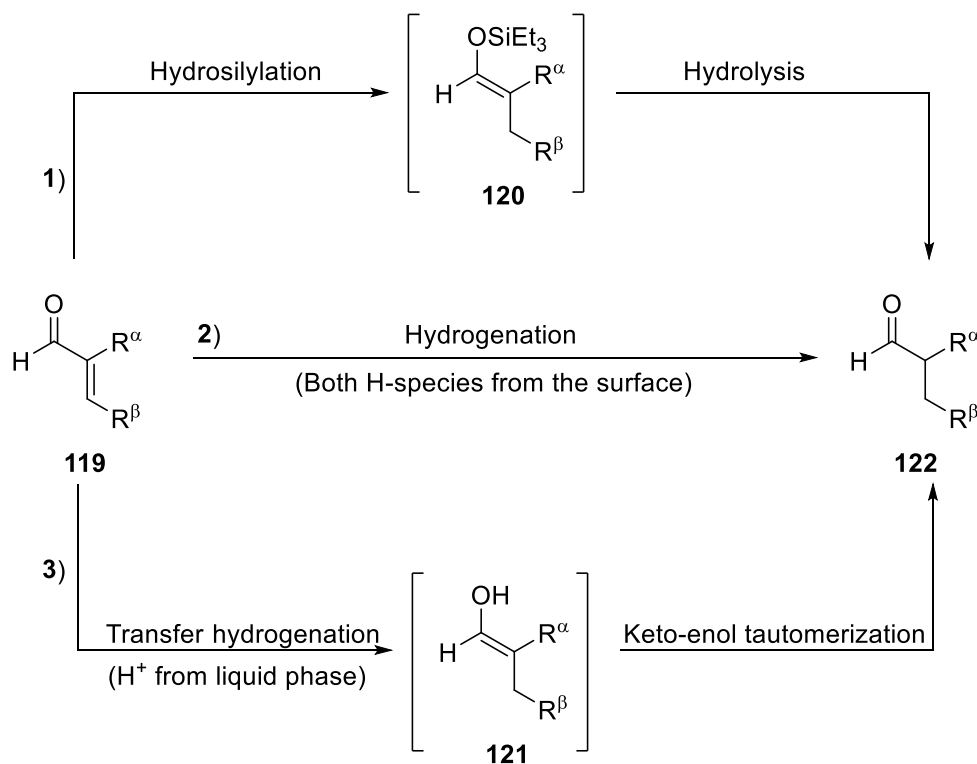
Supporting Information). Formation of silanol from adsorbed silyl-species and water is a well-documented reaction in literature.<sup>148,149,150,151,152,153,154</sup> This leads to the coverage of the surface with only hydrogen atoms. The enal **115** is then adsorbed *via* the C=C double bond. The hydrogen atom (“hydride”) attacks the  $\beta$ -position of enal, as the labeling experiments indicate (Scheme 27), followed by protonation and formation of enol **118** intermediate, either *via* a stepwise (showed in the Scheme 30) or concerted mechanism. The formation of the enol intermediate was observed in the  $^1\text{H}$  NMR experiments (see Article III: the Supporting Information).



Scheme 30. Proposed catalytic cycle for the transfer hydrogenation of enals with triethylsilane and Pd/C.

The formation of saturated aldehyde was also observed in the hydrosilylation conditions. At the beginning of the mechanistic studies, it was unclear whether the saturated aldehyde side-product was formed *via* the same or different mechanism as the saturated aldehyde product under the aqueous

conditions, i.e., transfer hydrogenation conditions. We then considered three different mechanistic pathways for **122** side-product formation: 1) *via* hydrolysis of enol silane **120**, 2) *via* hydrogenation mechanism or 3) *via* transfer hydrogenation mechanism, i.e., *via* enol **121** (Scheme 31).

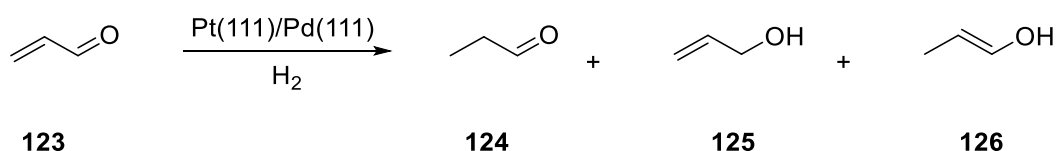


Scheme 31. Three different mechanistic pathways considered for the saturated aldehyde **122** side product formation.

The pathway 1 was not realistic, because the enol silanes were stable at the reaction conditions (see reaction monitoring in Article IV). According to DFT calculations, the *O*-silylation step had a significantly lower barrier than any of the H-additions to the acrolein. Consequently, pathway 2 could not compete with the hydrosilylation reaction (see Article IV). Additionally, in the labeling experiments with  $\text{Et}_3\text{SiD}$ , a D-incorporation was observed only in the  $\beta$ -position of the isolated saturated aldehyde side-product (see Article IV). We concluded that in the hydrosilylation conditions, the side-product is most likely formed *via* the transfer hydrogenation mechanism (pathway 3) by the excess moisture in the reaction mixture.

### 3.5 First principle calculations for the mechanism of hydrogenation of acrolein on Pd and Pt

The chemoselective reductions of  $\alpha,\beta$ -unsaturated carbonyl compounds to the corresponding allylic alcohols are important processes in the pharmaceutical and fine-chemical industries.<sup>155,156</sup> However, the origin of the chemoselectivity (C=C vs. C=O reduction) with metals such as Pd and Pt is still largely unknown.<sup>44,45,157</sup> Experimentally, the simplest unsaturated aldehyde, acrolein (**123**), is reduced to propanal (**124**) with over 98 % selectivity with Pt catalyst (Scheme 32).<sup>43,158,159</sup>



Scheme 32. Semihydrogenation of acrolein (**123**) leading to three isomeric products: propanal (**124**), allyl alcohol (**125**), and 1-propenol (**126**).

During the DFT studies of the hydrosilylation of acrolein (**123**) on Pd(111) surface (Article IV), we calculated several different hydrogenation pathways leading to propanal (**124**) on the Pd(111) surface. However, by comparing the obtained results with similar studies on the Pt(111) surface,<sup>44,45</sup> we noticed that the results did not completely engage, and we could present an alternative explanation for the observed chemoselectivity.

What we found out was that although the reduction of C=O functionality is kinetically favored over the C=C reduction, the mechanistic pathways leading to the allyl alcohol (**125**) (i.e., the reduction of C=O functionality) require the involvement of an ensemble of three (possibly even four) surface metal atoms. In contrast, the reactions at the C=C functionality are less space intensive and the size of the ensemble is one or two metal atoms (see Article II: the Supporting Information). Under experimental conditions, the surface is partially covered with the strongly binding species, such as fragmented species, which might block

one or several adsorption sites at once. In other words, pathways requiring access to several adjacent metal atoms are strongly disfavored at high coverage.

The calculations were done by varying the acrolein (**123**) coverage from 1/16 ML to 1/3 ML. The results clearly indicate that, when the number of available surface metal atoms is lowered, the mechanisms that require more metal atoms are simultaneously disfavored (see Article II: the Supporting Information for more details). The trend is illustrated in Figure 14.

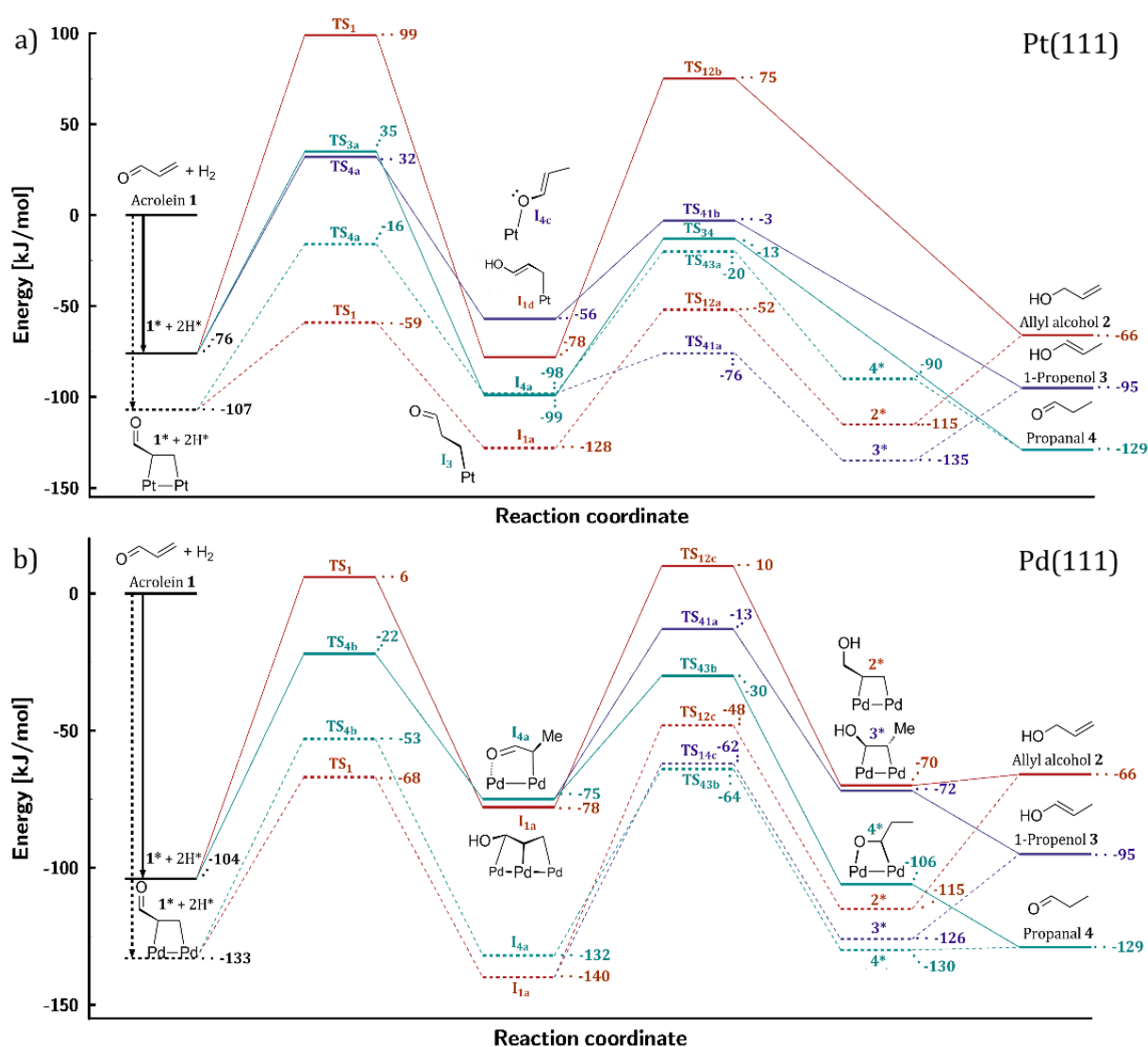


Figure 14. The potential energy surfaces for the key elementary steps in acrolein (**1**, in this Figure) reduction a) on Pt(111) and b) on Pd(111) surfaces together with the key molecular structures. The solid line refers to the results at 1/3 (1/4) ML acrolein coverage on Pt (Pd) and the dashed line for 1/9 ML coverage. For naming convention and coding, see Article II: the Supporting Information.

The other aspect that we found was related to the transition state scaling (TSS) relationship.<sup>160</sup> Typically, the “noise” in the TSS line is identified as resulting from a local variation in adsorption geometries and differences in transition-state bond lengths.<sup>161</sup> By carefully analyzing the reaction mechanism, and especially the internal electronic structures of the bound species, we found that the electronic structures of the initial or final state need to be similar to the transition state in order to form a TSS line. The scaling revealed that individual lines are formed for each type of mechanism (Figure 15). Even more specifically, we found that for similar mechanisms, the internal electronic structures of the bound species must be similar in order for the two elementary steps to form a single TSS line. For example, the internal electronic structures of the allyloxy and vinyloxy species differ, and thus a small variation in the TSS line is observed (Figure 16).

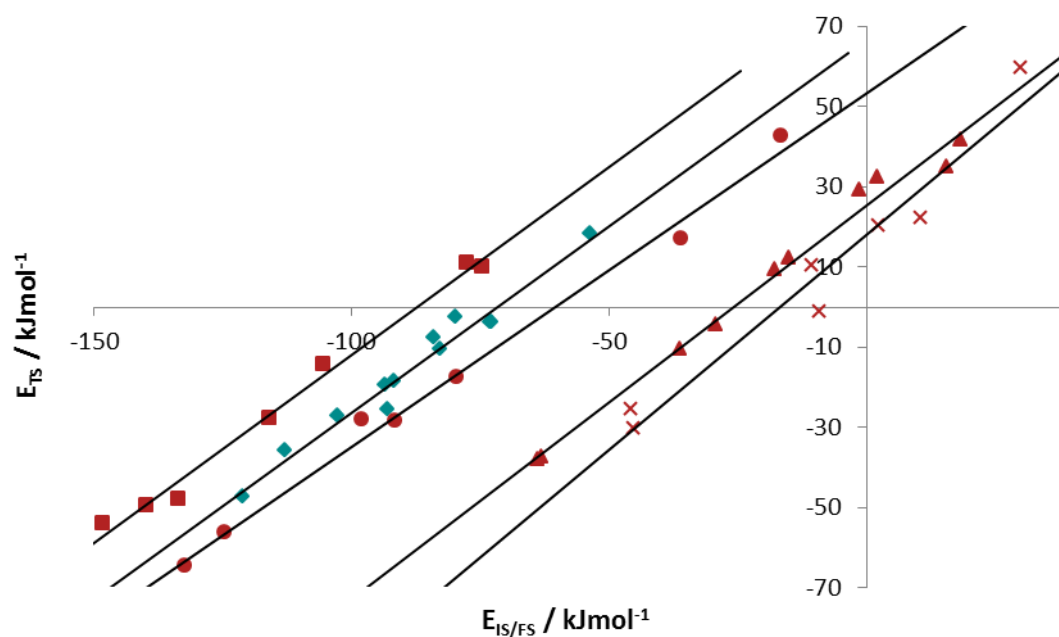


Figure 15. TSS relation for different mechanisms: ■ olefin insertion (1,2-addition,  $R^2 = 0.990$ ), ◆ reductive elimination (4,3-addition and 3,4-addition,  $R^2 = 0.969$ ), ● PCET (1- addition,  $R^2 = 0.993$ ), ▲ allyloxy protonation (2,1-addition,  $R^2 = 0.989$ ) and X hydride addition (2-addition,  $R^2 = 0.952$ ). For more details, see Article II: the Supporting Information.

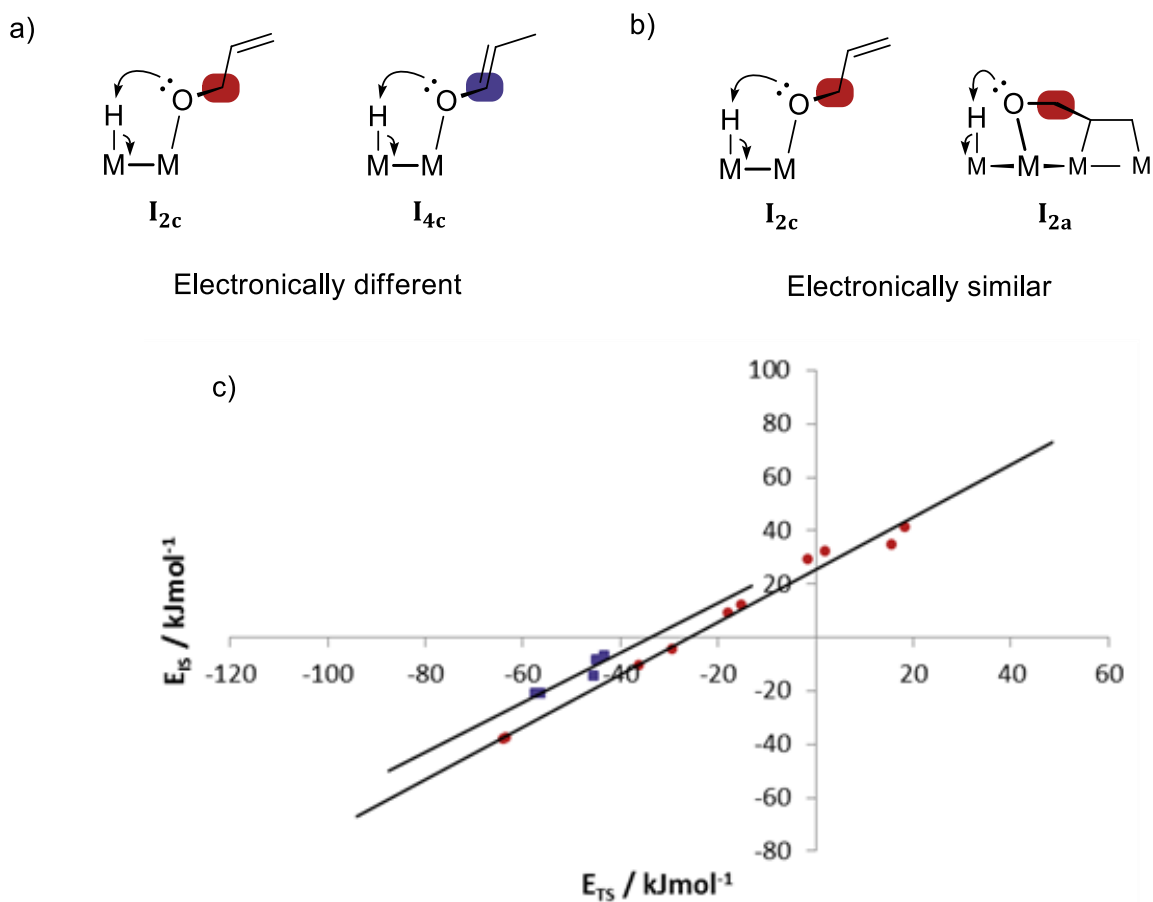


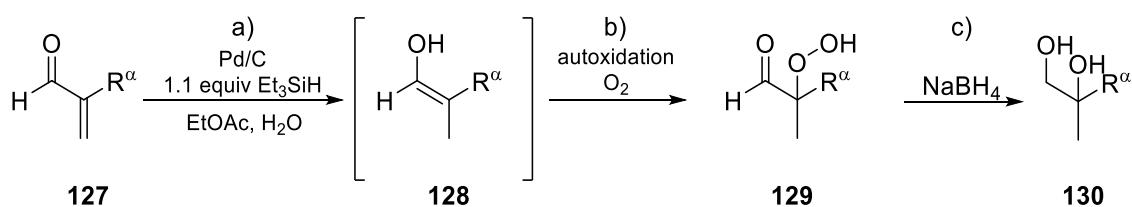
Figure 16. a) Electronically different structures do not form a single TSS relation while b) the electronically similar structures do. c) ● protonation of allyloxy species  $I_{2c}$  and  $I_{2a}$  (2,1-addition,  $R^2 = 0.988$ ) and ■ protonation of vinyloxy species  $I_{4c}$  (4,1-addition,  $R^2 = 0.896$ ) on a Pt(111) surface. For more details, see Article II: the Supporting Information.

### 3.6 3,4-Hydroperoxidation of $\alpha$ -substituted enals

$\alpha$ -Hydroxylations of saturated carbonyl compounds are well-known reactions in organic synthesis.<sup>162,163</sup> In these reactions, the  $\alpha$ -hydroxycarbonyl products are usually obtained after reductive work-up from the corresponding  $\alpha$ -hydroperoxycarbonyl intermediates. The hydroperoxy compounds are formed *via* oxidation of enolates or enols, which are obtained with acid or base treatment of the saturated carbonyl compounds. However, the formation of enols from saturated aldehydes is challenging due to their instability towards polymerization or aldol self-condensation under acidic or basic conditions.<sup>164</sup> An

alternative way to produce enols is *via* conjugated reduction of  $\alpha,\beta$ -unsaturated carbonyls.<sup>164,165,166</sup>

During the improvement of the transfer hydrogenation protocol, we observed a new product that was formed in significant quantities under the aqueous conditions (Table 2, entries 2 and 3). <sup>1</sup>H NMR experiments revealed the product to be an  $\alpha$ -hydroperoxide aldehyde **129**, which was formed *via* autoxidation of the initial reduction product enol **128** on a palladium surface. However, the new product was labile and could not be isolated, and full characterization was done for the reduced diol product **130** (Scheme 33).



Scheme 33. a) The transfer hydrogenation of  $\alpha$ -substituted enals **127**, b) the autoxidation of the metastable enols **128** and c) the reduction of the  $\alpha$ -hydroperoxides **129** to corresponding diol product **130**.

The key for the successful reaction was that the initial reduction on the palladium surface occurred in 1,4-fashion, which enabled the formation of the metastable enol **128**, and consequently its autoxidation, leading to the formation of hydroperoxide **129**. However, the hydroperoxidation reaction worked only with the  $\alpha$ -substituted enals. The reaction tolerated several reducible functional groups, such as aromatic, non-conjugated alkenes, and acetal protection (see Article III).

## SUMMARY AND CONCLUSIONS

The aim of the work was successfully realized, and a mechanism of the stereo- and chemoselective 1,4-hydrosilylation of enals and enones with heterogeneous palladium catalyst and triethylsilane was revealed. The reduction proceeds on the palladium surface *via* *O*-silylation, H-addition-sequence, i.e., 1,4-fashion. The stereoselectivity originates from the *s*-trans/*s*-cis ratio of the substrate in the solution phase, which is “frozen” by an almost barrier-less and irreversible *O*-silylation elementary step. The protocol was successfully improved to robust and highly chemoselective method to hydrosilylate and transfer hydrogenate enals and enones with stoichiometric amounts of triethylsilane as hydride source.

The mechanism studies performed with DFT for hydrosilylation reaction revealed a possible reason for the contradictions with experimental results and DFT calculations in chemoselective hydrogenation of acrolein with the heterogeneous platinum catalyst. The optimization studies for the transfer hydrogenation reaction also revealed a new synthetic route to produce  $\alpha$ -hydroperoxide aldehydes from  $\alpha$ -substituted enals with the heterogeneous palladium catalyst. The key for the reaction was that the transfer hydrogenation with triethylsilane and water occurs in 1,4-fashion, which enabled the metastable enol product to autoxidize to the corresponding hydroperoxide.

## REFERENCES

- <sup>1</sup> Berzelius, J. *Jahres-Bericht über die Fortschritte der Physichen Wissenschaften*, Vol. 15; H. Laupp: Tübingen, 1836.
- <sup>2</sup> A. D. McNaught, A. Wilkinson in *IUPAC Compendium of Chemical Terminology*, 2nd ed. (the "Gold Book"), Blackwell Scientific Publications, Oxford, 1997; XML on-line corrected version: <http://goldbook.iupac.org> (2006-), created by M. Nic, J. Jirat, B. Kosata, updates compiled by A. Jenkins.
- <sup>3</sup> George, S. M.; *Chem. Rev.* **1995**, *95*, 475–476.
- <sup>4</sup> Zaera, F. *Chem. Rec.* **2005**, *5*, 133–144.
- <sup>5</sup> Hatti-Kaul, R.; Törnvall, U.; Gustafsson, L.; Börjesson, P. *Trends Biotechnol.* **2007**, *25*, 119–124.
- <sup>6</sup> F. Zaera: *Topics in Catalysis* **2015**, *34*, 129–141.
- <sup>7</sup> <http://nacatsoc.org/above/what-is-catalysis>, J. Armor, Ed., North American Catalysis Society.
- <sup>8</sup> Somorjai, G. A.; Kliwer, C. J. *React. Kinet. Catal. Lett.* **2009**, *96*, 191–208.
- <sup>9</sup> Augustine, R. L. In *Heterogeneous Catalysis for the Synthetic Chemistry*; Marcel Dekker: New York, 1996.
- <sup>10</sup> Smith, G. V.; Notheisz, F. In *Heterogeneous Catalysis in Organic Chemistry*; Academic Press: New York, 1999.
- <sup>11</sup> Bartok, M.; Czombos, J.; Felfoldi, K.; Gera, L.; Gondos, G.; Molnar, A.; Notheisz, F.; Palinko, I.; Wittman, G.; Zsigmond, A. G. *Stereochemistry of Heterogeneous Metal Catalysis*; Wiley: New York, 1985.
- <sup>12</sup> Corma, A. *Chem. Rev.* **1997**, *97*, 2373–2420.
- <sup>13</sup> Gavia, D. J.; Shon, Y.-S. *ChemCatChem* **2015**, *7*, 892–900.
- <sup>14</sup> Phan, N. T. S.; Van Der Sluys, M.; Jones, C. W. *Adv. Synth. Catal.* **2006**, *348*, 609–679.
- <sup>15</sup> Pachón, L. D.; Rothenberg, G. *Appl. Organometal. Chem.* **2008**, *22*, 288–299.
- <sup>16</sup> Gellman, A. J.; *ACS Nano* **2010**, *4*, 5–10.
- <sup>17</sup> Rideal, E.; Bone, W. A.; Ingle-Finch, G.; Baly, E. C. C.; Lewis, W. C. M.; Edser, E.; Armstrong, E. F.; Hilditch, T. P.; Holtorp, H. E.; Langmuir, I.; Arrhenius, S. *Trans. Faraday Soc.* **1922**, *17*, 655–675.
- <sup>18</sup> Somorjai G. A.; Li Y. In *Introduction to Surface Chemistry and Catalysis*; 2nd Ed.; Wiley: Hoboken NJ, 2010.
- <sup>19</sup> Polanyi, M.; Horiuti, J. *Trans. Faraday Soc.* **1934**, *30*, 1164–1172.
- <sup>20</sup> Neurock, M.; van Santen, R. A. *J. Phys. Chem. B* **2000**, *104*, 11128–11145.
- <sup>21</sup> McQuarrie D. A.; Simon, J. D. In *Physical Chemistry: a molecular approach*; University Science Books: Sausalito CA, 1997.
- <sup>22</sup> Woodruff D. P.; Delchar T. A.; *Modern Techniques of Surface Science*; 2nd Ed.; Cambridge Univ. Press: New York, 1994.

- <sup>23</sup> Rylander, P. N. *Catalytic Hydrogenation over Platinum Metals*; Academic Press: New York, 1967.
- <sup>24</sup> Freifelder, M. *Practical Catalytic Hydrogenation*; Wiley-Interscience: New York, 1971.
- <sup>25</sup> Augustine, R. L. *Catalytic Hydrogenation*; Dekker: New York, 1965.
- <sup>26</sup> Rylander, P. N. *Catalytic Hydrogenation in Organic Synthesis*; Academic Press: New York, 1979.
- <sup>27</sup> Freifelder, M. *Catalytic Hydrogenation in Organic Synthesis, Procedures and Commentary*; Wiley: New York, 1978.
- <sup>28</sup> Cervený, L. *Catalytic Hydrogenation*; Elsevier: Amsterdam, 1986.
- <sup>29</sup> Polastro, E. *Chiral Reactions in Heterogeneous Catalysis*; Jannes, G.; Dubois, V., Eds.; Plenum Press: NY and London, 1995; pp 5-20.
- <sup>30</sup> Hiemenz P. C.; Rajagopalan R. *Principles of Colloid and Surface Chemistry*; 3rd Ed.; Marcel Dekker: New York, 1997.
- <sup>31</sup> Adamson A. W.; Gast A. P. *Physical Chemistry of Surfaces*; 6th Ed.; Wiley: New York, 1997.
- <sup>32</sup> Ertl G. *Reactions at Solid Surfaces*; Wiley: Hoboken NJ, 2009.
- <sup>33</sup> Nilsson A.; Pettersson L. G. M.; Norskov J. K. Eds.; *Chemical Bonding at Surfaces and Interfaces*; Elsevier Science & Technology: Amsterdam. 2008.
- <sup>34</sup> Augustine, R. L.; *Catal. Today* **1997**, 37, 419-440.
- <sup>35</sup> Molnár, A.; Sárkány, A. H.; Varga, M. J. *Mol. Catal.* **2001**, 173, 185-221.
- <sup>36</sup> Mallat, T.; Baiker, A. *Appl. Catal. A* **2000**, 200, 3-22.
- <sup>37</sup> Tungler, A.; Fogassy, G., *J. Mol. Catal.* **2001**, 173, 231-247.
- <sup>38</sup> de Vries, J. G.; Elsevier, C. J. In *The handbook of homogeneous hydrogenation* (3 Volumes), Wiley-VCH: Weinheim, 2007.
- <sup>39</sup> Zaera, F. *J. Phys.: Condens. Matter* **2004**, 16, S2299-S2310.
- <sup>40</sup> Haubrich, J.; Loffreda, D.; Delbecq, F.; Sautet, P.; Jugnet, Y.; Becker, C.; Wandelt, K. *J. Phys. Chem. C* **2010**, 114, 1073-1084.
- <sup>41</sup> Jones, W. H.; Benning, W. F.; Davis, P.; Mulvey, D. M.; Pollak, P. I.; Schaeffer, J. C.; Tull, R.; Weinstock, L. M. *Ann. N.Y. Acad. Sci.* **1969**, 158, 471-481.
- <sup>42</sup> Mahata, A.; Rai, R.K.; Choudhuri, I.; Singh, S.K.; Pathak, B. *Phys. Chem. Chem. Phys.* **2014**, 16, 26365-26374.
- <sup>43</sup> Marinelli, T. B. L. W.; Nabuurs, S.; Ponc, V. *J. Catal.* **1995**, 151, 431-438.
- <sup>44</sup> Loffreda, D.; Delbecq, F.; Vigné, F.; Sautet, P. *J. Am. Chem. Soc.* **2006**, 128, 1316-1323.
- <sup>45</sup> Loffreda, D.; Delbecq, F.; Vigné, F.; Sautet, P. *Angew. Chem. Int. Ed.* **2009**, 48, 8978-8980.
- <sup>46</sup> Tuokko, S.; Pihko, P. M.; Honkala, K. *Angew. Chem. Int. Ed.* **2016**, 55, 1670-1674.
- <sup>47</sup> Kozuch, S.; Shaik, S. *Acc. Chem. Res.* **2011**, 44, 101-110.
- <sup>48</sup> Nishimura, S.; Sakamoto, H.; Ozawa, T. *Chem. Lett.* **1973**, 2, 855-858.
- <sup>49</sup> Mitsui, S.; Imaizumi, S.; Nanbu, A.; Senda, Y. *J. Catal.* **1975**, 36, 333-337.

- <sup>50</sup> Sauvage, J.-F.; Baker, R. H.; Hussey, A. S. *J. Am. Chem. Soc.* **1960**, *82*, 6090–6095.
- <sup>51</sup> Burwell Jr, R. L. *Acc. Chem. Res.* **1969**, *2*, 289–296.
- <sup>52</sup> Patterson, W. R.; Burwell Jr, R. L.; Roth, J. A. *J. Am. Chem. Soc.* **1971**, *93*, 839–846.
- <sup>53</sup> McKervey, M. A.; Rooney, J. J.; Samman, N. G. *J. Chem. Soc., Chem. Commun.* **1972**, 1185–1185.
- <sup>54</sup> Accrombessi, G. C.; Geneste, P.; Olivé, J.-L. *J. Org. Chem.* **1980**, *45*, 4139–4143.
- <sup>55</sup> Meyer, E. F.; Burwell, R. L., Jr. *J. Am. Chem. Soc.* **1963**, *85*, 2881–2887.
- <sup>56</sup> Crombie, L.; Jenkins, P. A.; Mitchard, D. A. *J. Chem. Soc., Perkin 1* **1975**, 1081–1090.
- <sup>57</sup> Westmijze, H.; Meijer, J.; Vermeer, P. *Tetrahedron Lett.* **1975**, 2923–2924.
- <sup>58</sup> Kuhn, R.; Fischer, H. *Chem. Ber.* **1960**, *93*, 2285–2289.
- <sup>59</sup> Xu, C.; Koel, B. E. *Surf. Sci.* **1994**, *304*, 249–266.
- <sup>60</sup> Saeys, M.; Reyniers, M.-F.; Neurock, M.; Marin, G. B. *Surf. Sci.* **2006**, *600*, 3121–3134.
- <sup>61</sup> Delbecq, F.; Vigné-Maeder, F.; Becker, C.; Breitbach, J.; Wandelt, K. *J. Phys. Chem. C* **2008**, *112*, 555–556.
- <sup>62</sup> Siegel, S.; Dunkel, M.; Smith, G. V.; Halpern, W.; Cozort, J. *J. Org. Chem.* **1966**, *31*, 2802–2806.
- <sup>63</sup> Mitsui, S.; Shionoya, M.; Gohke, K.; Watanabe, F.; Imaizumi, S.; Senda, Y. *J. Catal.* **1975**, *40*, 372–378.
- <sup>64</sup> Van de Graaf, B. In *Studies on Overcrowding in Organic Molecules*; Delft University Press: Netherlands, 1978.
- <sup>65</sup> Mitsui, S.; Ito, M.; Nanbu, A.; Senda, Y. *J. Catal.* **1975**, *36*, 119–124.
- <sup>66</sup> Siegel, S.; Smith, G. V. *J. Am. Chem. Soc.* **1960**, *82*, 6082–6087.
- <sup>67</sup> Augustine, R. L.; Migliorini, D. C.; Foscante, R. E.; Sodano, C. S.; Sisbarro, M. J. *J. Org. Chem.* **1969**, *34*, 1075–1085.
- <sup>68</sup> Mallat, T.; Baiker, A. *Topics in Catalysis* **1998**, *8*, 115–124.
- <sup>69</sup> Carcía-Mota, M.; Gómez-Díaz, J.; Novell-Leruth, G.; Vargas-Fuentes, C.; Bellarosa, L.; Bridier, B.; Pérez-Ramírez, J.; López, N. *Theor. Chem. Acc.* **2011**, *128*, 663–673.
- <sup>70</sup> Gould, F.E.; Johnson, G.S.; Ferris, A.E. *J. Org. Chem.* **1960**, *25*, 1658–1660.
- <sup>71</sup> Blaser, H. U.; Jalett, H. P.; Monti, D. M.; Reber, J. F.; Wehrli, J. T. *Stud. Surf. Sci. Catal.* **1988**, *41*, 153–163.
- <sup>72</sup> Blaser, H. U.; Jalett, H. P.; Lottenbach, W. Studer, M. *J. Am. Chem. Soc.* **2000**, *122*, 12675–12682.
- <sup>73</sup> Murzin, D. Y.; Mäki-Arvela, P.; Salmi, T. *Kinet. Catal.* **2003**, *44*, 323–333.
- <sup>74</sup> Blaser, H. U.; Studer, M. *Acc. Chem. Res.* **2007**, *40*, 1348–1356.
- <sup>75</sup> Mallat, T.; Orglmeister, E.; Baiker, A. *Chem. Rev.* **2007**, *107*, 4863–4890.
- <sup>76</sup> Tálas, E.; Margittfalvi, J. L. *Chirality* **2010**, *22*, 3–15.
- <sup>77</sup> Baiker, A. *Chem. Soc. Rev.* **2015**, *44*, 7449–7464.
- <sup>78</sup> Diezi, S.; Hess, M.; Orglmeister, E.; Mallat, T.; Baiker, A. *Catal. Lett.* **2005**, *102*, 121–125.
- <sup>79</sup> Busygin, I.; Toukoniitty, E.; Sillanpää, R.; Murzin, D. Y.; Leino, R. *Eur. J. Org. Chem.* **2005**, 2811–2821.

- <sup>80</sup> Schürch, M.; Heinz, T.; Aeschimann, R.; Mallat, T.; Pfaltz, A.; Baiker, A. *J. Catal.* **1998**, *173*, 187–195.
- <sup>81</sup> Orglmeister, E.; Mallat, T.; Baiker, A. *Adv. Synth. Catal.* **2005**, *347*, 78–86.
- <sup>82</sup> Love, J. C.; Estroff, L. A.; Kriebel, J. K.; Nuzzo, R. G.; Whitesides, G. M. *Chem. Rev.* **2005**, *105*, 1103–1169.
- <sup>83</sup> Bartok, M. *Curr. Org. Chem.* **2006**, *10*, 1533–1567.
- <sup>84</sup> Zuo, X.; Liu, H.; Liu, M. *Tetrahedron Lett.* **1998**, *39*, 1941–1944.
- <sup>85</sup> Huck, W. R.; Mallat, T.; Baiker, A. *Adv. Synth. Catal.* **2003**, *345*, 255–260.
- <sup>86</sup> Török, B.; Felföldi, K.; Balázsik, K.; Bartók, M. *Chem. Commun.* **1999**, 1725–1726.
- <sup>87</sup> Schürch, M.; Künzle, N.; Mallat, T.; Baiker, A. *J. Catal.* **1998**, *176*, 569–571.
- <sup>88</sup> von Arx, M.; Mallat, T.; Baiker, A. *Catal. Lett.* **2002**, *78*, 267–271.
- <sup>89</sup> Nitta, Y.; Watanabe, J.; Okuyama, T.; Sugimura, T. *J. Catal.* **2005**, *236*, 164–167.
- <sup>90</sup> Huck, W. R.; Mallat, T.; Baiker, A. *New J. Chem.* **2002**, *26*, 6–8.
- <sup>91</sup> Minder, B.; Mallat, T.; Baiker, A.; Wang, G.; Heinz, T.; Pfaltz, A. *J. Catal.* **1995**, *1540*, 371–378.
- <sup>92</sup> Simons, K.E.; Wang, G.; Heinz, T.; Giger, T.; Mallat, T.; Pfaltz, A.; Baiker, A. *Tetrahedron: Asym.* **1995**, *6*, 505–518.
- <sup>93</sup> Schmidt, E.; Bucher, C.; Santarossa, G.; Mallat, T.; Gilmour, R.; Baiker, A. *J. Catal.* **2012**, *289*, 238–248.
- <sup>94</sup> Toukoniitty, E.; Franceschini, S.; Vaccari, A.; Murzin, D. Y. *Appl. Catal. A: Gen.* **2006**, *300*, 147–154.
- <sup>95</sup> Szöri, K.; Balázsik, K.; Felföldi, K.; Bartók, M. *J. Catal.* **2006**, *241*, 149–154.
- <sup>96</sup> Augustine, R. L.; Tanielyan, S. K. *J. Mol. Catal. A: Chem.* **1996**, *112*, 93–104.
- <sup>97</sup> Lavoie, S.; Laliberte, M. A.; Temprano, I.; McBreen, P. H. *J. Am. Chem. Soc.* **2006**, *128*, 7588–7593.
- <sup>98</sup> Vargas, A.; Ferri, D.; Baiker, A. *J. Catal.* **2005**, *236*, 1–8.
- <sup>99</sup> Baiker, A. *J. Mol. Catal. A: Chem.* **2000**, *163*, 205–220.
- <sup>100</sup> Meemken, F.; Maeda, N.; Hungerbühler, K.; Baiker, A. *Angew. Chem., Int. Ed.* **2012**, *51*, 8212–8216.
- <sup>101</sup> Diezi, S.; Reimann, S.; Bonalumi, N.; Mallat, T.; Baiker, A. *J. Catal.* **2006**, *239*, 255–262.
- <sup>102</sup> Vargas, A.; Hoxha, F.; Bonalumi, N.; Mallat, T.; Baiker, A. *J. Catal.* **2006**, *240*, 203–212.
- <sup>103</sup> Osawa, T.; Harada, T.; Takayasu, O. *Top. Catal.* **2000**, *13*, 155–168.
- <sup>104</sup> Tai, A.; Sugimura, T. In *Chiral Catalyst Immobilization and Recycling*; De Vos, D. E., Vankelecom, I. F. J., Jacobs, P. A., Eds.; Wiley-VCH: Weinheim, 2000; p 173.
- <sup>105</sup> Tungler, A.; Máthé, T.; Petró, J.; Tarnai, T. *J. Mol. Catal.* **1990**, *61*, 259–267.
- <sup>106</sup> Tungler, A.; Kajtár, M.; Máthé, T.; Tóth, G.; Fogassy, G.; Petró, J. *Catal. Today* **1989**, *5*, 159–171.
- <sup>107</sup> McIntosh, A. I.; Watson, D. J.; Burton, J. W.; Lambert, R. M. *J. Am. Chem. Soc.* **2006**, *128*, 7329–7334.

- <sup>108</sup> Rodríguez-García, L.; Hungerbühler, K.; Baiker, A.; Meemken, F. *J. Am. Chem. Soc.* **2015**, *137*, 12121–12130.
- <sup>109</sup> Watson, D. J.; Jesudason, R.; Beaumont, S. K.; Kyriakou, G.; Burton, J. W.; Lambert, R. M. *J. Am. Chem. Soc.* **2009**, *131*, 14584–14589.
- <sup>110</sup> Weng, Z.; Zaera, F. *J. Phys. Chem. C* **2014**, *118*, 3672–3679.
- <sup>111</sup> Schoenbaum, C. A.; Schwartz, D. K.; Medlin, J. W. *Acc. Chem. Res.* **2014**, *47*, 1438–1445.
- <sup>112</sup> Pang, S. H.; Medlin, J. W. *J. Phys. Chem. Lett.* **2015**, *6*, 1348–1356.
- <sup>113</sup> Marshall, S. T.; O'Brien, M.; Oetter, B.; Corpuz, A.; Richards, R. M.; Schwartz, D. K.; Medlin, J. *W. Nat. Mater.* **2010**, *9*, 853–858.
- <sup>114</sup> Marshall, S. T.; Schwartz, D. K.; Medlin, J. W. *Langmuir* **2011**, *27*, 6731–6737.
- <sup>115</sup> Medlin, J. W. *ACS Catal.* **2011**, *1*, 1284–1297.
- <sup>116</sup> Kahsar, K. R.; Schwartz, D. K.; Medlin, J. W. *J. Am. Chem. Soc.* **2014**, *136*, 520–526.
- <sup>117</sup> Benohoud, M.; Tuokko, S.; Pihko, P. M. *Chem. Eur. J.* **2011**, *17*, 8404–8413.
- <sup>118</sup> Mayes, P. A.; Perlmutter, P. In *Modern Reduction Methods*; Andersson, P. G., Munslow, I. J., Eds.; Wiley-VCH: New York, 2008; pp 87–106.
- <sup>119</sup> Keinan, E.; Greenspoon, N. In *Comprehensive Organic Synthesis*; Trost, B. M., Fleming, I., Eds.; Pergamon Press: Oxford, 1991; pp 553–557.
- <sup>120</sup> Mukaiyama, T. In *Organic Reactions*; Wiley: New York, 1982; Vol. 28, p 203.
- <sup>121</sup> Denmark, S. E.; Bui, T. *J. Org. Chem.* **2005**, *70*, 10190–10193.
- <sup>122</sup> Boxer, M. B.; Yamamoto, H. *J. Am. Chem. Soc.* **2007**, *129*, 2762–2763.
- <sup>123</sup> Herath, A.; Montgomery, J. *J. Am. Chem. Soc.* **2008**, *130*, 9132–8133.
- <sup>124</sup> Sumide, Y.; Yorimitsu, H.; Oshima, K. *J. Org. Chem.* **2009**, *74*, 7986–7989.
- <sup>125</sup> Dreizler, R. M.; Gros, E. K. U. *Density functional Theory, An Approach to the Quantum Many-Body Problem*; Springer-Verlag: New York, 1990.
- <sup>126</sup> Koch, W.; Holthausen, M. C. *A Chemist's Guide to Density Functional Theory*. 2nd Ed.; Wiley-VCH: Weinheim, 2002.
- <sup>127</sup> Martin, R. M. In *Electronic Structure*; Cambridge University Press: Cambridge, 2010.
- <sup>128</sup> von Barth, U. *Phys. Scripta* **2004**, *9*, T109.
- <sup>129</sup> Capelle, K. *Braz. J. Phys.* **2006**, *36*, 1318–1343.
- <sup>130</sup> Hohenberg, P.; Kohn, W. *Phys. Rev.* **1964**, *136*, 864–871.
- <sup>131</sup> Kohn, W.; Sham, L. J. *Phys. Rev.* **1965**, *140*, 1133–1138.
- <sup>132</sup> Jones, R. O.; Gunnarsson, O. *Rev. Mod. Phys.* **1989**, *61*, 689–746.
- <sup>133</sup> Perdew, J. P.; Schmidt. *AIP Conf. Proc.* **2001**, *577*, 1–20.
- <sup>134</sup> Perdew, J. P.; Burke, K.; Ernzerhof, M. *Phys. Rev. Lett.* **1996**, *77*, 2865–2870.
- <sup>135</sup> Hammer, B.; Hansen, L. B.; Nørskov, J. K. *Phys. Rev. B* **1999**, *98*, 5648–5652.
- <sup>136</sup> Eshuis, H.; Furche, F. *J. Phys. Chem. Lett.* **2011**, *2*, 983–989.

- <sup>137</sup> Dion, M.; Rydberg, H.; Schröder, E.; Langreth, D. C.; Lundqvist, B. I. *Phys. Rev. Lett.* **2004**, *92*, 246401.
- <sup>138</sup> Becke, A. D. *J. Chem. Phys.* **1993**, *98*, 5648–5652.
- <sup>139</sup> Stephens, P. J.; Devlin, F. J.; Chabalowski, C. F.; Frisch, M. J. *J. Phys. Chem.* **1994**, *98*, 11623–11627.
- <sup>140</sup> Enkovaara, J.; *et al.* *J. Phys.: Condens. Matter* **2010**, *22*, 253202.
- <sup>141</sup> <https://wiki.fysik.dtu.dk/gpaw>
- <sup>142</sup> Blöchl, P. E. *Phys. Rev. B.: Condens. Matter* **1994**, *50*, 17953–17979.
- <sup>143</sup> Wellendorff, J.; Nørskov, J. K.; *et al.* *Phys. Rev. B* **2012**, *85*, 235149.
- <sup>144</sup> Jónsson, H.; Mills, G.; Jacobsen, K. W. In *Classical and Quantum dynamics in Condensed Phase Simulations*. World Scientific: Singapore, 1998.
- <sup>145</sup> Jaguar, version 8.8, Schrödinger, LLC, New York, NY, 2009; Maestro, version 10.2.010, Schrödinger, LLC, New York, NY, 2009.
- <sup>146</sup> Ganesan, M.; Freemantle, R. G.; Obare, S. O. *Chem. Mater.* **2007**, *19*, 3464–3471.
- <sup>147</sup> Felpin, F.-X. *Synlett* **2014**, *25*, 1055–1067.
- <sup>148</sup> Shimizu, K.; Kubo, T.; Satsuma, A. *Chem.–Eur. J.* **2012**, *18*, 2226–2229.
- <sup>149</sup> Mitsudome, T.; Noujima, A.; Mizugaki, T.; Jitsukawa, K.; Kaneda, K. *Chem. Commun.* **2009**, 5302–5304.
- <sup>150</sup> Mitsudome, T.; Arita, S.; Mori, H.; Mizugaki, T.; Jitsukawa, K.; Kaneda, K. *Angew. Chem., Int. Ed.* **2008**, *47*, 7938–7940.
- <sup>151</sup> John, J.; Gravel, E.; Hagege, A.; Li, H.; Gacoin, T.; Doris, E. *Angew. Chem., Int. Ed.* **2011**, *50*, 7533–7536.
- <sup>152</sup> Jeon, M.; Han, J.; Park, J. *ChemCatChem* **2012**, *4*, 521–524.
- <sup>153</sup> Jeon, M.; Han, J.; Park, J. *ACS Catal.* **2012**, *2*, 1539–1549.
- <sup>154</sup> Kamachi, T.; Shimizu, K.-I.; Yoshihiro, D.; Igawa, K.; Tomooka, K.; Yoshizawa, K. *J. Phys. Chem. C* **2013**, *117*, 22967–22973.
- <sup>155</sup> Gallezot, P.; Richard, D. *Catal. Rev. Sci. Eng.* **1998**, *40*, 81–126.
- <sup>156</sup> Mäki-Arvela, P.; Hájek, J.; Salmi, T.; Murzin, D. Y. *Appl. Catal. A* **2005**, *292*, 1–49.
- <sup>157</sup> Kliewer, C. J.; Bieri, M.; Somorjai, G. A. *J. Am. Chem. Soc.* **2009**, *131*, 9958–9966.
- <sup>158</sup> Marinelli, T. B. L. W.; Ponec, V. *J. Catal.* **1995**, *156*, 51–59.
- <sup>159</sup> Ponec, V. *Appl. Catal. A* **1997**, *149*, 27–48.
- <sup>160</sup> Wang, S.; Petzold, V.; Tripkovic, V.; Kleis, J.; Howalt, J. G.; Skúlason, E.; Fernández, E. M.; Hvolbæk, B.; Jones, G.; Toftelund, A.; Falsig, H.; Björketun, M.; Studt, F.; Abild-Pedersen, F.; Rossmeisl, J.; Nørskov, J. K.; Bligaard, T. *Phys. Chem. Chem. Phys.* **2011**, *13*, 20760–20765.

- <sup>161</sup> Munter, T. R.; Bligaard, T.; Christensen, C. H.; Nørskov, J. K. *Phys. Chem. Chem. Phys.* **2008**, *10*, 5202–5206.
- <sup>162</sup> Jones A. B. In *Comprehensive Organic Synthesis*, Trost, B. M.; Fleming, I. Eds.; Pergamon Press Ltd.: Oxford, 1991; Vol. 7, pp. 151-191.
- <sup>163</sup> Chen, B.-C.; Zhou, P.; Davis, F. A.; Ciganek, E. In *Organic Reactions*; Overman L. E., Eds.; John Wiley & Sons Inc.: New York, 2003; Vol. 62, pp 1-356.
- <sup>164</sup> Enslin, P. R. *Tetrahedron* **1971**, *27*, 1909–1915.
- <sup>165</sup> Inoki, S.; Kato, K.; Isayama, S.; Mukaiyama, T. *Chem. Lett.* **1990**, 1869–1872.
- <sup>166</sup> Magnus, P.; Payne A. H.; Waring, M. J.; Scott, D. A.; Lynch, V. *Tetrahedron. Lett.* **2000**, *41*, 9725–9730.

## ORIGINAL PAPERS

### I

# PALLADIUM ON CHARCOAL AS A CATALYST FOR STOICHIOMETRIC CHEMO- AND STEREOSELECTIVE HYDROSILYLATIONS AND HYDROGENATIONS WITH TRIETHYLSILANE

by

Sakari Tuokko & Petri M. Pihko

*Org. Process Res. Dev.* **2014**, *18*, 1740–1751.

Reproduced with kind permission by 2015 American Chemical Society.

## II

# FIRST PRINCIPLES CALCULATIONS FOR HYDROGENATION OF ACROLEIN ON Pd AND Pt: CHEMOSELECTIVITY DEPENDS ON STERIC EFFECTS ON THE SURFACE

by

Sakari Tuokko, Petri M. Pihko & Karoliina Honkala

*Angew. Chem. Int. Ed.* **2015**, *55*, 1670–1674.

Reproduced with kind permission by 2016 Wiley-VCH Verlag GmbH & Co. KGaA,  
Weinheim.

### III

## PALLADIUM ON CHARCOAL CATALYZED 3,4- HYDROPEROXIDATION OF $\alpha$ -SUBSTITUTED ENALS WITH TRIETHYLSILANE AND WATER

by

Sakari Tuokko & Petri M. Pihko

*Synlett* **2016**, 27, 1649-1652.

Reproduced with kind permission by 2016 Georg Thieme Verlag Stuttgart · New  
York.

# IV

## **Pd/C CATALYZED HYDROSILYLATION OF ENALS AND ENONES WITH TRIETHYLSILANE: CONFORMER POPULATIONS CONTROL THE STEREOSELECTIVITY**

by

Sakari Tuokko, Karoliina Honkala & Petri M. Pihko

*Submitted.*



DEPARTMENT OF CHEMISTRY, UNIVERSITY OF JYVÄSKYLÄ  
RESEARCH REPORT SERIES

1. Vuolle, Mikko: Electron paramagnetic resonance and molecular orbital study of radical ions generated from (2.2)metacyclophane, pyrene and its hydrogenated compounds by alkali metal reduction and by thallium(III)trifluoroacetate oxidation. (99 pp.) 1976
2. Pasanen, Kaija: Electron paramagnetic resonance study of cation radical generated from various chlorinated biphenyls. (66 pp.) 1977
3. Carbon-13 Workshop, September 6-8, 1977. (91 pp.) 1977
4. Laihia, Katri: On the structure determination of norbornane polyols by NMR spectroscopy. (111 pp.) 1979
5. Nyrönen, Timo: On the EPR, ENDOR and visible absorption spectra of some nitrogen containing heterocyclic compounds in liquid ammonia. (76 pp.) 1978
6. Talvitie, Antti: Structure determination of some sesquiterpenoids by shift reagent NMR. (54 pp.) 1979
7. Häkli, Harri: Structure analysis and molecular dynamics of cyclic compounds by shift reagent NMR. (48 pp.) 1979
8. Pitkänen, Ilkka: Thermodynamics of complexation of 1,2,4-triazole with divalent manganese, cobalt, nickel, copper, zinc, cadmium and lead ions in aqueous sodium perchlorate solutions. (89 pp.) 1980
9. Asunta, Tuula: Preparation and characterization of new organometallic compounds synthesized by using metal vapours. (91 pp.) 1980
10. Sattar, Mohammad Abdus: Analyses of MCPA and its metabolites in soil. (57 pp.) 1980
11. Bibliography 1980. (31 pp.) 1981
12. Knuutila, Pekka: X-Ray structural studies on some divalent 3d metal compounds of picolinic and isonicotinic acid N-oxides. (77 pp.) 1981
13. Bibliography 1981. (33 pp.) 1982
14. 6th National NMR Symposium, September 9-10, 1982, Abstracts. (49 pp.) 1982
15. Bibliography 1982. (38 pp.) 1983
16. Knuutila, Hilikka: X-Ray structural studies on some Cu(II), Co(II) and Ni(II) complexes with nicotinic and isonicotinic acid N-oxides. (54 pp.) 1983
17. Symposium on inorganic and analytical chemistry May 18, 1984, Program and Abstracts. (100 pp.) 1984
18. Knuutinen, Juha: On the synthesis, structure verification and gas chromatographic determination of chlorinated catechols and guaiacols occurring in spent bleach liquors of kraft pulp mill. (30 pp.) 1984
19. Bibliography 1983. (47 pp.) 1984
20. Pitkänen, Maija: Addition of BrCl, B<sub>2</sub> and Cl<sub>2</sub> to methyl esters of propenoic and 2-butenic acid derivatives and <sup>13</sup>C NMR studies on methyl esters of saturated aliphatic mono- and dichlorocarboxylic acids. (56 pp.) 1985
21. Bibliography 1984. (39 pp.) 1985
22. Salo, Esa: EPR, ENDOR and TRIPLE spectroscopy of some nitrogen heteroaromatics in liquid ammonia. (111 pp.) 1985
23. Humppi, Tarmo: Synthesis, identification and analysis of

- dimeric impurities of chlorophenols. (39 pp.) 1985
24. Aho, Martti: The ion exchange and adsorption properties of sphagnum peat under acid conditions. (90 pp.) 1985
  25. Bibliography 1985 (61 pp.) 1986
  26. Bibliography 1986. (23 pp.) 1987
  27. Bibliography 1987. (26 pp.) 1988
  28. Paasivirta, Jaakko (Ed.): Structures of organic environmental chemicals. (67 pp.) 1988
  29. Paasivirta, Jaakko (Ed.): Chemistry and ecology of organo-element compounds. (93 pp.) 1989
  30. Sinkkonen, Seija: Determination of crude oil alkylated dibenzothiophenes in environment. (35 pp.) 1989
  31. Kolehmainen, Erkki (Ed.): XII National NMR Symposium Program and Abstracts. (75 pp.) 1989
  32. Kuokkanen, Tauno: Chlorocymenes and Chlorocymenenes: Persistent chlorocompounds in spent bleach liquors of kraft pulp mills. (40 pp.) 1989
  33. Mäkelä, Reijo: ESR, ENDOR and TRIPLE resonance study on substituted 9,10-anthraquinone radicals in solution. (35 pp.) 1990
  34. Veijanen, Anja: An integrated sensory and analytical method for identification of off-flavour compounds. (70 pp.) 1990
  35. Kasa, Seppo: EPR, ENDOR and TRIPLE resonance and molecular orbital studies on a substitution reaction of anthracene induced by thallium(III) in two fluorinated carboxylic acids. (114 pp.) 1990
  36. Herve, Sirpa: Mussel incubation method for monitoring organochlorine compounds in freshwater recipients of pulp and paper industry. (145 pp.) 1991
  37. Pohjola, Pekka: The electron paramagnetic resonance method for characterization of Finnish peat types and iron (III) complexes in the process of peat decomposition. (77 pp.) 1991
  38. Paasivirta, Jaakko (Ed.): Organochlorines from pulp mills and other sources. Research methodology studies 1988-91. (120 pp.) 1992
  39. Veijanen, Anja (Ed.): VI National Symposium on Mass Spectrometry, May 13-15, 1992, Abstracts. (55 pp.) 1992
  40. Rissanen, Kari (Ed.): The 7. National Symposium on Inorganic and Analytical Chemistry, May 22, 1992, Abstracts and Program. (153 pp.) 1992
  41. Paasivirta, Jaakko (Ed.): CEOEC'92, Second Finnish-Russian Seminar: Chemistry and Ecology of Organo-Element Compounds. (93 pp.) 1992
  42. Koistinen, Jaana: Persistent polychloroaromatic compounds in the environment: structure-specific analyses. (50 pp.) 1993
  43. Virkki, Liisa: Structural characterization of chlorolignins by spectroscopic and liquid chromatographic methods and a comparison with humic substances. (62 pp.) 1993
  44. Helenius, Vesa: Electronic and vibrational excitations in some biologically relevant molecules. (30 pp.) 1993

45. Leppä-aho, Jaakko: Thermal behaviour, infrared spectra and x-ray structures of some new rare earth chromates(VI). (64 pp.) 1994
46. Kotila, Sirpa: Synthesis, structure and thermal behavior of solid copper(II) complexes of 2-amino-2-hydroxymethyl-1,3-propanediol. (111 pp.) 1994
47. Mikkonen, Anneli: Retention of molybdenum(VI), vanadium(V) and tungsten(VI) by kaolin and three Finnish mineral soils. (90 pp.) 1995
48. Suontamo, Reijo: Molecular orbital studies of small molecules containing sulfur and selenium. (42 pp.) 1995
49. Hämäläinen, Jouni: Effect of fuel composition on the conversion of fuel-N to nitrogen oxides in the combustion of small single particles. (50 pp.) 1995
50. Nevalainen, Tapio: Polychlorinated diphenyl ethers: synthesis, NMR spectroscopy, structural properties, and estimated toxicity. (76 pp.) 1995
51. Aittola, Jussi-Pekka: Organochloro compounds in the stack emission. (35 pp.) 1995
52. Harju, Timo: Ultrafast polar molecular photophysics of (dibenzylmethine)borondifluoride and 4-aminophthalimide in solution. (61 pp.) 1995
53. Maatela, Paula: Determination of organically bound chlorine in industrial and environmental samples. (83 pp.) 1995
54. Paasivirta, Jaakko (Ed.): CEOEC'95, Third Finnish-Russian Seminar: Chemistry and Ecology of Organo-Element Compounds. (109 pp.) 1995
55. Huuskonen, Juhani: Synthesis and structural studies of some supramolecular compounds. (54 pp.) 1995
56. Palm, Helena: Fate of chlorophenols and their derivatives in sawmill soil and pulp mill recipient environments. (52 pp.) 1995
57. Rantio, Tiina: Chlorohydrocarbons in pulp mill effluents and their fate in the environment. (89 pp.) 1997
58. Ratilainen, Jari: Covalent and non-covalent interactions in molecular recognition. (37 pp.) 1997
59. Kolehmainen, Erkki (Ed.): XIX National NMR Symposium, June 4-6, 1997, Abstracts. (89 pp.) 1997
60. Matilainen, Rose: Development of methods for fertilizer analysis by inductively coupled plasma atomic emission spectrometry. (41 pp.) 1997
61. Koistinen, Jari (Ed.): Spring Meeting on the Division of Synthetic Chemistry, May 15-16, 1997, Program and Abstracts. (36 pp.) 1997
62. Lappalainen, Kari: Monomeric and cyclic bile acid derivatives: syntheses, NMR spectroscopy and molecular recognition properties. (50 pp.) 1997
63. Laitinen, Eira: Molecular dynamics of cyanine dyes and phthalimides in solution: picosecond laser studies. (62 pp.) 1997
64. Eloranta, Jussi: Experimental and theoretical studies on some

- quinone and quinol radicals. (40 pp.) 1997
65. Oksanen, Jari: Spectroscopic characterization of some monomeric and aggregated chlorophylls. (43 pp.) 1998
66. Häkkänen, Heikki: Development of a method based on laser-induced plasma spectrometry for rapid spatial analysis of material distributions in paper coatings. (60 pp.) 1998
67. Virtapohja, Janne: Fate of chelating agents used in the pulp and paper industries. (58 pp.) 1998
68. Airola, Karri: X-ray structural studies of supramolecular and organic compounds. (39 pp.) 1998
69. Hyötyläinen, Juha: Transport of lignin-type compounds in the receiving waters of pulp mills. (40 pp.) 1999
70. Ristolainen, Matti: Analysis of the organic material dissolved during totally chlorine-free bleaching. (40 pp.) 1999
71. Eklin, Tero: Development of analytical procedures with industrial samples for atomic emission and atomic absorption spectrometry. (43 pp.) 1999
72. Väliisaari, Jouni: Hygiene properties of resol-type phenolic resin laminates. (129 pp.) 1999
73. Hu, Jiwei: Persistent polyhalogenated diphenyl ethers: model compounds syntheses, characterization and molecular orbital studies. (59 pp.) 1999
74. Malkavaara, Petteri: Chemometric adaptations in wood processing chemistry. (56 pp.) 2000
75. Kujala Elena, Laihia Katri, Nieminen Kari (Eds.): NBC 2000, Symposium on Nuclear, Biological and Chemical Threats in the 21<sup>st</sup> Century. (299 pp.) 2000
76. Rantalainen, Anna-Lea: Semipermeable membrane devices in monitoring persistent organic pollutants in the environment. (58 pp.) 2000
77. Lahtinen, Manu: *In situ* X-ray powder diffraction studies of Pt/C, CuCl/C and Cu<sub>2</sub>O/C catalysts at elevated temperatures in various reaction conditions. (92 pp.) 2000
78. Tamminen, Jari: Syntheses, empirical and theoretical characterization, and metal cation complexation of bile acid-based monomers and open/closed dimers. (54 pp.) 2000
79. Vatanen, Virpi: Experimental studies by EPR and theoretical studies by DFT calculations of  $\alpha$ -amino-9,10-anthraquinone radical anions and cations in solution. (37 pp.) 2000
80. Kotilainen, Risto: Chemical changes in wood during heating at 150-260 °C. (57 pp.) 2000
81. Nissinen, Maija: X-ray structural studies on weak, non-covalent interactions in supramolecular compounds. (69 pp.) 2001
82. Wegelius, Elina: X-ray structural studies on self-assembled hydrogen-bonded networks and metallosupramolecular complexes. (84 pp.) 2001
83. Paasivirta, Jaakko (Ed.): CEOEC'2001, Fifth Finnish-Russian Seminar: Chemistry and Ecology of Organo-Element Compounds. (163 pp.) 2001
84. Kiljunen, Toni: Theoretical studies on spectroscopy and atomic dynamics in rare gas solids. (56 pp.) 2001

85. Du, Jin: Derivatives of dextran: synthesis and applications in oncology. (48 pp.) 2001
86. Koivisto, Jari: Structural analysis of selected polychlorinated persistent organic pollutants (POPs) and related compounds. (88 pp.) 2001
87. Feng, Zhinan: Alkaline pulping of non-wood feedstocks and characterization of black liquors. (54 pp.) 2001
88. Halonen, Markku: Lahon havupuun käyttö sulfaattiprosessin raaka-aineena sekä havupuun lahontorjunta. (90 pp.) 2002
89. Falábu, Dezső: Synthesis, conformational analysis and complexation studies of resorcarene derivatives. (212 pp.) 2001
90. Lehtovuori, Pekka: EMR spectroscopic studies on radicals of ubiquinones Q-*n*, vitamin K<sub>3</sub> and vitamine E in liquid solution. (40 pp.) 2002
91. Perkkalainen, Paula: Polymorphism of sugar alcohols and effect of grinding on thermal behavior on binary sugar alcohol mixtures. (53 pp.) 2002
92. Ihalainen, Janne: Spectroscopic studies on light-harvesting complexes of green plants and purple bacteria. (42 pp.) 2002
93. Kunttu, Henrik, Kiljunen, Toni (Eds.): 4<sup>th</sup> International Conference on Low Temperature Chemistry. (159 pp.) 2002
94. Väisänen, Ari: Development of methods for toxic element analysis in samples with environmental concern by ICP-AES and ETAAS. (54 pp.) 2002
95. Luostarinen, Minna: Synthesis and characterisation of novel resorcarene derivatives. (200 pp.) 2002
96. Louhelainen, Jarmo: Changes in the chemical composition and physical properties of wood and nonwood black liquors during heating. (68 pp.) 2003
97. Lahtinen, Tanja: Concave hydrocarbon cyclophane B-prismands. (65 pp.) 2003
98. Laihia, Katri (Ed.): NBC 2003, Symposium on Nuclear, Biological and Chemical Threats – A Crisis Management Challenge. (245 pp.) 2003
99. Oasmaa, Anja: Fuel oil quality properties of wood-based pyrolysis liquids. (32 pp.) 2003
100. Virtanen, Elina: Syntheses, structural characterisation, and cation/anion recognition properties of nano-sized bile acid-based host molecules and their precursors. (123 pp.) 2003
101. Nättinen, Kalle: Synthesis and X-ray structural studies of organic and metallo-organic supramolecular systems. (79 pp.) 2003
102. Lampiselkä, Jarkko: Demonstraatio lukion kemian opetuksessa. (285 pp.) 2003
103. Kallioinen, Jani: Photoinduced dynamics of Ru(dcbpy)<sub>2</sub>(NCS)<sub>2</sub> – in solution and on nanocrystalline titanium dioxide thin films. (47 pp.) 2004
104. Valkonen, Arto (Ed.): VII Synthetic Chemistry Meeting and XXVI Finnish NMR Symposium. (103 pp.) 2004
105. Vaskonen, Kari: Spectroscopic studies on atoms and small molecules isolated in low

- temperature rare gas matrices. (65 pp.) 2004
106. Lehtovuori, Viivi: Ultrafast light induced dissociation of Ru(dcbpy)(CO)<sub>2</sub>I<sub>2</sub> in solution. (49 pp.) 2004
107. Saarenketo, Pauli: Structural studies of metal complexing schiff bases, Schiff base derived *N*-glycosides and cyclophane  $\pi$ -prismans. (95 pp.) 2004
108. Paasivirta, Jaakko (Ed.): CEOEC'2004, Sixth Finnish-Russian Seminar: Chemistry and Ecology of Organo-Element Compounds. (147 pp.) 2004
109. Suontamo, Tuula: Development of a test method for evaluating the cleaning efficiency of hard-surface cleaning agents. (96 pp.) 2004
110. Güneş, Minna: Studies of thiocyanates of silver for nonlinear optics. (48 pp.) 2004
111. Ropponen, Jarmo: Aliphatic polyester dendrimers and dendrons. (81 pp.) 2004
112. Vu, Mân Thi Hong: Alkaline pulping and the subsequent elemental chlorine-free bleaching of bamboo (*Bambusa procera*). (69 pp.) 2004
113. Mansikkamäki, Heidi: Self-assembly of resorcinarenes. (77 pp.) 2006
114. Tuononen, Heikki M.: EPR spectroscopic and quantum chemical studies of some inorganic main group radicals. (79 pp.) 2005
115. Kaski, Saara: Development of methods and applications of laser-induced plasma spectroscopy in vacuum ultraviolet. (44 pp.) 2005
116. Mäkinen, Riika-Mari: Synthesis, crystal structure and thermal decomposition of certain metal thiocyanates and organic thiocyanates. (119 pp.) 2006
117. Ahokas, Jussi: Spectroscopic studies of atoms and small molecules isolated in rare gas solids: photodissociation and thermal reactions. (53 pp.) 2006
118. Busi, Sara: Synthesis, characterization and thermal properties of new quaternary ammonium compounds: new materials for electrolytes, ionic liquids and complexation studies. (102 pp.) 2006
119. Mäntykoski, Keijo: PCBs in processes, products and environment of paper mills using wastepaper as their raw material. (73 pp.) 2006
120. Laamanen, Pirkko-Leena: Simultaneous determination of industrially and environmentally relevant aminopolycarboxylic and hydroxycarboxylic acids by capillary zone electrophoresis. (54 pp.) 2007
121. Salmela, Maria: Description of oxygen-alkali delignification of kraft pulp using analysis of dissolved material. (71 pp.) 2007
122. Lehtovaara, Lauri: Theoretical studies of atomic scale impurities in superfluid <sup>4</sup>He. (87 pp.) 2007
123. Rautiainen, J. Mikko: Quantum chemical calculations of structures, bonding, and spectroscopic properties of some sulphur and selenium iodine cations. (71 pp.) 2007
124. Nummelin, Sami: Synthesis, characterization, structural and retrostructural analysis of self-assembling pore forming dendrimers. (286 pp.) 2008
125. Sopo, Harri: Uranyl(VI) ion complexes of some organic

- aminobisphenolate ligands: syntheses, structures and extraction studies. (57 pp.) 2008
126. Valkonen, Arto: Structural characteristics and properties of substituted cholanoates and *N*-substituted cholanamides. (80 pp.) 2008
127. Lähde, Anna: Production and surface modification of pharmaceutical nano- and microparticles with the aerosol flow reactor. (43 pp.) 2008
128. Beyeh, Ngong Kodiah: Resorcinarenes and their derivatives: synthesis, characterization and complexation in gas phase and in solution. (75 pp.) 2008
129. Väliisaari, Jouni, Lundell, Jan (Eds.): Kemian opetuksen päivät 2008: uusia oppimisympäristöjä ja ongelmalähtöistä opetusta. (118 pp.) 2008
130. Myllyperkiö, Pasi: Ultrafast electron transfer from potential organic and metal containing solar cell sensitizers. (69 pp.) 2009
131. Käkölä, Jaana: Fast chromatographic methods for determining aliphatic carboxylic acids in black liquors. (82 pp.) 2009
132. Koivukorpi, Juha: Bile acid-arene conjugates: from photoswitchability to cancer cell detection. (67 pp.) 2009
133. Tuuttila, Tero: Functional dendritic polyester compounds: synthesis and characterization of small bifunctional dendrimers and dyes. (74 pp.) 2009
134. Salorinne, Kirsi: Tetramethoxy resorcinarene based cation and anion receptors: synthesis, characterization and binding properties. (79 pp.) 2009
135. Rautiainen, Riikka: The use of first-thinning Scots pine (*Pinus sylvestris*) as fiber raw material for the kraft pulp and paper industry. (73 pp.) 2010
136. Ilander, Laura: Uranyl salophens: synthesis and use as ditopic receptors. (199 pp.) 2010
137. Kiviniemi, Tiina: Vibrational dynamics of iodine molecule and its complexes in solid krypton - Towards coherent control of bimolecular reactions? (73 pp.) 2010
138. Ikonen, Satu: Synthesis, characterization and structural properties of various covalent and non-covalent bile acid derivatives of N/O-heterocycles and their precursors. (105 pp.) 2010
139. Siitonen, Anni: Spectroscopic studies of semiconducting single-walled carbon nanotubes. (56 pp.) 2010
140. Raatikainen, Kari: Synthesis and structural studies of piperazine cyclophanes – Supramolecular systems through Halogen and Hydrogen bonding and metal ion coordination. (69 pp.) 2010
141. Leivo, Kimmo: Gelation and gel properties of two- and three-component Pyrene based low molecular weight organogelators. (116 pp.) 2011
142. Martiskainen, Jari: Electronic energy transfer in light-harvesting complexes isolated from *Spinacia oleracea* and from three photosynthetic green bacteria *Chloroflexus aurantiacus*, *Chlorobium tepidum*, and *Prosthecochloris aestuarii*. (55 pp.) 2011

143. Wichmann, Oula: Syntheses, characterization and structural properties of [O,N,O,X] aminobisphenolate metal complexes. (101 pp.) 2011
144. Ilander, Aki: Development of ultrasound-assisted digestion methods for the determination of toxic element concentrations in ash samples by ICP-OES. (58 pp.) 2011
145. The Combined XII Spring Meeting of the Division of Synthetic Chemistry and XXXIII Finnish NMR Symposium. Book of Abstracts. (90 pp.) 2011
146. Valto, Piia: Development of fast analysis methods for extractives in papermaking process waters. (73 pp.) 2011
147. Andersin, Jenni: Catalytic activity of palladium-based nanostructures in the conversion of simple olefinic hydro- and chlorohydrocarbons from first principles. (78 pp.) 2011
148. Aumanen, Jukka: Photophysical properties of dansylated poly(propylene amine) dendrimers. (55 pp.) 2011
149. Kärnä, Minna: Ether-functionalized quaternary ammonium ionic liquids – synthesis, characterization and physicochemical properties. (76 pp.) 2011
150. Jurček, Ondřej: Steroid conjugates for applications in pharmacology and biology. (57 pp.) 2011
151. Nauha, Elisa: Crystalline forms of selected Agrochemical actives: design and synthesis of cocrystals. (77 pp.) 2012
152. Ahkola, Heidi: Passive sampling in monitoring of nonylphenol ethoxylates and nonylphenol in aquatic environments. (92 pp.) 2012
153. Helttunen, Kaisa: Exploring the self-assembly of resorcinarenes: from molecular level interactions to mesoscopic structures. (78 pp.) 2012
154. Linnanto, Juha: Light excitation transfer in photosynthesis revealed by quantum chemical calculations and exciton theory. (179 pp.) 2012
155. Roiko-Jokela, Veikko: Digital imaging and infrared measurements of soil adhesion and cleanability of semihard and hard surfaces. (122 pp.) 2012
156. Noponen, Virpi: Amides of bile acids and biologically important small molecules: properties and applications. (85 pp.) 2012
157. Hulkko, Eero: Spectroscopic signatures as a probe of structure and dynamics in condensed-phase systems – studies of iodine and gold ranging from isolated molecules to nanoclusters. (69 pp.) 2012
158. Lappi, Hanna: Production of Hydrocarbon-rich biofuels from extractives-derived materials. (95 pp.) 2012
159. Nykänen, Lauri: Computational studies of Carbon chemistry on transition metal surfaces. (76 pp.) 2012
160. Ahonen, Kari: Solid state studies of pharmaceutically important molecules and their derivatives. (65 pp.) 2012
161. Pakkanen, Hannu: Characterization of organic material dissolved during alkaline pulping of wood and non-wood feedstocks (76 pp.) 2012
162. Moilanen, Jani: Theoretical and experimental studies of some

- main group compounds: from closed shell interactions to singlet diradicals and stable radicals. ( 80 pp.) 2012
163. Himanen, Jatta: Stereoselective synthesis of Oligosaccharides by *De Novo* Saccharide welding. (133 pp.) 2012
164. Bunzen, Hana: Steroidal derivatives of nitrogen containing compounds as potential gelators.(76 pp.) 2013
165. Seppälä, Petri: Structural diversity of copper(II) amino alcohol complexes. Syntheses, structural and magnetic properties of bidentate amino alcohol copper(II) complexes. (67 pp.) 2013
166. Lindgren, Johan: Computational investigations on rotational and vibrational spectroscopies of some diatomics in solid environment. (77 pp.) 2013
167. Giri, Chandan: Sub-component self-assembly of linear and non-linear diamines and diacylhydrazines, formylpyridine and transition metal cations. (145 pp.) 2013
168. Riisio, Antti: Synthesis, Characterization and Properties of Cu(II)-, Mo(VI)- and U(VI) Complexes With Diaminotetraphenolate Ligands. (51 pp.) 2013
169. Kiljunen, Toni (Ed.): Chemistry and Physics at Low Temperatures. Book of Abstracts. (103 pp.) 2013
170. Hänninen, Mikko: Experimental and Computational Studies of Transition Metal Complexes with Polydentate Amino- and Aminophenolate Ligands: Synthesis, Structure, Reactivity and Magnetic Properties. (66 pp.) 2013
171. Antila, Liisa: Spectroscopic studies of electron transfer reactions at the photoactive electrode of dye-sensitized solar cells. (53 pp.) 2013
172. Kemppainen, Eeva: Mukaiyama-Michael reactions with  $\alpha$ -substituted acroleins – a useful tool for the synthesis of the pectenotoxins and other natural product targets. (190 pp.) 2013
173. Virtanen, Suvi: Structural Studies Of Dielectric Polymer Nanocomposites. (49 pp.) 2013
174. Yliniemelä-Sipari, Sanna: Understanding The Structural Requirements for Optimal Hydrogen Bond Catalyzed Enolization – A Biomimetic Approach.(160 pp.) 2013
175. Leskinen, Mikko V: Remote  $\beta$ -functionalization of  $\beta'$ -keto esters (105 pp.) 2014
176. 12<sup>th</sup> European Conference on Research in Chemistry Education (ECRICE2014). Book of Abstracts. (166 pp.) 2014
177. Peuronen, Anssi: N-Monoalkylated DABCO-Based N-Donors as Versatile Building Blocks in Crystal Engineering and Supramolecular Chemistry. (54 pp.) 2014
178. Perämäki, Siiri: Method development for determination and recovery of rare earth elements from industrial fly ash. (88 pp.) 2014
179. Chernyshev, Alexander, N.: Nitrogen-containing ligands and their platinum(IV) and gold(III) complexes: investigation and basicity and nucleophilicity, luminescence, and aurophilic interactions. (64 pp.) 2014

180. Lehto, Joni: Advanced Biorefinery Concepts Integrated to Chemical Pulping. (142 pp.) 2015
181. Tero, Tiia-Riikka: Tetramethoxy resorcinarenes as platforms for fluorescent and halogen bonding systems. (61 pp.) 2015
182. Löfman, Miika: Bile acid amides as components of microcrystalline organogels. (62 pp.) 2015
183. Selin, Jukka: Adsorption of softwood-derived organic material onto various fillers during papermaking. (169 pp.) 2015
184. Piisola, Antti: Challenges in the stereoselective synthesis of allylic alcohols. (210 pp.) 2015
185. Bonakdarzadeh, Pia: Supramolecular coordination polyhedra based on achiral and chiral pyridyl ligands: design, preparation, and characterization. (65 pp.) 2015
186. Vasko, Petra: Synthesis, characterization, and reactivity of heavier group 13 and 14 metallylenes and metalloid clusters: small molecule activation and more. (66 pp.) 2015
187. Topić, Filip: Structural Studies of Nano-sized Supramolecular Assemblies. (79 pp.) 2015
188. Mustalahti, Satu: Photodynamics Studies of Ligand-Protected Gold Nanoclusters by using Ultrafast Transient Infrared Spectroscopy. (58 pp.) 2015
189. Koivisto, Jaakko: Electronic and vibrational spectroscopic studies of gold-nanoclusters. (63pp.) 2015
190. Suhonen, Aku: Solid state conformational behavior and interactions of series of aromatis oligoamide foldamers. (68 pp.) 2016
191. Soikkeli, Ville: Hydrometallurgical recovery and leaching studies for selected valuable metals from fly ash samples by ultrasound-assisted extraction followed by ICP-OES determination. ( 107 pp.) 2016
192. XXXVIII Finnish NMR Symposium. Book of Abstracts. (51 pp.) 2016
193. Mäkelä, Toni: Ion Pair Recognition by Ditopic Crown Ether Based bis-Urea and Uranyl Salophen Receptors. ( 75 pp.) 2016
194. Lindholm-Lehto, Petra: Occurrence of pharmaceuticals in municipal wastewater treatment plants and receiving surface waters in Central and Southern Finland. (98 pp.) 2016
195. Härkönen, Ville: Computational and Theoretical studies on Lattice Thermal conductivity and Thermal properties of Silicon Clathrates (89 pp.) 2016